Late Jurassic to Early Cretaceous black shale formation and paleoenvironment in high northern latitudes

Spätjurassische bis Frühkretazische Schwarzschiefergenese und Paläoumwelt in hohen nördlichen Breiten

---

Uwe Langrock

Ber. Polarforsch. Meeresforsch. 472 (2004)
ISSN 1618 - 3193

»There are many things in the deep water; and seas and lands may change. And it is not our part here to take thought only for a season, or for a few lives of Men, or for a passing age of the world.«

"The Fellowship of the Ring" by J.R.R. Tolkien

Uwe Langrock

Alfred Wegener Institute for Polar and Marine Research
Department of Geosciences
Columbus St.
27568 Bremerhaven
Germany

Die vorliegende Arbeit ist die inhaltlich unveränderte Fassung einer Dissertation, die 2003 dem Fachbereich 5 Geowissenschaften der Universität Bremen vorgelegt wurde.

Table of content

Abstract

The present study investigates the mechanisms which have controlled input and preservation of organic carbon in Late Jurassic to Early Cretaceous marine sediments from high northern paleolatitudes. Special emphasis is given to the origin, composition, and preservation of particulate organic matter in order to assess its response to paleoenvironmental changes. During the Late Jurassic to Early Cretaceous the long meridional Norwegian-Greenland-Seaway was one of only two marine connections between the boreal northwestern Tethys and the paleo-Arctic Ocean, the other being a much shallower seaway across the Russian Platform. To carry out this study, sediments from four cores taken along the Norwegian continental shelf were investigated using geochemical and petrographic approaches. With this it was possible to investigate late Mesozoic black shale formation in high northern paleolatitudes during times of a low global sea level.

The results show clear differences in the paleoenvironment from lower to higher latitudes, which can be explained by the great meridional distance and its paleoecologic, paleoceanographic, and paleoclimatic effect on the local sedimentary environment. On the other hand, a general change in depositional conditions was observed during a period of about 10 My from the Volgian to the Valanginian, which resulted in the termination of black shale formation as sea level rose. Microscopic analysis of the particulate organic matter revealed that, without regard to the paleolatitudes, both terrestrial and marine-aquatic macerals were deposited in the sediments. However, towards higher latitudes the amount of macerals from various marine, brackish, and limnic sources increases, reflecting more favorable conditions for preservation of the lipid-rich fraction. The accumulation of organic carbon in the sediments from the low-latitudinal location is primarily controlled by the input of terrigenous "woody" organic matter, whereas primary control towards higher latitudes is the input and preservation of lipid-rich organic matter.

Interpretations of framboidal pyrite distribution, C/S and C/N ratios, Mo/Al ratios, and TOC-Fe-S relationships revealed that preservation of organic matter

becomes more and more associated with anoxic bottom waters towards higher latitudes. Estimates of paleoproductivity, the relationship between C_{ORG} and initial sedimentation rate, and carbonate dissolution in the water column indicate that anoxia was unlikely caused by increased marine productivity. It is much more likely that a low sea level favored the formation of paleoceanographic isolated basins where probably reduced vertical circulation caused stratification of the water column. The lack of oxygen eventually resulted in persistent anoxic bottom waters, whilst the organic carbon content was influenced by more short-term periodic changes in primary production and input of clastic material. This scenario, similar to the stagnation model, is supported by the subsequent termination of black shale formation due to a sea-level rise that reached its maximum in the Valanginian and Hauterivian. This is clearly reflected by the composition of the organic matter, which shows a decrease of hydrocarbon potential and an enrichment of refractory material that may be explained by the increased circulation of O_2-rich water masses and the associated re-establishment of the benthic fauna.

Kurzfassung

Im Rahmen der vorliegenden Arbeit wurde untersucht, welche Mechanismen den Eintrag und die Erhaltung von organischem Kohlenstoff (C_{ORG}) in fossilen marinen Sedimenten hoher nördlicher Breiten steuern. Der inhaltliche Schwerpunkt liegt dabei auf der geochemischen und mikroskopischen Charakterisierung des partikulären organischen Materials und welche Rückschlüsse aus dessen Herkunft, Zusammensetzung und Erhaltung auf die Paläoumweltbedingungen gezogen werden können. Dafür wurden Sedimente aus 4 Bohrkernen entlang des norwegischen Kontinentalschelfs ausgewählt, die während des Oberjura und der Unterkreide abgelagert wurden. Der 300 km breite und über 2000 km lange meridionale Seeweg zwischen Norwegen und Grönland war zu dieser Zeit die einzige direkte Verbindung zwischen den äquatorialen Gefilden der nordwestlichen Tethys und den sub-polaren Gebieten

des heutigen arktischen Ozeans. Die spezielle Zeitscheibe wurde ausgewählt, um Bildungsbedingungen von organisch-reichen Sedimenten des späten Mesozoikum zu dokumentieren, die in hohen nördlichen Paläobreiten und während eines niedrigen globalen Meeresspiegels vorherrschten.

Die Ergebnisse zeigen zum einen deutliche Unterschiede in den Paläoumweltbedingungen von niedrigen zu hohen Breiten, was auf den großen meridionalen Unterschied und die möglicherweise damit verbundenen paläoökologischen, paläozeanographischen, und paläoklimatischen Auswirkungen auf die lokalen Sedimentationsräume zurückgeführt werden kann. Zum anderen ist eine allgemeine Änderung in den Bildungsbedingungen über einen Zeitraum von etwa 10 Mio Jahren vom Volgium bis in das Valanginium zu erkennen, die eine Termination der Schwarzschieferbildung zur Folge hat und auf einen deutlichen Meerespiegelanstieg zurückgeführt werden kann.

Die mikroskopische Analyse des partikulären organischen Materials (Mazerale) hat gezeigt, dass ungeachtet der Breiten sowohl terrigene als auch marin-aquatische Mazerale eingetragen wurden. Allerdings nimmt der Anteil an Mazeralen, die verschiedenen marinen, brackischen und limnischen Habitaten zugeordnet werden können, mit zunehmend höheren Breiten zu und reflektiert Bedingungen, die eine bessere Erhaltung der lipid-reichen Fraktion begünstigen. In diesem Zusammenhang konnte ebenfalls gezeigt werden, dass der Gehalt an C_{ORG} im Sediment in der südlichen Lokalität primär vom terrigenen Eintrag gesteuert wird, während in höheren Breiten der Gehalt an C_{ORG} zunehmend durch erhöhte Erhaltung von lipid-reichen Mazeralen kontrolliert wird.

Ferner konnte durch das Verteilungsmuster framboidaler Pyrite sowie C/S-, C/N-, TOC-Fe-S- und Mo/Al-Verhältnissen gezeigt werden, dass die Erhaltung des organischen Materials in höheren Breiten immer deutlicher mit anoxischen Bedingungen im Bodenwasser verknüpft ist. Berechnungen der Paläoproduktivitäten sowie das Verhältnis zwischen C_{ORG} und der ursprünglichen Sedimentationsrate unter besonderer Berücksichtigung möglichen Karbonatabbaus in der Wassersäule deuten darauf hin, dass eine

erhöhte marine Produktivität nicht in erster Linie ursächlich für die anoxischen Bedingungen gewesen sein kann. Vielmehr führte ein niedriger Meeresspiegel wahrscheinlich zu einer paläozeanographischen Isolation, wodurch es zur Stratifizierung der Wassersäule und zur Reduzierung der Bodenwasserzirkulation kam. Der Mangel an Sauerstoff führte dann zur Bildung von Anoxia, wobei die Auswirkungen auf den Gehalt an C_{ORG} durch eher periodische Schwankungen in der Primärproduktion auf der einen und klastischen Eintrag auf der anderen Seite beeinflusst wurden. Diese Modellvorstellung, ähnlich dem *Stagnations-Modell*, wird dadurch unterstützt, dass den kontinuierlichen Niedergang der Schwarzschieferbildung von einem Anstieg des Meeresspiegels begleitet wird, der seinen Höhepunkt im Valanginium und Hauterivium hat. Die Zusammensetzung des organischen Materials spiegelt dies u.a. durch eine Verschlechterung des Kohlenwasserstoffpotentials und eine Anreicherung von refraktärem Material wider, was durch eine intensivere Zirkulation O_2-reicher Wassermassen und die damit verbundene Re-etablierung des Benthos erklärt werden kann.

1. Introduction

1.1. Late Mesozoic black shale formation

There were two periods in the geological record where the formation of fossil energy resources became a crucial dimension on a global scale – one in the late Paleozoic and one in the late Mesozoic [e.g. Larson, 1991; Hallam and Wignall, 1999].

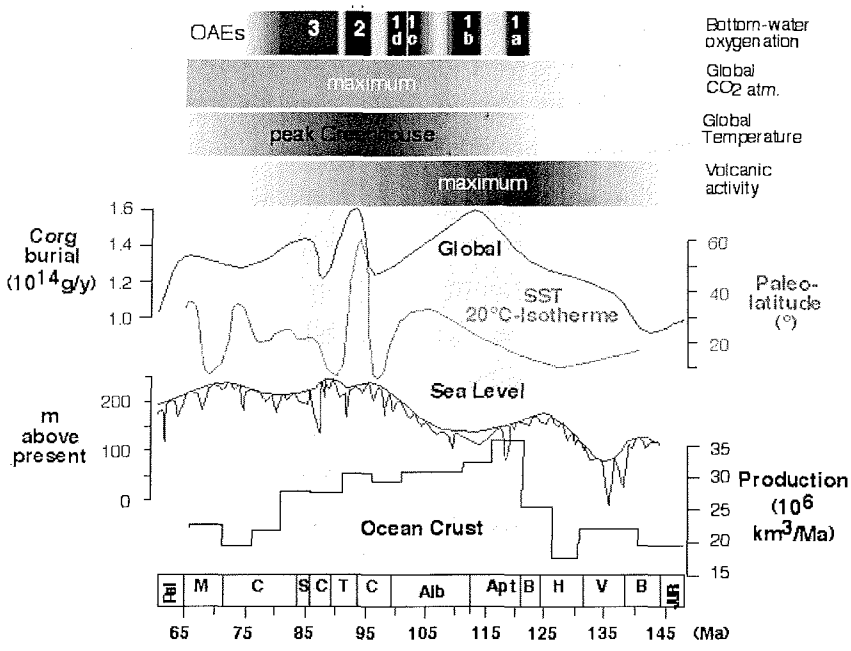

Fig. 1-1 Comparison between oceanic anoxic events (OAEs), global CO_2 (atm.) pressure, global paleotemperature, volcanic activity, ocean crust production, global sea level, and organic carbon burial rate according to paleolatitude in the Cretaceous period (modified after Larson, 1991 and Wagner et al.,, 2003).

During the Upper Carboniferous and Permian period one half of the world's coal reserves were generated from the burial of a vast terrestrial flora, containing nine times more fossil fuel energy than all oil and gas combined. During the Jurassic and Cretaceous period, on the other hand, the source rocks for two thirds of the world's oil and gas reserves were formed in marine and lacustrine sediments [e.g. Tissot and Welte, 1984]. Even though that formation of coal

and organic carbon-rich sediments occurred throughout the geological past, and even today, such "productive" periods that lasted for several tens of millions of years require special conditions that exceed a regional scale. Magmatic superplumes are thought to have caused an episode of constant normal magnetic polarity in the mid-Cretaceous (124 – 83 Ma), which resulted in high oceanic spreading rates, high sea level, and high paleotemperatures [Larson, 1991] (Fig. 1-1). Along with this, increased rifting, oceanic plateau production, and island-arc volcanism subsequently caused an elevated atmospheric CO_2 partial pressure, which was crucial for creating "greenhouse conditions" during these times. The constant availability of nutrients and CO_2 stimulated primary production, and is thought to have caused anoxic conditions in large parts of the oceans [e.g. Schlanger and Jenkyns, 1976; Demaison and Moore, 1980; Arthur et al., 1987; Erbacher et al., 2001]. These major episodes are known as Oceanic Anoxic Events (OAEs) and have probably occurred worldwide. For example, the southern North Atlantic is presumed to have been almost completely anoxic during the Cenomanian/Turonian, when the oxygen-depleted waters sporadically reached up into the photic zone [e.g. Sinninghe Damsté and Köster, 1998]. Such extreme conditions favored the accumulation and preservation of organic carbon-rich marine sediments, which eventually became petroleum source rocks. The OAEs are also a likely cause for mass extinction [e.g. Hallam and Wignall, 1999], and this may have even more "snowballed" the organic carbon accumulation.

The deposition of sediments rich in organic matter, including petroleum source rocks with more than 0.5 to 1.0 % by weight organic carbon, is usually restricted to sub-aquatic environments in which organic matter is provided faster than it can be destroyed (Tissot and Welte, 1984). In subaerial sediments the organic matter is easily recycled by chemical and microbial oxidation. Most of the organic carbon-rich sediments, so-called black shales, are found along the continental margins. This is because of high primary productivity of coastal waters, high input from land-plant derived material, and shallow water depths, which allow for more of organic matter to reach the seafloor. In particular, fine-grained sediments are associated with high organic carbon contents because

most organic particles (including bacteria) are hydrodynamically equivalent to the clay and silt fraction. The organic matter usually originates from both aquatic (marine, brackish, and freshwater) and terrestrial sources, and can vary widely in composition. However, it is imperative for the formation of black shales that the organic matter becomes preserved, regardless of its sources. All organic matter is unstable and hence susceptible to oxidation and biochemical decomposition during transport and settling. The degree of susceptibility depends largely on the chemical properties of the organic matter; nitrogen- and hydrogen-rich (aliphatic) components are preferably consumed by animal and bacteria because they provide more energy. There are two primary mechanisms, one chemical and one physical, which lead to enhanced preservation. The presence of anoxia in the bottom water is probably the most important factor (Demaison and Moore, 1980) because the resulting absence of benthic life may inhibit one major remineralization process of organic matter (Meyers, 1997). Anoxia emerges when the demand of oxygen for bacterial decomposition of organic matter exceeds the supply. As a consequence, other oxidants (e.g. sulfate) are used by anaerobic bacteria, producing H_2S that is toxic to most species. The formation of organic carbon-rich sediments is therefore often attributed to episodes of anoxic bottom waters, particularly in response to extreme climate changes. Early discussion on the preservation of organic carbon in sediments has largely been based on material from the mid-Cretaceous of the Central and North Atlantic. Two models have been discussed by many authors [e.g. Schlanger and Jenkyns, 1976; Thiede and van Andel, 1977; Brumsack, 1980; Demaison and Moore, 1980; De Graciansky et al., 1984; Stein et al., 1986; Pedersen and Calvert, 1990, Caplan and Bustin, 1999; Saelen et al., 2000; Nijenhuis et al., 2001; Röhl et al., 2001]. The "***stagnation model***" involves a stratified water mass, where a low rate of circulation, especially vertical circulation, ultimately results in oxygen deficiency of the bottom waters. High preservation of organic matter results from the absence of oxygen, rather than high primary productivity. Modern examples are the Black Sea and Lake Tanganyika (Huc, 1988). The "***productivity model***" assumes increased rates of marine productivity that stimulate oxygen consumption by

aerobic bacteria, causing an oxygen minimum zone (OMZ) just below the zone of primary production. When the OMZ expands and impinges on the seafloor the bottom waters become dysoxic or suboxic and enhance preservation of organic matter. This model requires high nutrient supply and sufficient sunlight, as has been observed in upwelling areas such as offshore Peru (Suess and Thiede, 1983; Pedersen and Calvert, 1990). Rapid burial of organic matter may also lead to enhancing preservation, because biochemical decomposition by bacteria is most prominent in the upper 0.5 meters of the sediment. Whereas a high rate of clastic input may have a dilution effect on the organic carbon content, increased supply of terrigenous (woody) organic matter seems to be an important mechanism to enhance accumulation and preservation of organic carbon in some marine sediments (Stein et al., 1986).

Under certain conditions organic carbon-rich sediments may become petroleum source rocks (Tissot and Welte, 1984; Boussafir and Lallier-Vergès, 1997; Welte et al., 1997). A minimum organic carbon content of ≥ 1 % by weight and an elevated amount of hydrogen-rich components are required for the formation of petroleum source rocks. These components may be derived by selective preservation of lipid-rich OM beneath anoxic bottom waters, or by polycondensation of bio-macromolecules of various sources (e.g. Tissot and Welte, 1984).

1.2. Main objectives

The primary goal of this work was to identify the mechanisms that may have controlled input, accumulation, and preservation of organic carbon-rich sediments in high northern paleolatitudes during the late Jurassic-early Cretaceous interval, and their significance for paleoenvironmental reconstruction. Sedimentary organic matter has its precursors in different marine and terrestrial sources, which response directly and indirectly to paleoenvironmental changes. These responses become eventually preserved in the sediment, and so may act as a paleoenvironmental logbook. The

formation of organic carbon-rich sediments is often attributed to distinct periods in the geological past, where a special configuration of paleogeographic, paleoceanographic, and paleoclimatic conditions existed (see section 1.1). Such conditions have prevailed particularly during the late Mesozoic, where black shale formation is documented from many parts of the oceans, e.g. during the Cenomanian-Turonian boundary event (CTBE black shales). These events are connected to the worldwide development of anoxia during the long mid-Cretaceous magnetic "normal" episode, which is marked by a relatively high sea level (Fig. 1-1). Much has since been reported of sediments which were deposited during the mid-Cretaceous, especially from the central and southern North Atlantic, and the South Atlantic Ocean (e.g. Arthur et al., 1987; De Graciansky et al., 1984, Stein, 1990; Stein et al., 1986; Demaison and Moore, 1980; Wagner, 2002; Sinninghe Damsté and Köster, 1998). It has been also reported from these and many other studies that formation of black shales is not limited to the mid-Cretaceous or periods of high sea level.

The Jurassic and Cretaceous periods periodically underwent significant climate changes from "ice-house" to "greenhouse" conditions, replacing the somewhat antiquated view of constant equable warmth and sluggish oceanic circulation during the late Mesozoic (e.g. Hay, 1995; Hay et al. 1999; Price et al., 2000; Mutterlose and Kessels, 2000; Mutterlose et al., 2003). The higher latitudes have recently received much attention, because there climate changes should be more clearly reflected in the sedimentary record. The northern North Atlantic is of special interest because in the late Jurassic to early Cretaceous large amounts of organic carbon-rich sediments accumulated in the shallow margins of the opening part of this ocean (e.g. Larsen et al., 1990; Leith et al., 1990; Doré, 1991; Hay, 1998). The formation of these black shales occurred during times of an exceptionally low sea level (Haq et al., 1988; Hay, 1995; Jongepier et al., 1996; Brekke et al., 1999), which is reflected by the occurrence of shallow-marine and non-marine sediments in large parts of Europe, e.g. the Wealden facies. Due to this situation, the late Jurassic to early Cretaceous was also characterized by a distinctive provincialism of marine biota and a clear

differentiation into the Tethyan and Boreal realms (e.g. Mutterlose et al., 2003). Much work has since been focussed on sediments from various localities in NW Europe, France, Italy, Romania, and Poland; however these locations reflect paleolatitudes, which were below 30° N during this time. The Norwegian-Greenland-Seaway provides the rare opportunity to compliment these sites with material from true high paleolatitudes, connecting the northwestern Tethys and the proto-Arctic seas. Due to the extreme meridional extension of the seaway it should be possible to reveal changes in the paleoenvironmental conditions, and probably different mechanisms of black shale formation between the Boreal and Arctic realms. Four locations were selected that represent paleolatitudes from 42° N up to 59° N along the Norwegian continental shelf into the south-central Barents Sea.

1.3. The Norwegian Greenland Seaway

The Norwegian Greenland Seaway (NGS) is the Mesozoic ancestor of the modern northern North Atlantic, which is bounded by Greenland and Norway at its flanks and extends more or less from Rockall and Hatton Banks to Svalbard (Fig. 1-2). The primary structural elements of the Norwegian-Greenland-Seaway (NGS) were defined during the Caledonian orogenesis by the collision of Laurentia and Eurasia, forming the "Old Red Continent" in the Devonian (e.g. Brekke, 2000).

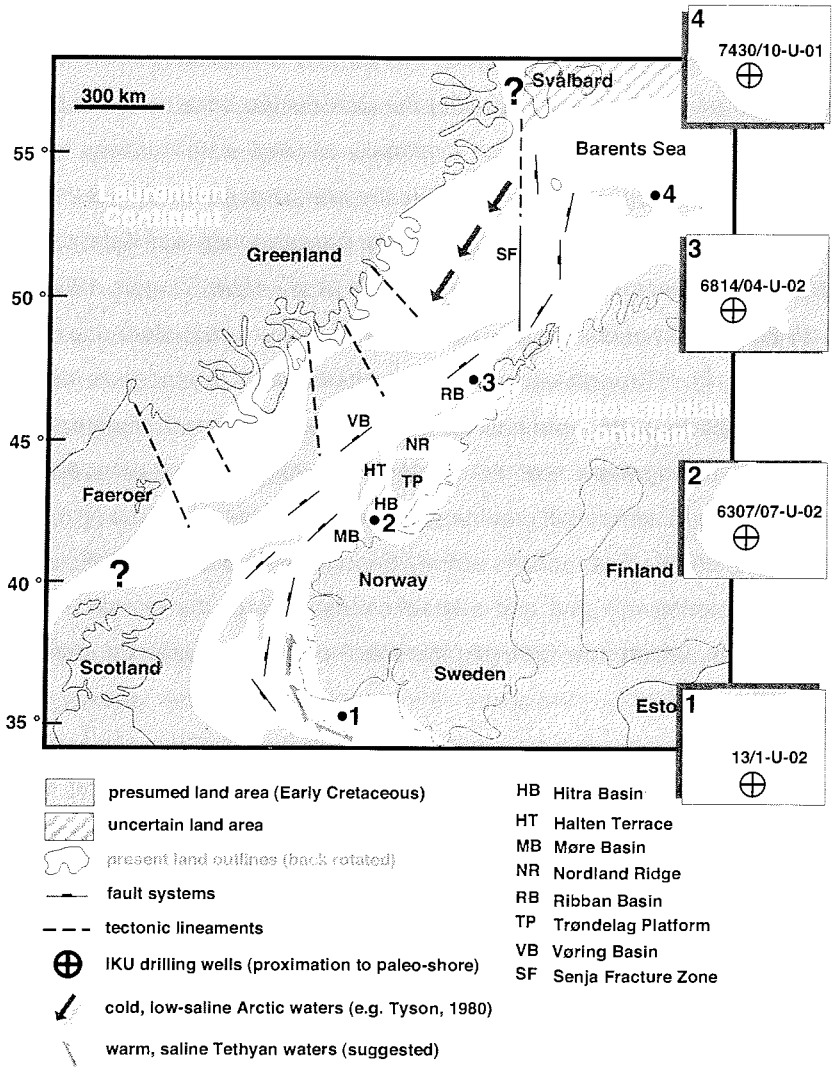

Fig. 1-2 Suggested paleogeographic situation of the Norwegian-Greenland-Seaway during the Early Cretaceous (modified after Larson, 1987; Ziegler, 1988; Doré, 1992; Jongepier et al., 1996; Brekke et al., 1999; Hay et al., 1999; Brekke, 2001; Mutterlose et al. 2003).

The overall NE-SW structural trend, which has been established during the formation of the metamorphic basement, played a crucial role during the later re-opening between the two continental blocks. As the impulse from the first opening of the Central Atlantic Ocean in the Jurassic reached the collapsing Caledonian Orogen, a long episode of extensional tectonism along the

continental boundaries was initiated, beginning with intra-plate continental rifting (e.g. Doré, 1991). Although Greenland still formed a continuous unit with the Scandinavian part of Europe by sharing the Caledonian basement, continuous pulses of extension and subsidence eventually allowed water masses to enter the region from the north and the south. By the late Jurassic an almost 2000 km long NE – SW oriented epicontinental marine passage was well established – the Norwegian-Greenland-Seaway [e.g. Larsen et al., 1990; Ziegler, 1988; Hay et al., 1999; Kazmin and Napatov, 1998; Brekke et al., 1999; Mutterlose et al., 2003] (Fig. 1-2). Through subsequent Jurassic and Cretaceous times a fundamental differentiation into basins, bounding platforms, and marginal highs started within the seaway, e.g. the Vøring Basin, the Møre Basins, and the Trøndelag Platform, which still dominate the modern Norwegian Sea (e.g. Doré, 1991; Brekke, 2000). The tectonic activity through this period also left its mark on older sediments, e.g. the sub-arcosic sandstones of the middle Jurassic Garn Formation, which now provides important petroleum reservoir units [e.g. Storvoll et al., 2002]. Whereas the existence of the seaway was unquestionable, its extension provided some controversy. Early reconstruction of the seaway included space for the Vøring Plateau [e.g. Barron et al, 1981], because an overlap of such a large section (60.000 km^2) with Greenland was unacceptable. Hence, the seaway was estimated to be about 300 to 450 km wide [e.g. Ziegler, 1988; Doré, 1991]. Using the reconstruction of Hay et al. (1999), and considering that deep-sea drilling revealed a much younger, Eocene age for the Vøring Plateau [e.g. Thiede, 1980] the true width of the early Cretaceous seaway may have been only 200 to 300 km. During the late Jurassic to early Cretaceous the NGS was one of only two connections between the proto-Arctic Ocean and the Tethyan realm, the other being across the Russian Platform. Due to its long meridional extension it may have played a crucial paleoceanographic role as a conduit for heat transport and exchange of water-masses between the low and high latitudes [e.g. Kazmin and Napatov, 1998; Gradstein et al., 1999; Hay et al., 1999; Mutterlose et al., 2003] (Fig. 1-2). The other seaway was further east, left ending from the present Caspian region northward along the western margin of the Ural, and via the Moscow Platform

into the Barents Sea (e.g. Hay et al., 1999) (Fig. 1-3). It is uncertain whether this shallow seaway was always open, which is particularly questionable during the Jurassic-Cretaceous transition. While the Tethys and the Pacific formed large open oceans, only part of the North Atlantic from about the equator to 25° N paleo-latitude (Azores Fracture Zone) was already open. The existence of a shallow marine framework bounding the western European continental landmasses from about 25° to 35° N paleo-latitude [e.g. Ziegler, 1988] is highly speculative, and does not support a direct open connection between the North Atlantic and the NGS. This is also supported by the fact that the Rockall-Hatton-Bank was still closed to Greenland and Europe during that time [Hay et al., 1999].

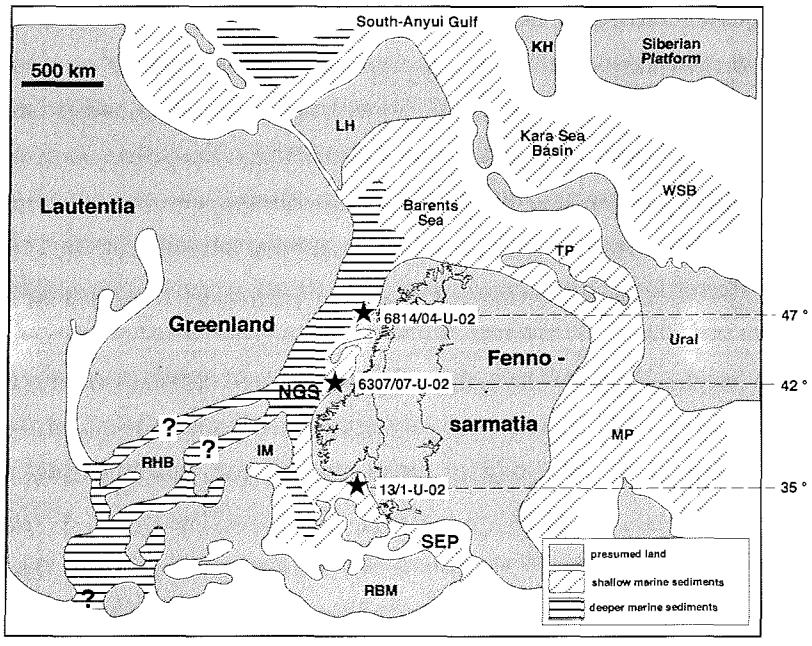

Fig. 1-3 Paleogeographic situation of the seaways surrounding Eurasian continental masses during the Early Cretaceous (modified after Ziegler, 1988 and Mutterlose et al., 2003)

The Labrador Sea did not begin to open before the mid-Cretaceous magnetic-quiet interval about 115 Ma ago [e.g. Larson, 1991; Mutterlose et al., 2003]. Stretching along the continental margins did not start until the late Cretaceous

(80 Ma) when Hatton and Rockall Banks separated from Greenland, and from each other [Hay et al., 1999]. The initial continental breakup between Eurasia and Greenland occurred during the early Eocene, about 53.7 Ma (Chron 24B). This initiated an episode of both intense compression and extension, which was driven by plume-enhanced ridge push, and caused broad uplifts and subsidence in the entire seaway [e.g. Lundin and Doré, 2001]. The principal structural elements caused by the post-breakup deformation still dominate the present region.

A large two-way current system that we observe in the present-day North Atlantic did not exist in the late Jurassic to early Cretaceous. This is primarily owing to a different paleogeographic and paleoceanographic situation. The Gulf Stream, which is considered as the pace-maker of the modern global current system, transporting warm, saline waters into the Arctic Ocean via the North Atlantic Drift (NAD) and the Norwegian Current (NC) was not yet established during this time (e.g. Hay et al., 1999). Continental landmasses and structural highs, such as the Iberian Massif and the Rockall-Hatton Bank, likely prevented a direct connection between the tropical North Atlantic and the Norwegian-Greenland-Seaway. Another important point is that the long axis of the Central and North Atlantic tends to be more zonal (East-West), which is unfavorable for a significant heat transport towards higher latitudes. The formation of a paleo-Arctic deep-water like the present one and its southward transport via the East Greenland Current (EGC) was also very unlikely, because the paleo-Arctic realm was about 2000 km north of those landmasses, which enclose the present Arctic Ocean [e.g. Kazmin and Napatov, 1998; Hay et al., 1999]. A southward flow of cold, low-salinity waters from the paleo-Arctic Ocean into the NGS was inhibited by landmasses between Nowaja Semlja and NE-Greenland [e.g. Mutterlose et al., 2003]. Hence, a large two-way current system in the Norwegian-Greenland-Seaway similar to the present one is unlikely, because the connection between the two large physical pumps (Central Atlantic and Arctic Ocean) was probably blocked, both from the north and the south. However, the long meridional NE-SW extension of the seaway itself provides the potential for an exchange of surface waters and heat transport between

lower and higher latitudes. Beyond that, there is still a suggested southeasterly connection to the Boreal NW-Tethys, and a northeasterly connection via the Barents Sea to the South Anyui Gulf (the paleo-Arctic Ocean) [e.g. Kazmin and Napatov, 1998] (Fig. 1-3). During the late Jurassic the low sea level and the emergence of structural highs and landmasses within the seaway [e.g. Doré, 1991; Brekke, 2000] may have limited a large meridional current system. Riley and Tyson (1980) suggested that cooler water masses entered the seaway from the north in early Cretaceous times, which would fit into the picture of moderate "ice-house" conditions in the Valanginian [e.g. Price et al. 2000; Hay, 1995, Hay et al., 1999]. With sea-level rise and change to a more cool, arid climate in the earliest Cretaceous (Late Volgian – Valanginian) [e.g. Mutterlose et al., 2003] a merging of water-masses in the seaway probably favored the development of a more complex current system. It is very likely that during this period more warm, oxygenated waters from the Tethys region successively entered the investigated sedimentary basins along the eastern seaway from the south.

1.4. Research area

To the present day some of the sediments deposited during the late Mesozoic represent important petroleum source rocks. The first exploration licenses in the area were allocated in 1980 and during the next fifteen years the activity of exploration and scientific studies increased both from the oil industry and academic institutions. Aside from great advances in seismic, gravimetric, and magnetic data a large number of sediment cores penetrating Cretaceous and Jurassic strata were obtained. The continental margin of the present Norwegian Sea consists of a complex sea-floor physiography, including different troughs, ridges and basins that were primarily formed during and in response to the main tectonic episodes (late Jurassic, late Cretaceous, Eocene, Oligocene, and Miocene).

The primary structural elements in the Norwegian Sea are the NE-SW oriented deep Cretaceous basins, e.g. the Vøring and Møre Basins between 62° and 69° present latitude, surrounded by paleo-highs and platforms, and the mainland [e.g. Doré, 1991; Brekke, 2000]. To carry out this study four locations were selected at almost regular intervals from the western Skagerrak along the Norwegian shelf to the Barents Sea, reflecting a meridional transect of about 2000 kilometers (Table 1-1). The advantage of the selected core positions is that the inner parts of the Scandinavian continental margin and the Barents Sea have not been severely affected by the major tectonic processes since the late Jurassic [Brekke, 2001; Bugge et al., 2002]. The post-Cretaceous continental breakup occurred along the NE-SW axis of the seaway, the Senja Fracture Zone, Hornsund Fault Zone, and into the Beaufort Sea [e.g. Lundin and Doré, 2001].

Site	Latitude	Longitude	Water Depth	Paleolatitudes		
				150 Ma	135 Ma	120 Ma
7430/10-U-01	74.12 °N	30.14 °E	338 m	54° N	55° N	56° N
6814/04-U-02	68.39 °N	14.09 °E	233 m	47° N	48° N	50° N
6307/07-U-02	63.27 °N	07.14 °E	290 m	42° N	43° N	45° N
13/1-U-02	57.48 °N	08.12 °E	505 m	38° N	39° N	41° N

Table 1-1 Latitudinal and longitudinal grid reference, water depth at drilling site, and paleolatitudes of the sediment cores investigated.

Hence, the distances between the core locations remained relatively constant, so that this transect reflects the paleogeographic configuration during late Jurassic to early Cretaceous. A low sea-level during the Jurassic-Cretaceous transition influenced the NGS by forming of a number of isolated epicontinental seas along the shelf, e.g. the shallow Trøndelag Platform and its adjacent basins [Ziegler, 1988; Jongepier et al., 1996; Bugge et al., 1999; Hansen et al., 1991; Doré, 1991]. Fine-grained organic carbon-rich sediments were probably deposited under dominantly anoxic conditions, e.g. the Spekk Formation in the middle part and the correlating Hekkingen Formation in the northern part of the

Norwegian-Greenland-Seaway, which can be traced laterally into the western Barents Sea (e.g. Bugge et al., 1989; Smelror et al., 1998; Bugge et al., 2002) (Fig. 1-3).

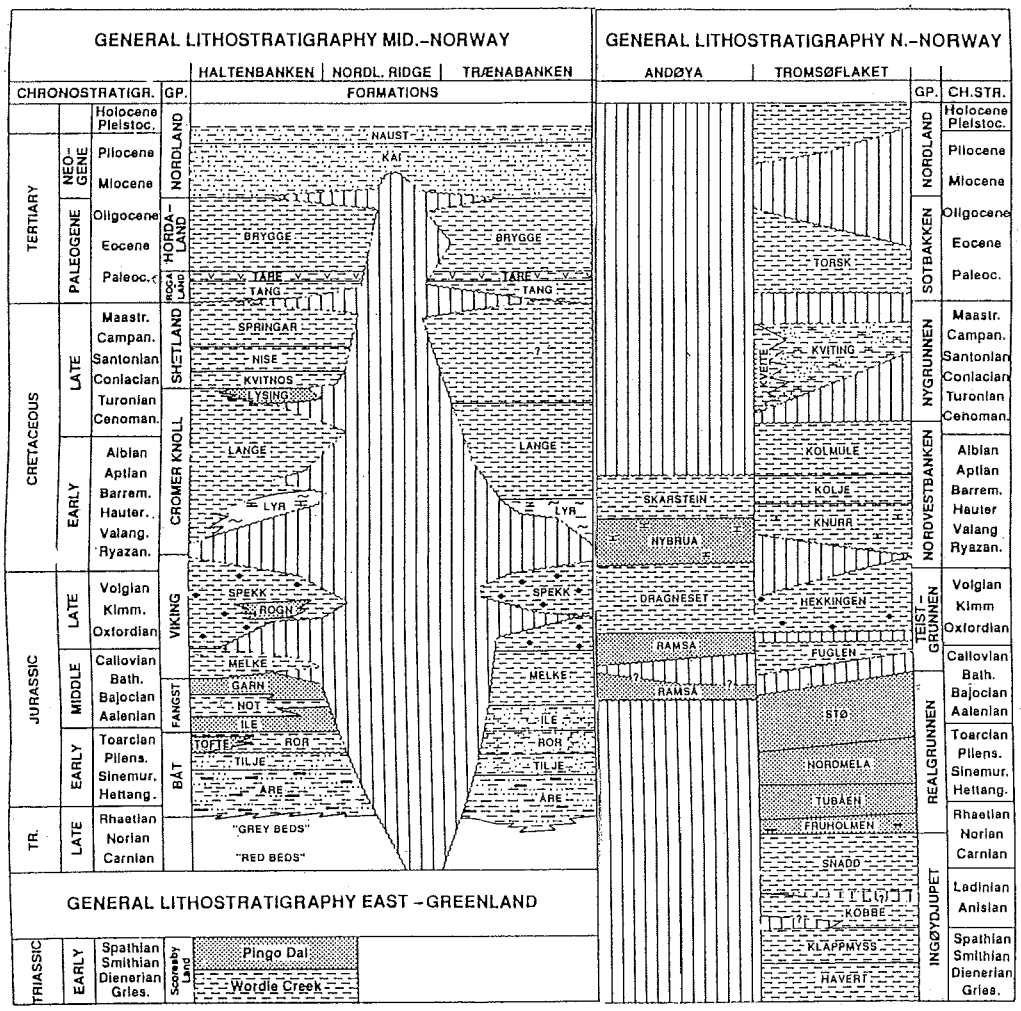

Fig. 1-4 General lithostratigraphic units of mid- and upper Norway and the Barents Sea (see Skarbø et al., 1988).

Large volumes of relatively fine-grained clastic sediments were deposited in the basins off mid-Norway and in the Barents Sea, whereas the structural highs are characterized by condensed carbonates. A widespread hiatus in earliest Cretaceous time is thought to be due to differential subsidence with local uplifts and erosion (Surlyk, 1990; Brekke, 2000). Siliciclastic sedimentation prevailed in the mid to high latitudes, while the Tethys was characterized by carbonate-rich pelagic sedimentation. The sedimentary successions and their spatial distributions found along the Norwegian shelf margin are presented in Figure 1-4. In the southern parts dark claystones of Tithonian to Berriasian age are best represented by the Spekk Formation. These black shale sequences are successively overlain by gray and red marls of the late Berriasian to early Valanginian Lange Formation. Further north, and in the central Barents Sea, a similar trend from siliciclastic towards calcareous sediments can be observed by dark, organic carbon-rich claystones of the Kimmeridgian to late Berriasian Hekkingen Formation. These black shales are succeeded by marly limestones of the early Valanginian to Barremian Klippfisk Formation.

1.5. Time control

Stratigraphic control of marine sediments is essential for the purpose of paleoenvironmental reconstruction. However, only a few methods are applicable on consolidated sedimentary rocks as old as 140 million years. The general problem of marine sediments containing thick laminated black shale sequences is the relative scarcity of fossils within these sequences. In the present case, short-term and long-term episodes of anoxic to dysoxic conditions dominated the bottom waters, which resulted in the almost complete absence of benthic fossils. Calcareous nannofossils and foraminifers show low to moderate abundance in most of the cored sequences (Mutterlose et al., 2003). Stratigraphic assess ment of the investigated cores was obtained from various lithostratigraphic, palynological, and biostratigraphic investigations [e.g. Hansen et al., 1991; Johansen et al., 1993; Mørk et al., 1993; Mutterlose et al., 2003;

Smelror, 1994; Smelror et al., 1998, 2001b; Vigran et al., 1998; Worsley et al., 1988].

Period	Linear Sedimentation Rate (cm/1000 years)			
	7430/10-U-01	6814/04-U-02	6307/07-U-02	13/1-U-02
Early Barremian	0,1	0,6		
Hauterivian	0,1	0,3	0,2	
Valanginian	0,1	0,4	0,3	
Ryazanian	0,2	0,6	0,3	
Late Volgian	0,2	1,5	0,4	0,7
Middle Volgian	0,2	0,8	0,6	1,0
Early Volgian	0,1	0,6	0,8	0,9
Late Kimmeridgian	0,5			

Table 1-2 Linear sedimentation rates per stage for all cores investigated

Resulting linear sedimentation rates (LSR) of the investigated sediment sequences using the time scale of Hardenbol et al. (1998) are summarized in Table 1-2. A general overview of stratigraphic range, lithological thickness and formational boundaries of the two cores from the mid-Norwegian shelf (6307/07-U-02, 6814/04-U-02) and the one from the south-central Barents Sea (7430/10-U-01) is shown in Figure 1-5.

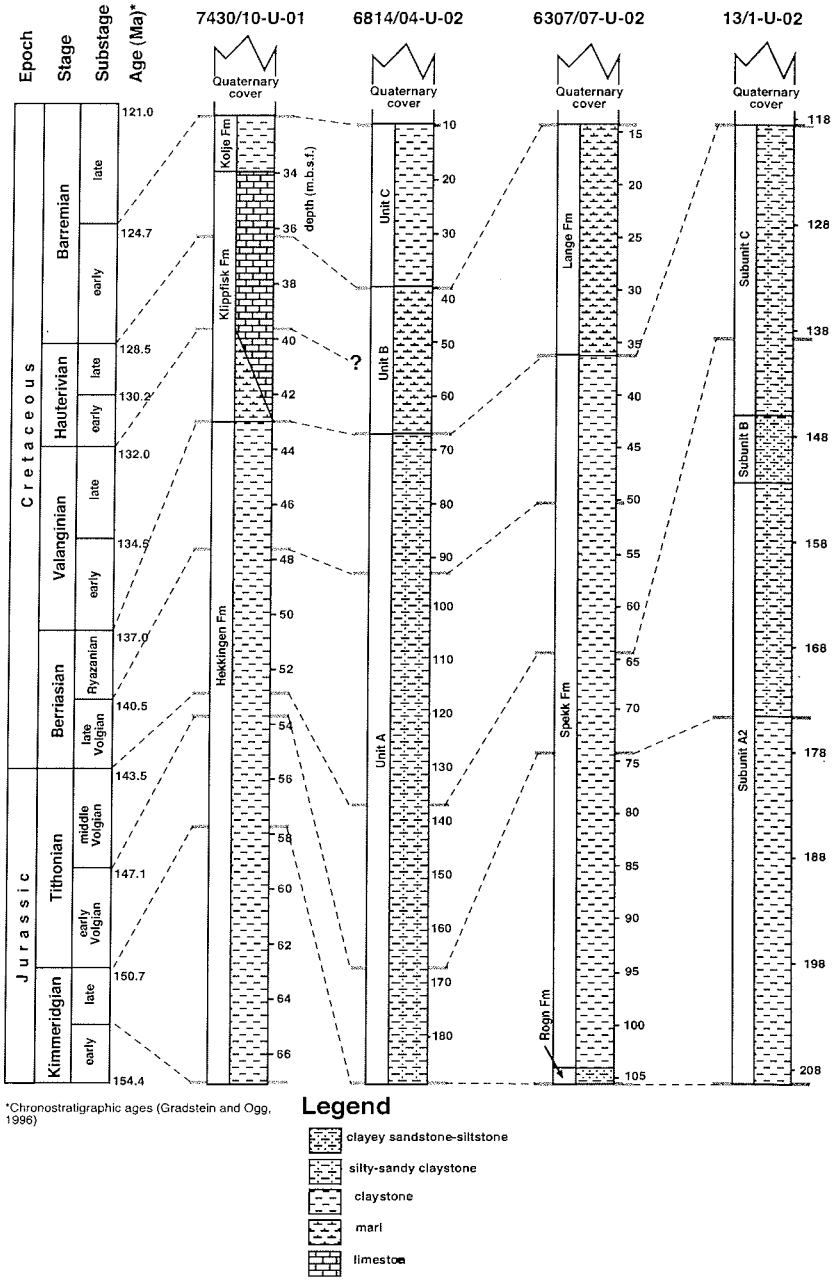

Fig. 1-5 General overview of stratigraphic range, lithological thickness and formation boundaries of the cores investigated (modified after Mutterlose et al.,2003).

1.6. Material and methods

1.6.1. Sampling

In total 648 samples were investigated from four cored sections taken along the Norwegian continental shelf, from the Skagerrak north into the western Barents Sea. A general overview of the sampling and processing is given in Figure 1-6.

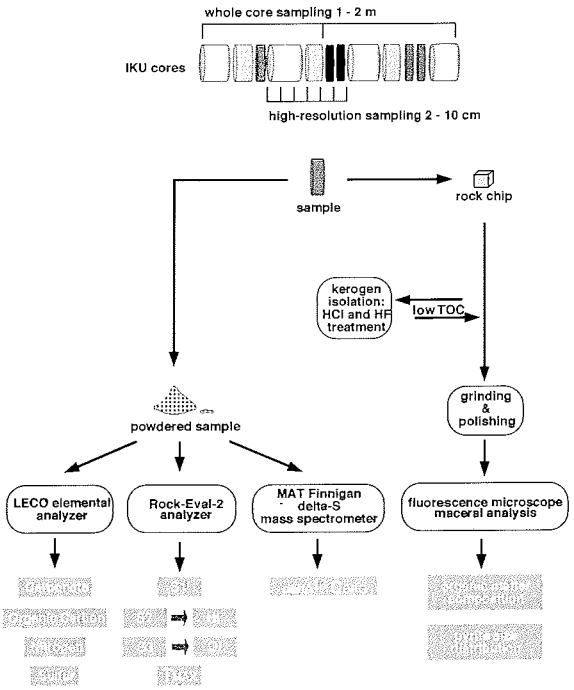

Fig. 1-6 Sample treatment scheme and methods applied

The cores were initially collected and described by Sintef Petroleum Research in Trondheim, Norway (former IKU) in the course of several shallow-drilling projects carried out from 1985 to 1991 [Fjerdingstad et al., 1985; Århus et al., 1987; Skarbø et al., 1988; Rokoengen et al., 1988; Bugge et al., 1989; Lippard and Rokoengen, 1989; Hansen, et al., 1991; Leith et al., 1992; Smelror et al., 1994, 1998, 2001]. Locations including grid references and paleolatitudes are summarized in Table 1-1. In a first approach we sampled the cores at an

irregular spacing of about 1.5 to 2.0 m, depending on availability and condition of the material. Assuming a mean sedimentation rate of 0.5 cm/1000 years (Table 1.2), this would represent a time interval of about 300 – 400 ky allowing detection of long-term trends. In a second approach, high-resolution analysis was applied to the organic-rich sequences of core 6307/07-U-02, 6814/04-U-02, and 7430/10-U-01 close to the Jurassic-Cretaceous boundary (Fig. 1-5, 5-1). We sampled a few meters of each core at an interval of 2 and 10 cm, so obtaining a time resolution of about 2 to 20 ky. With this it was possible to detect depositional changes at a relatively small scale, permitting recognition of obliquity and eccentricity cycles.

1.6.2. Elemental analysis

Total carbon (TC), total nitrogen (TN) and total sulfur (TS) contents were analyzed on homogenized samples using a LECO CNS-2000 and CS-400 elemental analyzer. The organic carbon content (TOC) was determined with a LECO CS-125 elemental analyzer after carbonate was removed from the samples using 12% hydrochloric acid. The carbonate content was determined by inorganic CaO measurements with a CM-5012-CO_2 coulometer and expressed as $CaCO_3$ [cf. Lipinski et al., 2003]. To evaluate the reproducibility of carbon and organic carbon data duplicates were measured routinely.

1.6.3. Rock-Eval pyrolysis

Rock-Eval pyrolysis of whole rock samples [cf. Espitalié et al., 1977; Peters, 1986] was performed with a Rock-Eval II unit. This method is used to rapidly evaluate the quantity, quality, petroleum-generative potential, and thermally maturity of the associated organic matter (OM). The pulverized samples are gradually heated in an oxygen-free helium atmosphere up to 550°C. In the first stage easy-to-liberate hydrocarbons are measured with a flame-ionization-

detector (FID) at 300°C (constant for 3 to 4 minutes) and are expressed as the S1 peak in milligrams of hydrocarbons in one gram of rock. The more complex kerogens are cracked during a programmed pyrolysis to 550°C at a rate of 25°C/min and deliver the S2 peak in milligrams of hydrocarbons in one gram of rock. The third peak (S3) represents the milligrams of CO_2 generated during the interval of 300°C to 390°C and are released from a molecular sieve after S2 detection is completed. The Hydrogen Index (HI) corresponds to the quantity of pyrolizable hydrocarbons relative to the total organic carbon (TOC) and the oxygen index (OI) corresponds to the carbon dioxide liberated relative to the total organic carbon and are expressed as:

Hydrogen Index (HI) = (S2 * 100)/TOC in [mg HC/g TOC]
Oxygen Index (OI) = (S3 x 100) / TOC in [mg CO_2/g TOC]

These parameters were adapted to the Van Krevelen-diagram and used to estimate the type I – IV kerogens (Espitalié et al., 1977; Peters, 1986) and the source of the organic matter (marine vs. terrigenous). The interpretation of the results provides different problems of which one is the "mineral matrix effect" that influences argillaceous (clay-rich) rocks containing less than 0.5 wt. % TOC [e.g. Peters, 1986]. Here, the HI is likely to be too low and T_{MAX} to high because the pyrolytic organic compounds can be easily adsorbed by clay minerals, especially illite and montmorillonite [Espitalié et al., 1980]. It is therefore important to interpret Rock-Eval results under consideration of organic carbon content and sedimentary facies.

1.6.4. Alternative kerogen typing

The S2/TOC relationship is used as an alternative way to estimate different kerogen types, without interference by mineral matrix effects. The diagram is limited to display type I to III kerogen, because type IV kerogen does not contain any S2 hydrocarbons. However, the intersection of the data point series

with the TOC axis indicates the amount of "dead" organic carbon, which is in fact type IV kerogen [e.g. Lüniger and Schwark, 2001]. An example of a S2/TOC diagram is presented in Figure 1-7. The fields of kerogen types are separated by lines of a constant S2/TOC ratio, equivalent to a discrete HI value (HI = S2/TOC * 100).

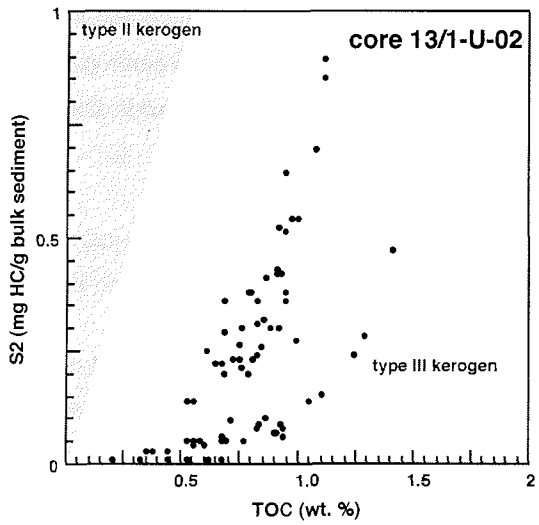

Figure 1-7 S2 against TOC diagram to determine kerogen types of the OM avoiding mineral matrix effects. Good correlation indicates that the TOC is primarily controlled by preservation and terrestrial/marine OM mixing (e.g. Langford and Blanc-Valleron, 1990, Horsfield et al., 1994; Lüniger and Schwark, 2002; Tribovillard et al., 2001). Intersection with TOC indicates the percentage of „dead" organic carbon, such as inertinite (e.g. Cornford et al., 1998).

A high correlation coefficient (r^2) within a set of S2 and TOC values, not to be confused with a high S2/TOC ratio (= HI), is considered to indicate that TOC accumulation is primarily controlled by selected preservation [Horsfield et al., 1994], e.g. oxic to anoxic changes.

1.6.5. Maceral analysis

For a detailed study of the composition of the organic matter (OM) a qualitative and quantitative microscopic determination of the organic particles (macerals)

has been employed on selected samples. For this purpose small blocks of rock were embedded in a 30 mm latex crucible with liquid epoxy resin and hardened for 48 hours at 30°C. Some samples were additionally orientated parallel to the bedding to detect particles, which appear very flat due to compaction in the vertical profile. Samples were then gradually ground with 600, 800 and 1200 abrasive powder and finally polished with 9μm, 3μm and 1μm diamond paste and 0.05 μm Al_2O_3 paste on an automatic polish-grinding unit. Observation was performed on a ZEISS Axioscop using reflected white light and fluorescence light with blue light irradiation. Standard oil immersion objectives of 20x and 50x magnification and oculars of 10-fold magnification were used. All photographs were taken with a ZEISS AxioCam digital (fluorescence-) color video camera. We usually distinguish between three maceral groups: vitrinite, inertinite and liptinite (formerly exinite). The groups are subdivided into individual macerals, e.g. telinite, cutinite, alginite or fusinite, representing different biological precursors from land or water and were determined according to the classification of Taylor et al. (1998). We differentiate between particulate organic matter (POM), which was quantified by point counting and unstructured, amorphous organic matter (bituminite), which was obtained by estimating the area volume percentages. Four statistical accuracy at least 300 macerals were counted on each sample using a 25-point cross-hair ocular.

1.6.6. Carbon isotope analysis

Different fractionation of ^{12}C and ^{13}C stable isotopes is a crucial geochemical characteristic of all organisms. In general, the marine biomass utilizes oceanic HCO_3^- and produces organic carbon that is enriched in ^{13}C, whereas the terrestrial biomass utilizes atmospheric CO_2 by the C3 pathway, producing organic carbon that is depleted in ^{13}C [e.g. Waples, 1981; Arthur et al., 1985; Müller et al., 1994; Meyers, 1997]. Based on the international Vienna PDB standard [see Coplen, 1995] variations in the isotopic signature ($\delta^{13}C$) appear to be a useful tool for estimating the sources of organic carbon in marine

sediments. However, a major problem in the present work is that isotopic fractionation in the Mesozoic appears to be substantially different from recent sediments [Arthur et al., 1985; Rau et al., 1987; Dean and Arthur, 1999; Hofmann et al., 2000; Sælen et al, 2000; Langrock et al., 2003b]. For example, organic carbon derived from marine phytoplankton of Cretaceous and older rocks is relatively depleted in ^{13}C, which results in a shift of 5 to 7‰ to more negative $\delta^{13}C_{ORG}$ values than marine organic carbon in Holocene sediments. The reason for this phenomenon, however, is still controversial and it is suggested that photosynthetic ^{13}C fractionation of marine phytoplankton was more extensive in the Mesozoic than today [Arthur et al., 1985]. This was probably a consequence of the increased atmospheric CO_2 partial pressure, which was six to eight times higher in the Cenomanian and Turonian than today [e.g. Larson, 1991]. On the other hand, it is unlikely that diagenesis had a great effect, because it did not produce a significant shift of $\delta^{13}C_{ORG}$ in Miocene to Holocene sediments, and so probably did not during the Cretaceous [Dean et al., 1986]. The strange isotopic "behavior" is most clearly reflected when $\delta^{13}C_{ORG}$ values are plotted against the Hydrogen Index (HI), obtained from Rock-Eval pyrolysis. Langrock et al. (2003b) (chapter 3) demonstrated this "abnormal" relationship between more positive $\delta^{13}C_{ORG}$ and low HI values, and more negative $\delta^{13}C_{ORG}$ and high HI values. As a consequence, organic petrography was applied and revealed that more negative $\delta^{13}C_{ORG}$ values indicate organic matter was derived from marine-aquatic sources, and more positive $\delta^{13}C_{ORG}$ values indicate organic matter was derived from terrestrial sources. In general, and particularly in late Mesozoic sediments, $\delta^{13}C_{ORG}$ data may be inconsistent and produce contradictory results when used independently.

1.6.7. Application of C/N ratios

The C/N ratio can be used to estimate the relative proportions of terrestrial and marine organic matter, because different groups of organisms contain different organic carbon and nitrogen contents (Meyers, 1997, and references therein). The average C/N ratio for most lower plants, marine animals, and bacteria is

less than about 10, whereas higher plants, such as *Zostera* (aquatic grass) and deciduous trees, are characterized by C/N ratios of more than 15 and 25, respectively (e.g. Scheffer and Schachtschabel, 1984). However, the application has some constraints because the ratio, which is supposed to be C_{ORG}/N_{ORG}, is usually measured and given as C_{ORG}/N_{TOT}. It must be considered that in organic carbon-poor sediments the inorganic nitrogen fixed in clay minerals becomes a major portion of the total nitrogen content [Stein et al., 1994; Schubert, 1995], resulting in low C_{ORG}/N_{TOT} ratios. For this purpose N_{ORG} content was determined by two separate measurements in a LECO CN-2000 elemental analyzer after the organic fraction was removed by combustion in one set of samples.

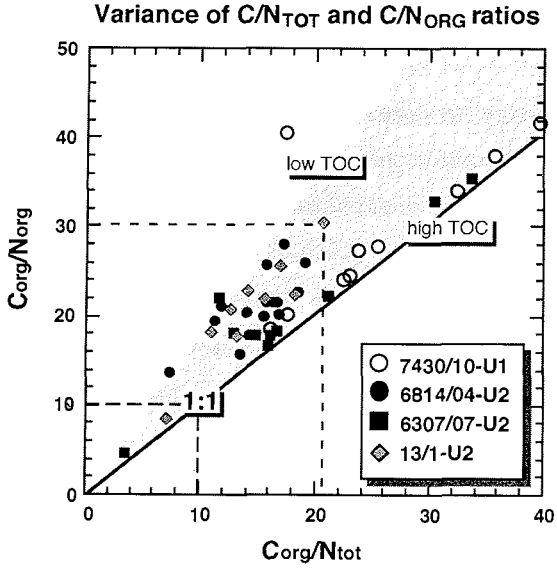

Fig. 1-8 Differences between C_{ORG}/N_{TOT} and C_{ORG}/N_{ORG} ratios. Increasing difference from the equation line indicates a higher amount of inorganic nitrogen, e.g. from clay minerals. The samples with the higher amount of inorganic nitrogen have lower organic carbon contents. If the increasing amount of clay minerals represents a higher sediment input this may suggest a dilution effect. Moreover, this effect appears more severe in core 13/1-U-02 (more oxic environment) and less severe in core 7430/10-U-01 (anoxic

This is particularly reflected by the sediments of the present work, showing that C_{ORG}/N_{ORG} ratios are much higher compared to C_{ORG}/N_{TOT} ratios in samples with low TOC content than in samples with moderate, or high TOC content (Fig. 1-8). As a result, a sample (1.2 % by weight TOC) with a C_{ORG}/N_{TOT} ratio of 21 will have a true C_{ORG}/N_{ORG} ratio of 30 when using organic instead of total nitrogen (center, dashed line). On the other hand, a high C_{ORG}/N_{TOT} ratio may be

generated due to increased marine productivity, because nitrogen compounds are preferably utilized in the water

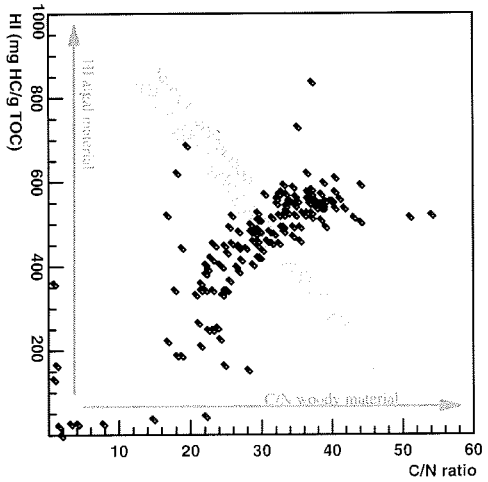

Fig. 1-9 High positive correlation between C/N ratio and HI of core 7430/10-U-01, suggesting that high C_{ORG}/N_{TOT} ratios do not reflect terrigenous input, but an increased preservation of lipid-rich OM by accelerated anoxia.

column, especially in upwelling areas. In restricted environments, such as anoxic basins or lakes, the C_{ORG}/N_{TOT} ratio is reported to be inconsistent, or even inverted. In the absence of oxygen bacterial utilization of nitrogen may be strongly enhanced, decreasing the C_{ORG}/N_{TOT} ratio [Lüniger and Schwark, 2002; Twichell et al., 2002; Langrock et al., 2003a,b]. As a result, most sediments investigated in the present study show a positive correlation between C/N ratios and the amount of hydrogen-rich organic matter derived largely from marine-aquatic sources (Fig. 1-9).

1.7. Individual Studies

The following three chapters report on different aspects of the present study. Each chapter represents a paper, which is already published or pending for publication in a peer-reviewing international journal. The following paragraphs give a brief overview of each paper. For convenience, references were removed from these chapters and included into the main reference list at the end of the present work – chapter 7.

In Chapter 2 "Paleoenvironment and sea-level change in the early Cretaceous Barents Sea – implications from near-shore marine sapropels" the depositional environment and long-term paleoceanographic changes of the late Jurassic Hekkingen Formation from the central Barents Sea were approached by detailed geochemical and organic-petrographic investigation. These exceptionally organic carbon-rich sapropelic shales have likely formed in a stratified epicontinental basin with an almost completely anoxic water column and display very good petroleum generative potential. Detailed maceral analysis indicates proximity to land in the central Barents Sea during this time and a continuous sea-level rise through the late Volgian. No evidence was found that the Mjølnir meteorite hit the Barents Sea before the top of our investigated sequence.

In Chapter 3 "Late Jurassic to early Cretaceous black shale formation and paleoenvironment in high northern latitudes – examples from the Norwegian-Greenland Seaway" a combination of organic petrography and organic- and inorganic-geochemical analysis was applied to investigate changes in the accumulation of organic carbon-rich sediments from low to high northern paleolatitudes. Three examples from the Norwegian-Greenland-Seaway reflect the heterogeneity of black shale formation, its different controls, and its sensitivity to long-term sea-level changes, which eventually lead to its successive termination. Stable isotope analysis of organic carbon confirmed earlier observations on late Mesozoic sediments with respect to the opposite signals of the marine and terrestrial biomass relative to Recent sediments.

In Chapter 4 "Origin of marine petroleum source rocks from the Late Jurassic to Early Cretaceous Norwegian Greenland Seaway – evidence for stagnation and upwelling" origin, accumulation and preservation of potential petroleum source rocks from the Hitra Basin (southern Trøndelag Platform) and the Ribban Basin (west of the Lofoten ridge) were investigated based on a detailed petrographic examination. Common proxies were combined with results obtained from

geochemical and sedimentological studies to gain new insights in the fate of the organic matter in the nascent Norwegian Sea and its potential for generating petroleum. Due to recent progress in sedimentation rate estimates, accumulation rates and paleoproductivities of organic carbon were calculated. Results were surprisingly clear and suggested that black shale formation followed largely two opposite depositional models, e.g. the "stagnation model" and the "productivity model".

CHAPTER 2 Geo-Marine Letters 23, Vol.1, 2003, 34-42, DOI 10.1007/s00367-003-0122-5

Paleoenvironment and sea level change in the early Cretaceous Barents Sea – implications from near-shore marine sapropels

U. Langrock[1], R. Stein[1], M. Lipinski[2], and H.-J. Brumsack[2]

[1]Alfred Wegener Institute for Polar and Marine Research, Department of Geosciences, Columbusstrasse, 27568 Bremerhaven, Germany

[2]Institute for Chemistry and Biology of the Marine Environments (ICBM), Carl von Ossietzky University, 26111 Oldenburg, Germany

Received: 13 August 2002, Accepted: 20. January 2003; Published: 3. April 2003

Abstract

The late Volgian (early "Boreal" Berriasian) sapropels of the Hekkingen Formation of the central Barents Sea show total organic carbon (TOC) contents from 3 to 36 wt%. The relationship between TOC content and sedimentation rate (SR), and high Mo/Al ratios indicate deposition under oxygen-free bottom water conditions, and suggests that preservation under anoxic conditions has largely contributed to the high accumulation of organic carbon. Hydrogen index values obtained from Rock-Eval pyrolysis are exceptionally high, and the organic matter is characterized by well-preserved type II kerogen. However, the occurrence of spores, freshwater algae, coal fragments, and charred land-plant remains strongly suggest proximity to land. Short-term oscillation probably reflecting Milankovitch-type cyclicity are superimposed on the long-term trend of constantly changing depositional conditions during most of the late Volgian. Progressively smaller amounts of terrestrial organic matter and larger amounts of marine organic matter upwards in the section may have been caused by a continuous sea-level rise.

2.1. Introduction

The late Jurassic – early Cretaceous time interval is characterized by low North Atlantic spreading rates, which resulted in a relative sea-level low-stand. This increased the prominence of shallow marine basins along the continental shelf, thereby promoting the development of restricted depositional environments, and favored the accumulation and preservation of organic matter. As a result, dark-colored organic carbon-rich sediments, so-called black shales, occurred widely during this period, e.g. in the marginal seas of the North Atlantic (e.g. Schlanger and Jenkyns 1976; Stein 1986; De Graciansky et al. 1987), along the Norwegian-Greenland-Seaway (e.g. Doré et al. 1991; Smelror et al. 2001b; Mutterlose et al. in press), and in the adjacent Barents Sea (e.g. Bugge et al. 1989; Bugge et al. 2002). The formation of black shales is often attributed to "oceanic anoxic events" (OEAs) on a global scale, e.g. during the Cenomanian/Turonian, which is characterized by a relatively high sea-level stand (e.g. Arthur et al. 1987; Erbacher et al. 2001). The Cretaceous Barents Sea was located in a high paleo-latitude realm (e.g. Haq et al. 1988; Hardenbol et al. 1998; Street and Brown 2000) and was dominated by fine-grained clastic sediments with thick black shales sequences (e.g. Worsley et al. 1988; Ziegler 1988). Some of these shallow marine black shales have received much commercial attention in the past because of their high petroleum source rock potential (e.g. Johansen et al. 1990; Larsen et al. 1990; Leith et al. 1990). Much of the scientific interest in these sequences was also raised by the Mjølnir meteorite (e.g. Gudlaugsson 1993; Dypvik et al. 1996), which impacted the paleo-Barents Sea close to the Volgian – Ryazanian (early/late Berriasian) boundary 142 ± 2.6 Ma ago (e.g. Smelror et al. 2001b). Core 7430/10-U-01 is located only 30 kilometers off the outer rim of the impact crater, and comprises the late Kimmeridgian to early Ryazanian Hekkingen Formation (e.g. Worsley et al. 1988; Bugge et al. 1989; Århus et al. 1990), of which the late Volgian sequence (Fig. 2-2a for age control) shows an exceptional suite of organic carbon-rich laminated black shales, which are actually marine sapropels. The section from 47.65 to 46.85 meters below seafloor (m.b.s.f.) forms the so-called

"ejecta-unit" assigned to the meteorite impact (e.g. Dypvik et al. 1996), but there are new indications, which suggest that the impact may have occurred earlier, probably below 50 m.b.s.f. (Smelror et al. 2001b).

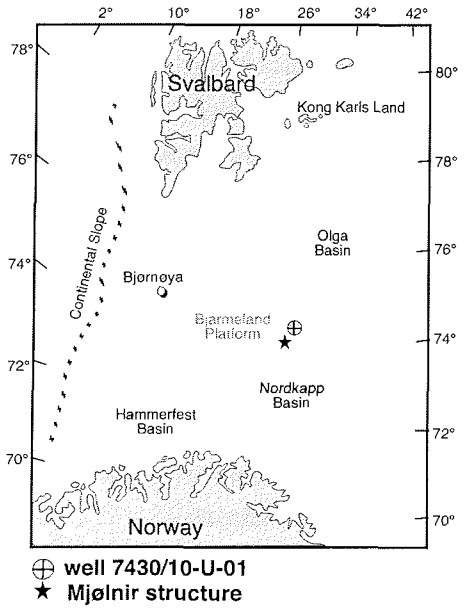

Figure 2-1
Location of IKU well 7430/10-U 01 on the Bjarmeland Platform in the western central Barents Sea (335 m water depth)

To obtain information about the origin of the late Volgian sapropels of core 7430/10-U-01 and their relation to paleoenvironmental and sea-level changes, as well as their possible relation to the Mjølnir meteorite impact, a detailed organic geochemical and microscopic study has been performed.

2.2. Material and Methods

Geochemical and microscopic investigations were carried out on selected samples from the organic carbon-rich Hekkingen Formation of core 7430/10-U-01. The core was taken at 74° 13´ N and 30° 14´ E on the Bjarmeland Platform in the central Barents Sea north of the Nordkap Basin (Fig. 2-1) in a water depth of 335 m, and penetrated 57.10 m of late Jurassic to early Cretaceous bedrock. The drilling was performed by Sintef Petroleum Research Norway (former IKU)

in the year 1989. Total carbon (TC), total organic carbon (TOC), total nitrogen (TN), and total sulfur (TS) were measured on 148 samples after combustion using LECO CS-240 and CNS-2000 elemental analyzers, including 126 samples of a high-resolution section from 51 to 49 m.b.s.f. TOC was measured on a LECO CS-400 after carbonate was removed with hydrochloric acid. All TOC results were re-checked by CaO (total inorganic carbon TIC) determination on a CM-5012 CO2 coulometer (e.g. Engleman et al. 1985) using the equation TOC = TC – TIC. Estimates for quantity, quality, and maturity of the organic matter were drawn from hydrogen index (HI) values, oxygen index (OI) values, S2 values, and T_{MAX} values obtained from Rock-Eval pyrolysis (cf. Espitalié et al. 1977; Peters 1986). HI and OI signatures allow a rough distinction between algal/marine (types I and II kerogen) and woody/terrestrial (types III and IV kerogen) organic matter. Properties of the particulate organic matter, such as type, abundance and degree of preservation, can provide most valuable information about sources (marine, lacustrine, or terrigenous) and conditions under which the OM was deposited (oxic, dysoxic, or anoxic).

For a more detailed qualitative and quantitative determination of the particulate organic matter, a petrographic analysis on 15 selected whole rock samples was conducted by reflected light microscopy using white and fluorescent light. For statistical accuracy at least 300 macerals were counted in each sample using a 25-point crosshair grid. We can generally distinguish between terrestrial (vitrinite, vitrodetrinite, inertinite, sporinite, and resinite) and marine/aquatic macerals (alginite, liptodetrinite, and acritarchs/dinocysts) following largely the nomenclature described in Taylor et al. (1998). For example, vitrinite and inertinite are derived from relatively hydrogen-poor (woody) land plant remains, whereas sporinite is a collective term for spores and pollen, which, although originating from terrestrial sources, may contribute to a relatively nitrogen- and hydrogen-rich sediment. Resinite is a product of waxy, fatty, or oily substances, which also originates from land plants. Alginite, on the other hand, may be differentiated in marine (e.g. marine prasinophytes), more cosmopolitan (e.g. dinocysts and acritarchs), or freshwater genera (e.g. *Botryococcus*), which commonly produce hydrogen-rich types I and II kerogens.

Particles that are smaller than 5 - 10 μm are given the suffix "detrinite", but it is often hard to specify their origin.

In addition to the organic matter, all major and trace elements were determined by XRF and/or ICP-MS analysis (see Mutterlose et al. in press), but in this paper only Mo/Al ratios were used to indicate bottom-water anoxia. To support this, pyrite size distribution is used for evaluating bottom-water redox conditions in ancient sedimentary rocks (e.g. Wilkin et al. 1996, 1997). Framboidal pyrite in sediments of modern anoxic basins, e.g. the Black Sea, is typically smaller and less variable in size than those in sediments underlying an oxic or dysoxic water column. A semi-quantitative analysis on five samples was carried out under the microscope to determine the proportion of framboidal pyrite in the total amount of pyrite, and its size distribution.

2.3. Results

The Hekkingen Formation core has TOC contents that vary widely from 5 to more than 20 wt% with a prominent maximum of 36 wt% at about 50 m.b.s.f. (Fig. 2-2a). There is a continuous increase towards this maximum, followed by a similar decrease (Fig. 2-2b). The late Volgian – early Ryazanian section (51 – 49 m.b.s.f.) was investigated in greater detail by high-resolution analyses (118 of the total 144 samples) to elucidate what may have caused and controlled the dramatic increase in organic carbon enrichment and preservation. To obtain information about the type of organic matter, several independent parameters were considered including C/N ratios, HI and OI values, and especially, maceral composition.

Results of TOC content, Rock-Eval S2 and HI values, C/N and Mo/Al ratios are compiled in Figure 2-2b, and all show a high positive correlation. C/N ratios range from 20 to 50, which would commonly indicate a strong terrestrial signal in the case of modern sediments (see below). Mo/Al ratios are very high (10 – 40 x 10^{-4}) compared to average shale (e.g. Wedepohl 1970), and approach maximum values of 120 x 10^{-4} where all parameters reveal their maximum. HI

values of 400 – 600 mg HC/g TOC and low OI values (≤ 20 mg CO_2/g TOC) were plotted as a van Krevelen-type diagram (Fig. 2-3), which indicates predominantly types I and II kerogen with a very good source rock potential for oil (cf. Espitalié et al. 1977; Peters 1986). Thermal immaturity of the organic matter is evident in T_{MAX} values of 410 – 430°C (Langrock and Stein 2001; Mutterlose et al., 2003).

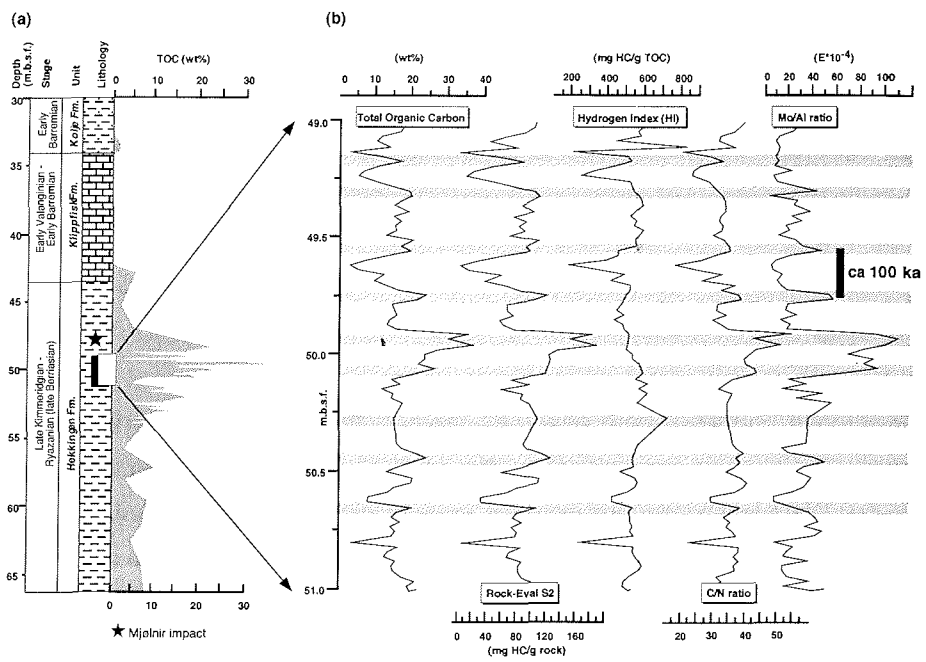

Figure 2-2 (a) Core depth, stratigraphic correlation (e.g. Gradstein et al. 1998; Smelror et al. 1998), lithology and regional formational limits of core 7430/10-U-01 showing TOC contents of the whole core, and a high-resolution sequence (extracted box). (b) High-resolution section from 51 to 49 m.b.s.f. showing down-core variations in TOC content, Rock-Eval S2 and HI values, and C/N and Mo/Al ratios. Maximum peaks are highlighted by shaded lines. Spacing between peaks may represent app. 100 ka, revealing changing sedimentation rates (based on 0.2 cm/per 1000 years).

The maceral compositions of the sediments are dominated by lipid-rich organic matter derived from different marine/aquatic sources (Fig. 2-4), supporting the type II kerogen characterization by Rock-Eval pyrolysis. Massive occurrences of well-preserved marine Prasinophycean algae (mainly *Leiosphaeridia*), minor abundance of juvenile *Botryococcus*-type algae (freshwater), a few *Tasmanites*-type algae (brackish), and *Reinschia*-type algae (freshwater puddle), as well as

a few low-diverse dinocysts (or acritarchs) were recorded at various depths. The terrigenous organic matter is mainly composed of terrestrial liptinite (sporinite, and resinite), which may also contribute to the high HI values.

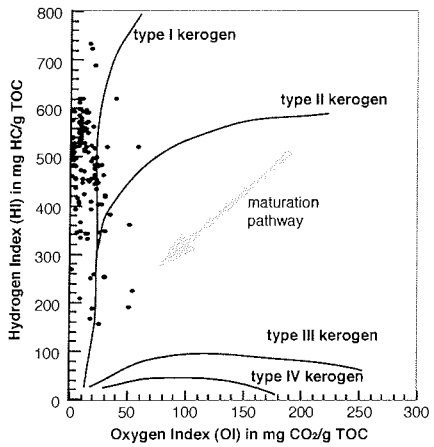

Figure 2-3 Rock-Eval van Krevelen-type diagram shows dominantly type I and II kerogen, which may represent algal/marine OM of different preservation, or a mixture of fresh algal/marine and lipid-rich terrigenous OM (e.g. spores, resins).

Inertinite, vitrinite, and clasts of bituminous coal are less abundant. However, vitrinite and inertinite particles are occasionally up to 150 μm in length and well preserved. Most inertinite may be derived from charred plants (fusinites), and fungal spores (funginite). We particularly observed a continuous upward decrease of inertinite plus sporinite (which seem to be closely related in this case) along with an increase of marine-derived alginites (from about 60 % at 52 m.b.s.f. to more than 95 % at 50 m.b.s.f.). The amount of vitrinite and vitrodetrinite does not exceed 5 % and remains relatively stable throughout this sequence. A vast abundance (up to 15 vol% of the sediment) of small-sized pyrite framboids appeared with diameters of 4 to 5 μm, implicating small absolute sizes, and a low size variability. In Fig. 2-2b the maximum peaks of all values appear in a more or less regular interval (shaded bars), which probably reflect a cyclicity. Based on a mean sedimentation rate of about 0.2 cm/1000 years for the late Volgian (Smelror et al. 1998, 2001; Mutterlose et al. 2003) this frequency may represent the 100 ky orbital Milankovitch cycle. The different

thickness of the intervals may then be a result of little variations in the sedimentation rate.

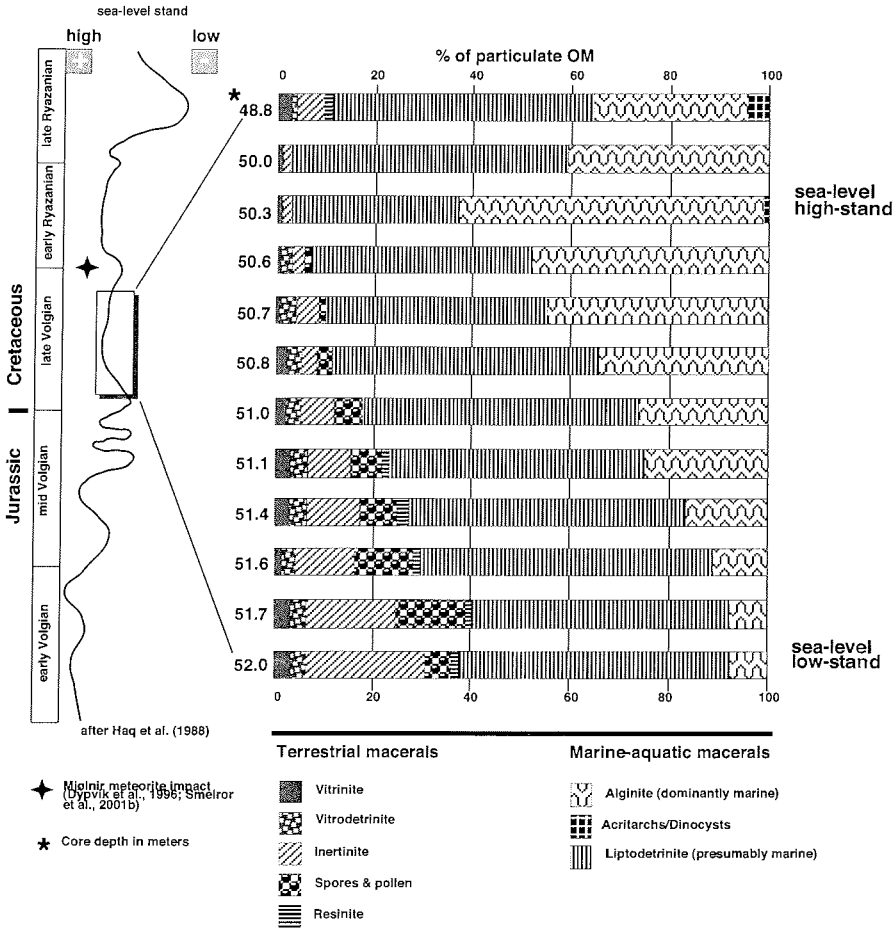

Figure 2-4 Organic matter composition based on maceral analysis results against depth (note this section ranges from 52 to 49 m.b.s.f.), and the correlation to the global sea-level curve suggested by Haq et al. (1988).

2.4. Discussion and conclusions

2.4.1. Depositional conditions

The causes for the deposition of organic carbon-rich sediments in Cretaceous marine environments have been controversial for a long time. Several authors favor basin-wide to global "stagnation" of deep waters, e.g. deep basins with reduced vertical circulation that inhibits a renewal of water masses (e.g. Brumsack 1980, 1988; De Graciansky et al 1987). Others explain the occurrence of these black shales by an increased oceanic "productivity" that may lead to the formation of oxygen minimum layers, which impinge on the seafloor (e.g. Schlanger and Jenkyns 1976). Furthermore, increased supply of terrigenous organic matter seems to be an important mechanism for the enrichment of organic carbon in some Mesozoic sediments (e.g. Stein et al. 1986, Stein 1991). However, contents of lipid-rich organic carbon in the sedimentary record as high as 36 wt% can hardly be explained without invoking a combination of elevated primary productivity, improved organic matter preservation, and limited dilution by clastic material from the continents.

The dark, laminated, and non-bioturbated sequence of core 7430/10-U-01 indicates a lack of benthic life and the absence of bottom-water oxygen, which inhibits a major part of the whole organic matter remineralization process that occurs at the sediment surface. In addition, the high amount of uniformly small framboidal pyrite suggests that pyrite was almost exclusively formed within the water column. Consequently, not only the sediments surface but at least part of the water column was (at least frequently) anoxic, which may have enhanced OM preservation. This situation is also reflected by high TOC and HI values, and the abundance of well preserved autochthonous algal organic matter. The extraordinarily high Mo/Al ratios suggest that anoxic conditions extended beyond the sediment surface (e.g. Brumsack 1980, 1988; Mutterlose et al. in press). The expansion of anoxia in the water column due to fluctuations in sea level and surface productivity may also lead to mass extinctions (e.g. Hallam

and Wignall 1999), not only of primary producers but also of vast amounts of aerobic bacteria, which contribute to high TOC and HI values.

In recent and sub-recent marine environments, a high C/N ratio is often interpreted as an indicator for terrigenous (woody) organic carbon input (e.g. Stein 1991; Meyers 1997). In our case, however, the high C/N ratios correlate positively with the TOC, HI, and Mo/Al ratios, which are considered as indicators for marine (lipid-rich) OM and anoxia. Positive correlation between high TOC contents, marine organic carbon, and high C/N ratios is also reported from other organic carbon-rich sediments (e.g. Meyers 1997; Twichell et al. 2002), which may reflect enhanced paleoproductivity and/or improved preservation of OM. It is thereby considered that during sinking partial degradation of algal OM may selectively diminish N-rich proteinaceous components, and raises the C/N ratio. This may, of cause, be a direct response to enhanced primary productivity but probably requires greater water depths and a more oxic water column. Also nitrogen can become strongly recycled if the supply of nutrients is limited (e.g. Waples and Sloan 1980), e.g. in isolated stratified basins, which may also raise the C/N ratio.

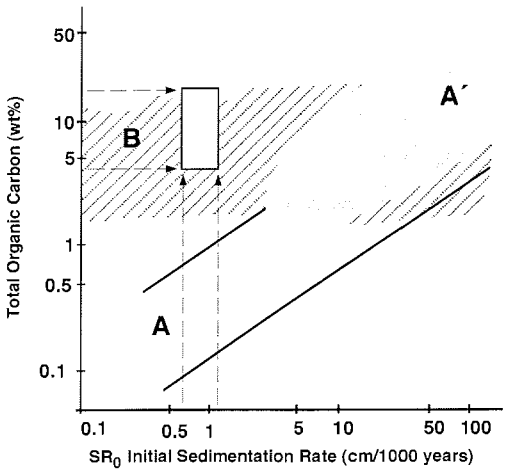

Figure 2-5 TOC/SR relationship shows different fields of depositional conditions for marine sediments (cf. Stein 1990). Field A is characterized by a positive correlation between TOC content and sedimentation rate indicating open oxic deep-water conditions. Field A´ indicates conditions of high oceanic primary productivity. Field B indicates anoxic depositional conditions where no correlation exists between TOC content and sedimentation rate. Sedimentation rates are given as initial (or decompacted) SR_0 (c.f. Stein 1990 for details). The open box represents the field of most likely depositional conditions of the investigated sequence based on minimum/maximum SR_0 values (interpolated, estimated), and minimum/maximum TOC contents (measured).

However, maceral analysis has clearly shown that high C/N ratios do not indicate an increased terrigenous input but instead likely reflect greater OM preservation due to anoxia. Very low sedimentation rates in the late Volgian of core 7430/10-U-01 indicate that clastic dilution is strongly limited and that OM preservation was not controlled by rapid burial. In combination with very high TOC contents deposition in the presence of anoxic bottom water is the most reasonable mechanism rather than under conditions of high primary production (Fig. 2-5) (e.g. Stein 1991). For a high primary productivity system 10 to 50 times higher initial sedimentation rates would be required (according to Fig. 2-5). It is unlikely that such large amounts of carbonate were dissolved in the water column, because the average $CaCO_3$ content is still 10 wt%. It has also to be considered, however, that the age control on these sediments is very difficult, and that a long-term mean sedimentation rate has to be used. It can therefore not be excluded that periods of elevated primary productivity may also have occurred (along with the peak TOC values). This would have favored OM preservation by establishing an oxygen minimum zone (e.g. Arthur et al. 1987) probably extending over the entire water-column (e.g. Sinninghe Damsté and Köster 1998).

2.4.2. Sea-Level Change

In order to evaluate an effect of a global sea-level change on the accumulation of organic carbon the section from 52 – 50 m.b.s.f. was investigated with a detailed microscopic analysis, because it is associated with a continuous change in the OM composition (Fig. 2-4). Over this depth interval a decreasing amount of sporinite plus inertinite is apparent, which strongly suggests an increasing distance from their terrestrial sources (e.g. Littke et al. 1997; Taylor et al. 1998), probably associated with a sea-level rise (Fig. 2-6). Since the base of the investigated sequence (52.00 m.b.s.f.) is assigned to the base of the late Volgian (Smelror et al. 2001b), the change in the OM composition can be correlated with the global sea-level curve postulated by Haq et al. (1988) (Fig.

2-4). The upward-increasing amount of marine/aquatic alginite may reflect an increasing primary production that was promoted by the rising sea level (e.g. Sheridan 1987). Since the primary production is positively correlated with the "anoxia parameters", the variations are probably controlled by an additional preservation signal, probably caused by an expanded oxygen minimum zone. In summary, the remarkably high and increasing OM content in the late Volgian section from the Barents Sea (core 7430/10-U-01) was most likely caused by a combination of increasing preservation by bottom water anoxia, coupled with periods of increasing primary production, as well as a low and decreasing dilution of clastic material, which we relate to a marked rise in sea-level.

2.4.3. Paleogeographic Position

The analysis of the particulate organic matter provides strong evidence for a depositional environment in proximity to the paleo-shore (Fig. 2-6) because high abundance of spores and pollen is typically found in near-shore marine or estuarine environments, and decrease substantially with increasing distance from land (e.g. Littke et al. 1997; Taylor et al. 1998). The occurrence of well-preserved algae (such as *Botryococcus* or *Pila*, *Tasmanites*, and *Reinschia* types) from freshwater and brackish habitats further points towards a near-shore environment. This is due to lipid-rich organic matter is more susceptible to biochemical degradation than, for example, inertinite, and would therefore be less preserved if transported over greater distances (e.g. Littke et al. 1997). Furthermore, clasts of limnic coal facies, such as bog-head coal, show good preservation and suggest short transport ways from their source. In addition, patchy distributed, coarse-grained minerals (apparently quartz) are found as big as 60 to 200 μm in diameter that could not have been transported along with the claystone facies, but by another mechanism. Due to the patchy distribution they might have been transported by episodic events, e.g. storms, but they are too large to be transported far offshore (e.g. Fuechtbauer 1976). However, there is another (though not yet proven) possible mechanism for the input of these

large sand grains – by ice rafting. Episodes of a relatively cool climate were already suggested for the earliest Cretaceous Boreal realm (e.g. Price et al. 2000; Mutterlose et al. in press), and another significant temperature drop was postulated for the Hauterivian Vocontian Basin at 30° N paleo-latitude (e.g. Van de Schootbrugge et al. 2000). Hence, episodic (or even seasonal) IRD input cannot be excluded for the late Volgian Barents Sea, which reveals a paleo-latitude of almost 55° North.

According to previous paleogeographic estimates, the location of core 7430/10-U-01 was at least 300 kilometers away from any coastline during the late Jurassic to early Cretaceous (e.g. Ziegler 1988; Bugge et al. 1989; Dypvik et al. 1996; Smelror et al. 1998). However, our results suggest a much more proximal position below wave base, which is indicated by the origin, the preservation, and the grain size of the organic material.

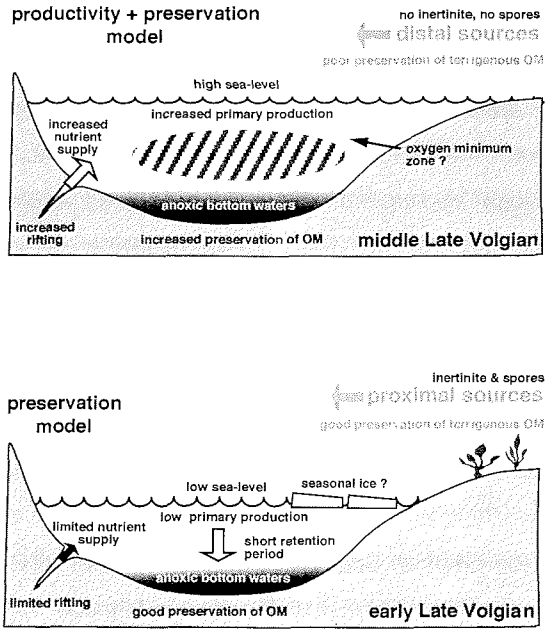

Figure 2-6 Contrasting paleoenvironments and depositional conditions of the upper *Hekkingen Formation* best explained by the "preservation model" during low sea-level (lower Late Volgian) and the "preservation + productivity model" during elevated sea-level (upper Late Volgian).

During the relative sea-level low stand in the early late Volgian Barents Sea, tectonic highs and basin ridges may have emerged as land areas, separating a number of isolated, sediment-starved marine environments as has been suggested for the Norwegian-Greenland-Seaway (e.g. Doré 1991; Brekke et al. 1999). Although such areas may have provided little clastic input by rivers due to their limited sizes, they could have supported spore-producing land plants and freshwater habitats, which eventually became the proximal sources for the organic matter of the upper Hekkingen Formation in the middle of the paleo-Barents Sea.

2.4.4. Influence by the Mjølnir meteorite impact

Our investigation provides a continuous geochemical and microscopic record of the upper Hekkingen Formation, and reveals no evidence for an impact event before 50 m.b.s.f. in core 7430/10-U-01. In view of exceptionally low sedimentation rates, drastic impact and/or post-impact effects caused by an impact of this dimension (see Gudlaugsson 1993; Dypvik et al. 1996) on the paleoenvironment, such as huge amounts of mobilized sediments, mass extinctions (e.g. Tsikalas et al. 1998b), disturbance of water-column stratification, extinction of case-sensitive organic matter sources, etc. would have left distinct marks in the sedimentary record, which we could not detect.

Acknowledgments

Financial support by the German Science Foundation (grant STE 412-13/1) is gratefully acknowledged. Sintef Petroleum Research, Norway, kindly provided access to sensitive core material and unpublished data. We also thank Dr. Tom Wagner (Woodshole Oceanographic Institution) and two anonymous reviewers for their helpful comments to improve this contribution.

CHAPTER 3 *Paleoceanography* 18, Vol. 3, 2003, DOI: 10.1029/2002PA000867

Late Jurassic to Early Cretaceous black shale formation and paleoenvironment in high northern latitudes – examples from the Norwegian Greenland Seaway

U. Langrock[1], R. Stein[1], M. Lipinski[2], and H.-J. Brumsack[2]

[1]Alfred Wegener Institute for Polar and Marine Research, Bremerhaven, Germany
[2]Institute for Chemistry and Biology of the Marine Environment ICBM, Oldenburg, Germany

Received: 25.November 2002 Accepted: 26. February 2003

Abstract

The Late Jurassic to Early Cretaceous (Volgian-Ryazanian) was a period of a second-order sea level low-stand, and it provided excellent conditions for the formation of shallow-marine black shales in the Norwegian-Greenland-Seaway (NGS). IKU drilling cores taken offshore along the Norwegian shelf were investigated with geochemical and microscopic approaches to (1) determine the composition of the organic matter, (2) characterize the depositional environments, and (3) discuss the mechanisms which may have controlled production, accumulation and preservation of the organic matter. The black shale sequences show a wide range of organic carbon contents (0.5 to 7.0 wt. %), and consist of thermally immature organic matter of type II to II/III kerogen. Rock-Eval pyrolysis revealed fair to very good petroleum source rock potential, suggesting a deposition in restricted shallow marine basins. Well developed lamination and the formation of autochthonous pyrite framboids further indicate suboxic to anoxic bottom water conditions. In combination with very low sedimentation rates it seems likely that preservation was the principal control on organic matter accumulation. However, a decrease of organic carbon

preservation and an increase of refractory organic matter from the Volgian to the Hauterivian is superimposed on short-term variations (probably reflecting Milankovitch cycles). Various parameters indicate that black shale formation in the NGS was gradually terminated by increased oxidative conditions in the course of a sea-level rise.

3.1. Introduction

High primary production of coastal waters, a stratified water column, anoxic bottom waters, low influx of clastic material (low dilution), and high supply of terrestrial organic matter may promote the formation of organic carbon-rich sediments (Schlanger and Jenkyns, 1976; Hallam, 1987; Calvert and Pedersen, 1992; Meyers, 1997). Favorable conditions for the formation of argillaceous, organic carbon-rich sedimentary rocks, the so-called black shales, are most known from the mid-Cretaceous where most of our present-day petroleum reserves were generated [e.g. Larson, 1991a,b and references therein]. Widespread formation of black shales is reported from the Aptian/Albian and Cenomanian/Turonian and is associated with "oceanic anoxic events" (OAEs) [e.g. Arthur et al., 1987; Bralower and Thierstein, 1987; Larson, 1991b; Schlanger et al., 1987; Sinninghe Damsté and Köster, 1998]. Two principal models have been under controversial discussion during the past three decades: (1) ocean wide episodes of "stagnation" in restricted stratified basin similar to the Black Sea, and (2) an increased primary production which causes oxygen minimum zones that impinge on the sea floor and thereby limit the remineralization of organic matter on the sea-floor [e.g. Pedersen and Calvert, 1990, Caplan and Bustin, 1999; Saelen et al., 2000; Nijenhuis et al., 2001; Röhl et al., 2001]. An increased supply of terrigenous organic matter may also be an important mechanism for the accumulation of organic carbon in marine sediments [e.g. Stein et al., 1986]. However, many of these studies are derived from the "middle" Cretaceous low-latitudinal North Atlantic where black shale formation is associated with a relatively high sea-level. Because the oil and gas

reservoirs of the North Sea were generated in the late Jurassic much attention has more recently been focussed on the Jurassic-Cretaceous boundary. In contrast to the "middle" Cretaceous the Jurassic-Cretaceous boundary was characterized by very low North Atlantic spreading rates, which caused a second-order sea level low-stand [e.g. Haq et al., 1988] and formed a large number of restricted marine environments [e.g. Ziegler, 1988; Hardenbol et al., 1998].

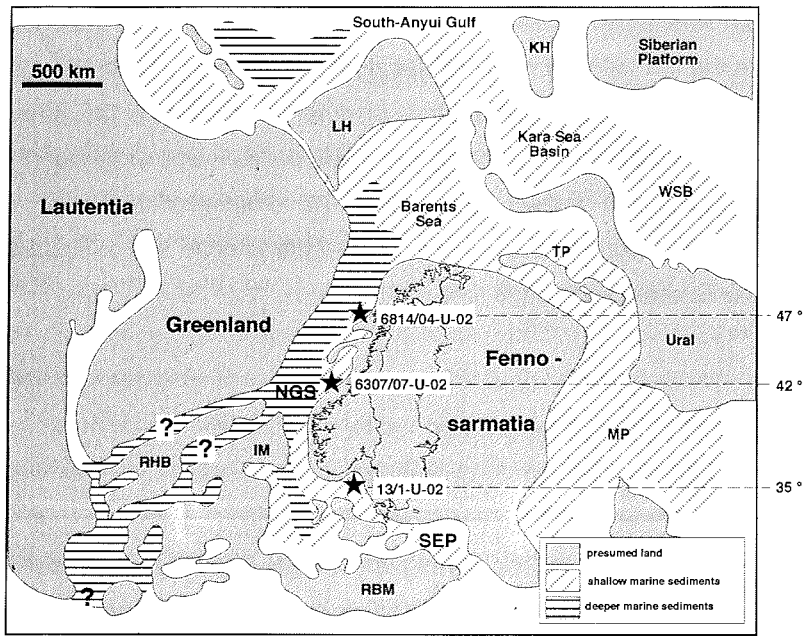

Fig. 3-1 Paleogeographic situation of the Norwegian-Greenland-Seaway and surrounding continental masses in the Ryazanian (middle to late Berriasian) [modified after Ziegler, 1988]. Core locations are shown relative to the modern coast line (outlines of Norway) and indicated by the asterisk. Paleolatitudes are taken from Mutterlose et al. (in press). Abbreviations: IM = Irish Massif, KH = Kara High, LH = Lomonossov High, MP = Moscow Platform, RBM = Rhenish Bohemian Massif, RHB = Rockall-Hatton Bank, TP = Timan Pechora Area, WSB = West Siberian Basin, NGS = Norwegian-Greenland-Seaway, SEP = Southeastern Passage.

During this time the only direct connection between the North Atlantic and the proto-Arctic Ocean was a narrow and shallow-marine passage between Greenland and Fennoscandia, which was more than 1500 km long and only 200 to 300 km wide – the Norwegian-Greenland-Seaway [e.g. Ziegler, 1988; Doré, 1991; Brekike et al., 1999; Hay et al., 1999; Mutterlose et al., 2003] (Fig. 3-1).

The paleogeographic and paleoceanographic situation along the margins of this seaway provided excellent conditions for the formation of black shales, which became eventually petroleum source rocks, e.g. the Hekkingen and Spekk formations exposed along the Norwegian shelf and the adjacent Barents Sea [e.g. Århus et al., 1987; Worsley et al., 1988; Bugge et al., 1989; Århus, 1991; Leith et al., 1992, Smelror et al., 1998, 2001; Mutterlose et al., 2003]. The high petroleum generative potential of these late Jurassic to early Cretaceous sequences is also supported by our data (Table 3-1; cf. Peters, 1986). Therefore, the Norwegian-Greenland-Seaway (NGS) provides rare opportunity to investigate the formation of black shales during times of sea level low-stand and really high northern paleo-latitudes. In order to determine the primary mechanisms that controlled the formation of black shales it was essential (1) to assess the inorganic and organic geochemistry, (2) to determine the origin and preservation of the organic matter, and (3) to characterize the depositional conditions and its changes through time.

3.2. Material and analytical approach

We investigated 257 samples from 3 sediment cores drilled offshore of southern and middle Norway (Fig. 3-1). The cores were initially collected and described by Sintef Petroleum Research (former IKU) during economic shallow-drilling projects in the late 1980s [e.g. Århus et al., 1987; Rokoengen et al., 1988; Bugge et al., 1989; Hansen et al., 1991; Leith et al., 1992]. The southernmost drilling hole 13/1-U-02 is located 57° 48' 42.78" N and 08° 12' 13.97" E in the western Skagerrak about 50 km south of Kristiansand. Hole 6307/07-U-02 is located 63° 27' 54.35" N and 07° 14' 44.26" E in the southern part of the Hitra Basin (off Smøla Island) some 120 km west of Trondheim, and hole 6814/04-U-02 is located 68° 39' 45.80" N and 14° 09' 47.10" E in the northern part of the Ribban Basin (off the Lofoten Islands). We sampled the entire cores with a spacing that represents time intervals of about 100 to 500 ka.

Total carbon (TC), total nitrogen (TN) and total sulfur (TS) contents were analyzed on homogenized samples using a LECO CNS-2000 and CS-400 elemental analyzer. The organic carbon content (TOC) was determined with a LECO CS-125 elemental analyzer after carbonate was removed from the samples by hydrochloric acid. The carbonate content was determined by inorganic CaO measurements with a CM-5012-CO_2 coulometer [e.g. Huffmann, 1977; Engleman et al., 1985] and expressed as $CaCO_3$. To evaluate the reproducibility of carbon and organic carbon data, duplicates were measured routinely. Fe_2O_3, Al_2O_3 [wt%] and Zr [ppm] were measured by XRF analysis using a Philips PW 2400 analyzer. The amount of reactive iron was calculated using the empirical formula $Fe_{reactive}$ = Fe - 0.25 * Al (wt. %). TOC-Fe-S relationships were used to estimate the depositional conditions [e.g. Brumsack, 1988; Dean and Arthur, 1989; Lückge et al., 1996; Hofmann et al., 2000], whereas Zr/Al ratios describe changes of the relative distance to the paleo-shore, because high Zr/Al ratios usually indicate an increased aeolian input and the proximity to the land (e.g. Hinrichs et al., 2001). In normal marine sediments the C/N ratio may improve the differentiation between terrestrial and marine organic matter, where a high ratio indicates a more terrestrial signal (e.g. Meyers, 1997, and references therein). But in modern and ancient sediments, especially under anoxic conditions, C/N ratios are reported to be irrational and non-indicative [e.g. Rau et al., 1987; Lueniger and Schwark, 2002; Twichell et al., 2002]. However, Langrock et al., [2003a] demonstrate that strictly inverse C/N ratios in late Jurassic black shales from the Barents Sea indicate changes in the degree of anoxia.

Stable carbon isotopic composition of bulk sediment organic carbon ($\delta^{13}C_{org}$) was measured on de-carbonated samples from core 6307/07-U2 and 6814/04-U2. Samples were analyzed by high-temperature combustion in a Heraeus CHN elemental analyzer connected to a Finnigan MAT Delta S isotope ratio mass-spectrometer [see Fry et al., 1992] at the Alfred Wegener Institute, Potsdam. The isotopic composition is reported as δ-values [in ‰] relative to the international Vienna PDB standard [Coplen, 1995]. The analytical reproducibility based on replicate analyses was better than ± 0.2 ‰.

Kerogen typing, determination of source rock generative potential and organic matter (OM) maturity were conducted according to Espitalié et al. (1977, 1985) and Peters (1986) using a Rock-Eval II (plus S3 unit). The hydrogen index (HI) was calculated from the amount of pyrolyzable hydrocarbons (S2 value) based on the TOC content, and the oxygen index (OI) was calculated from the amount of associated carbon dioxide (S3 value) based on the TOC content. Indices were used in a HI/OI diagram to estimate kerogen types (I – IV), their potential sources and thermal maturity [cf. Espitalié et al, 1977; Peters, 1986]. The alternative presentation of S2 values against TOC contents is an additional kerogen type determination to avoid mineral matrix effects, and to estimate the amount of "dead" (inert) organic carbon [e.g. Langford and Blanc-Valleron, 1990; Horsfield et al., 1994; Cornford et al., 1998; Lüniger and Schwark, 2002]. However, the kerogen type classification is only a rough estimate that depends on composition, preservation and thermal maturity of the organic matter. Hence, interpretation is difficult without invoking other parameters such as maceral data obtained by petrographic studies.

Consequently, reflected light microscopy was performed on polished blocks of rock and kerogen isolates using a Zeiss Axiophot equipped with normal white and ultraviolet light. The organic matter composition was determined by point-counting maceral analysis following largely the ICCP nomenclature described in Taylor et al. (1998). In general, macerals are divided into three main groups: vitrinite, inertinite and liptinite. Vitrinites (e.g. telinite, vitrodetrinite) are cellulose and lignin-rich remains of land-plants, and they are usually associated with type III kerogen. Inertinites (e.g. semifusinite, funginite) are also derived from various herbaceous sources, but have experienced moderate to severe oxidation, e.g. fusinite is a primary charred plant remain (ash particle). Hence, inertinite behaves virtually "inert" during pyrolysis and usually produces type IV kerogen. Liptinite is a collective term for both terrestrial and marine organic matter that is relatively rich in lipids and proteins with relatively high hydrogen and/or nitrogen contents. Terrestrial liptinite (e.g. sporinite, cutinite) is predominantly derived from land-plant precursors (e.g. pollen, spores, cuticles) and may produce type I/II to II/III kerogen. Marine-aquatic liptinites (e.g. alginite) originate from aquatic

precursors (e.g. freshwater algae, marine dinocysts) and may produce the rare type I kerogen. In this paper we summarized the observed macerals into vitrinite, inertinite, terrigenous liptinite and marine-aquatic liptinite. Particles less than 5 μm in size and small nonspecific fragments were given the suffix detrinite, e.g. liptodetrinite.

To estimate the level of oxygenation in the water column we performed a pyrite size distribution analysis using incident white light [cf. Wilkin et al., 1996, 1997]. We determined the amount and diameters of total pyrite, pyrite framboids, and idiomorphic crystals on 10 representative samples counting at least 100 grains each.

3.3. Lithology and stratigraphy

The Late Jurassic to Early Cretaceous sedimentary successions of the Norwegian-Greenland-Seaway (NGS) were described by several authors [e.g. Århus et al., 1987; Rokoengen et al., 1988; Worsley et al., 1988; Bugge et al., 1989; Lippard and Rokoengen, 1989; Århus, 1991; Leith et al., 1992; Smelror et al., 2001; Mutterlose et al., 2003]. The sediment deposited during the Volgian and Ryazanian is characterized by dark, dominantly laminated and relatively organic carbon-rich claystones and silty claystones. Some of these black shales are also considered as oil shales, e.g. the Spekk Formation and the Hekkingen Formation (Fig. 3-2), because they yield liquid hydrocarbons when artificially matured. However, during the Ryazanian and early Valanginian these facies were gradually succeeded by more and more light-colored, silty and/or calcareous sediments typically associated with a decrease in organic carbon. This calcareous facies is called the Klippfisk Formation, which dominated the northern part of the NGS and the western Barents Sea (e.g. Smelror et al., 1998; Bugge et al., 2002), whereas the time-equivalent Lange Formation dominates the middle NGS. The late Hauterivian (not always documented in the sedimentary record) is usually barren of organic carbon, and signals the end of an approximately 10 Ma episode of black shale formation. These calcareous

open-marine sequences are locally succeeded (usually after a hiatus) by dark claystones or silty claystones of the Barremian Kolje Formation, containing moderate organic carbon contents (Fig. 3-2).

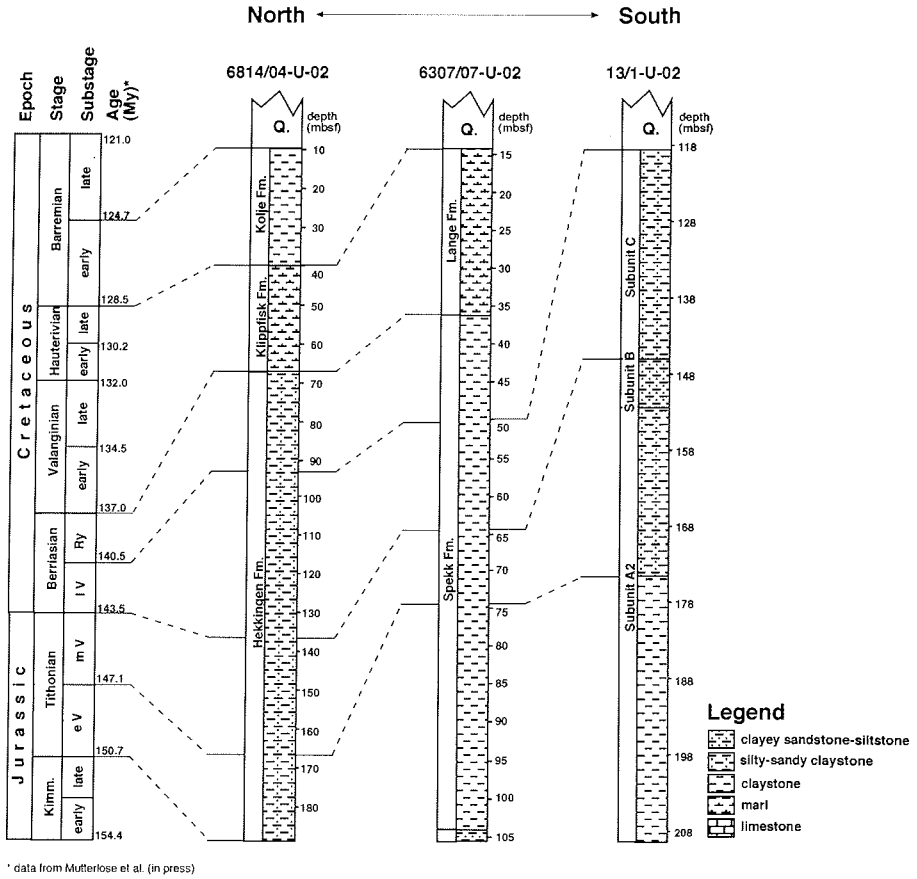

Fig. 3-2 Lithostratigraphic correlation between the investigated cores [after Århus et al., 1987; Rokoengen et al., 1988; Mutterlose et al., in press] using the ages of Hardenbol et al. (1998). The lithological units are also displayed by their regional terminology, usually given fish names, e.g. the *Hekkingen Formation*. Note the differences in sedimentation rate from South to North. (abbreviations: Kimm. = Kimmeridgian, eV = early Volgian, mV = middle Volgian, lV = late Volgian, Ry = Ryazanian)

The investigated cores from the NGS reflect these regional sedimentary patterns, whereas the core from the Skagerrak was selected to represent the Southeastern Passage (SEP) to the Tethys realm.

The problem of stratigraphic control on marine sediments containing thick laminated black shale sequences is the relative scarcity of fossils within these

sequences. Low clastic sedimentation inhibits fast burial and preservation, and allows scavenging. Therefore, a combined investigation on palynomorphs, macrofossils, and foraminifers was performed to gain stratigraphic control [e.g. Hansen et al., 1991; Smelror et al., 1998, 2001b; Mutterlose et al., 2003]. The latter produced a reasonable stratigraphic framework by comparing peaks from spectral analysis (assumed as astronomical sedimentation rates) with linear sedimentation rates obtained from the investigations mentioned above (see Figure 3-2).

3.4. Results

3.4.1. Bulk geochemical parameters

For all three cores, average values of bulk elemental composition and Rock-Eval data according to time intervals are summarized in Table 3-1.

Total organic carbon (TOC) contents of core 13/1-U-02 range from 0.1 to 1.7 wt. %, but most values remain below 1 wt. %. There is a continuous decrease in TOC from the base early Volgian to the middle Volgian, until a single maximum of 1.7 wt. % introduces the base late Volgian (Fig. 3-3). Hydrogen Index (HI) values are very low, ranging between 10 and 40 [mg HC/g TOC] in the early and middle Volgian, and somewhat higher values of about 20 to 100 [mg HC/g TOC] in the late Volgian. Values for Fe_2O_3 are relatively high and range from 3 to 10 wt. %, whereas sulfur values are relatively low and range from 1 to 3 wt. %. The Zr/Al ratio is about 15 in the lower early Volgian and continuously increases to about 65 in the middle Volgian. Core 6307/07-U-02 is characterized by TOC contents between 0.1 and 7.0 wt. % that continuously decrease from the early Volgian to the late Ryazanian. The decrease is particularly rapid through the Ryazanian (Fig. 3-4). Except for a few fluctuations in the early Valanginian the uppermost 20 meters of the core are virtually barren of organic carbon. HI values show high variability between 200 to 600 [mg HC/g TOC] from the early Volgian to the late Ryazanian. In the Valanginian values

core	depth (m.b.s.f.)	interval	TC (wt. %)	TN (wt. %)	TS (wt. %)	CaCO3 (wt. %)	Fe2O3 (wt. %)	TOC (wt. %)	HI *1	OI *2	T_{MAX} (°C)	S1 *3	S2 *3	S3 *3	S2/S3	PI	source rock potential
6814/04-U-02	7 - 39 m	Barremian	3,40	0,15	1,0	8,0	9,0	2,40	58	48	436	0,1	1,5	1,2	2,1	0,07	poor/fair
	39 - 44 m	late	1,70	0,04	3,6	13,9	6,0	0,10	77	292	494	0,0	0,1	0,2	0,1	0,08	none
	44 - 70 m	Valanginian	1,90	0,06	2,9	10,8	6,6	0,60	112	98	460	0,1	0,6	0,4	1,9	0,11	none
	70 - 89 m	Ryazanian	2,10	0,12	2,3	4,1	5,0	1,60	100	90	423	0,1	1,9	1,2	1,7	0,05	fair
	89 - 136 m	late Volgian	4,30	0,19	3,9	11,6	7,6	2,90	187	35	430	0,3	5,9	0,9	8,7	0,04	fair/good
	136 - 167 m	middle	4,80	0,22	3,9	10,8	7,5	3,50	219	25	429	0,4	7,6	0,9	19,0	0,04	good/very good
	167 - 191 m	early	3,70	0,20	3,5	8,4	5,4	2,70	247	22	425	0,3	6,5	0,6	16,4	0,05	good/very good
6307/07-U-02	13 - 34 m	Valanginian	3,20	0,04	1,8	15,7	7,8	0,40	56	152	410	0,2	0,8	0,9	0,7	0,17	poor
	34 - 50 m	Ryazanian	4,70	0,15	4,3	2,8	6,4	2,70	275	66	413	0,3	8,8	1,5	4,9	0,05	good
	50 - 62 m	late Volgian	6,30	0,21	3,3	0,8	4,0	4,30	348	49	409	0,7	14,6	2,0	7,3	0,05	very good
	62 - 74 m	middle	6,30	0,19	4,5	1,9	5,4	3,90	371	62	406	0,6	14,2	2,4	6,1	0,04	very good
	74 - 105 m	early	6,80	0,18	5,4	2,8	6,1	4,20	373	99	407	0,8	16,0	1,9	8,5	0,05	very good
13/1-U-02	118 - 145 m	late Volgian	1,40	0,05	1,0	4,5	5,4	0,80	44	79	421	0,1	0,4	0,6	1,5	0,20	poor
	145 - 152 m	middle	0,80	0,04	0,5	3,6	8,7	0,30	6	x	367	0,0	0,0	0,0	0,0	0,56	poor
	152 - 208 m	early	1,80	0,05	1,0	9,4	6,5	0,70	10	68	381	0,1	0,1	0,4	0,2	0,56	poor

*1 = mg HC/g TOC; *2 = mg CO2/g TOC; *3 = mg HC/g rock

Table 3-1 Average values of bulk parameters from organic and inorganic geochemical analysis and Rock-Eval pyrolysis for major time intervals. Estimates of source rock potential according to Espitalié et al. (1977) and Peters (1986).

drop below 200 [mg HC/g TOC] and reach zero in the Hauterivian. Stable carbon isotope analysis yields $\delta^{13}C_{ORG}$ values from –29 ‰ in the Volgian and –20‰ in the Valanginian. The sediments show high Fe_2O_3 and sulfur contents ranging from 3 to 13 wt. %, and 0.1 to 13 wt. %, respectively. The Zr/Al ratio is about 15 in the early Volgian and decreases to about 6 in the Ryazanian.

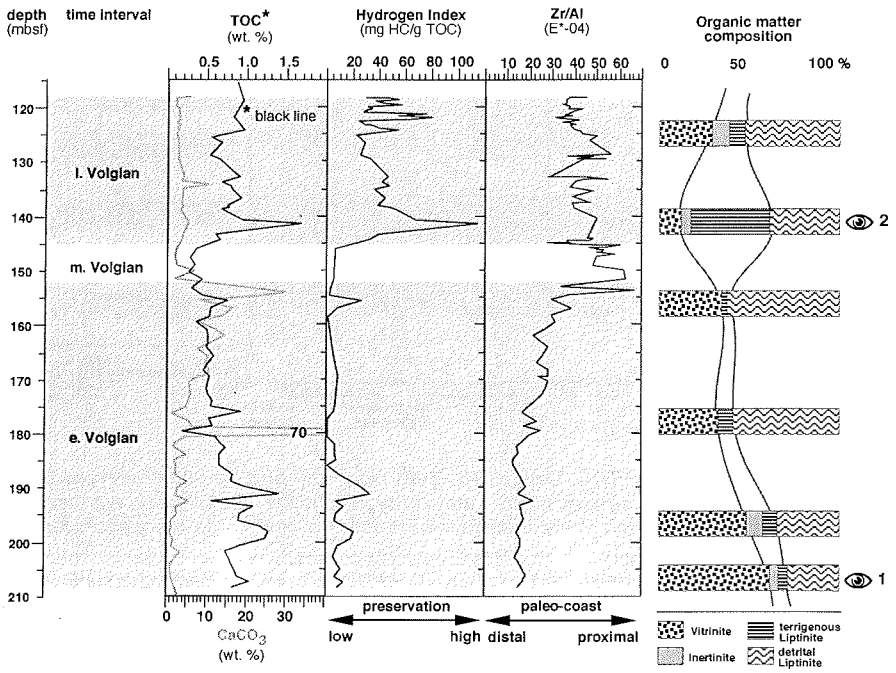

Fig. 3-3 Diagram showing TOC, $CaCO_3$, HI, Zr/Al ratio, and organic matter composition of core 13/1-U-02 plotted against depth. Terms of organic matter preservation are displayed along with the HI value, and interpretations of the relative position to the paleo-coast are displayed with the Zr/Al ratio. The collective quantity of inertinite plus terrestrial liptinite is enveloped by solid lines, because they may be derived by wind. (👁 digital picture of OM composition, see Plate I in appendix)

TOC contents of core 6814/04-U-02 range from 0.1 to 4.8 wt. % and decrease similar to those in core 6307/07-U-02 (Fig. 3-4, 3-5). Fluctuations in the early Valanginian are also comparable to core 6307/07-U-02, and the succeeding Hauterivian is virtually barren of organic carbon. HI values range from 200 to 400 [mg HC/g TOC] in the early Volgian and from 100 to 200 in the Ryazanian.

The Valanginian is marked by values below 100 [mg HC/g TOC], whereas no values can be calculated in the Hauterivian because the TOC is too low.

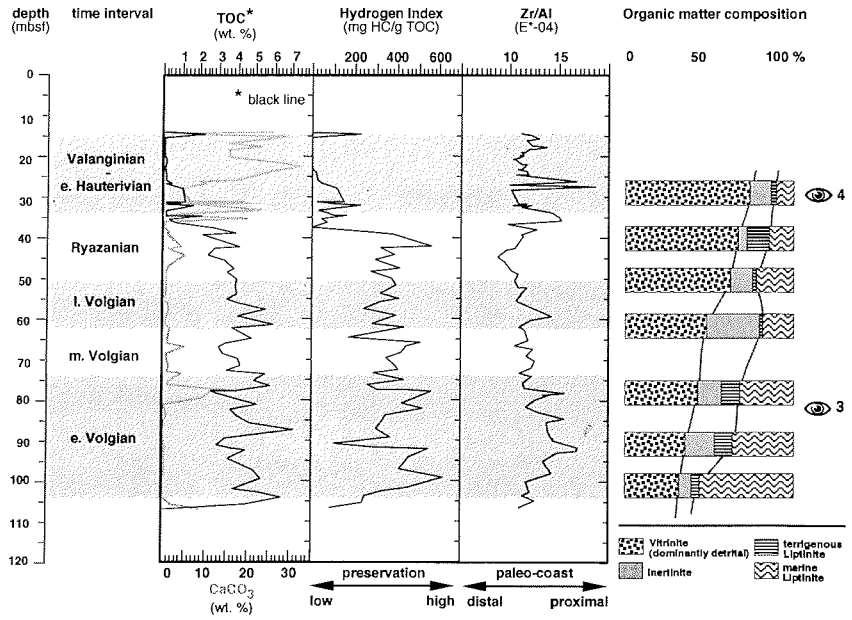

Fig. 3-4 Diagram showing TOC, $CaCO_3$, HI, Zr/Al ratio, and organic matter composition of core 6307/07-U-02 plotted against depth. Terms of organic matter preservation are displayed along with the HI value, and interpretations of the relative position to the paleo-coast are displayed with the Zr/Al ratio. The collective quantity of inertinite plus terrestrial liptinite is enveloped by solid lines, because they may be derived by wind. (👁 digital picture of OM composition, see Plate II in appendix)

Stable carbon isotope analysis reveals $\delta^{13}C_{ORG}$ values from –30 ‰ in the Volgian and –26‰ in the Valanginian. Fe_2O_3 concentrations range from 2.6 to 21.4 wt. %, and sulfur values range from 0.1 to 6.9 wt. %. The Zr/Al ratio is about 25 (2 x higher compared to core 6307/07-U-02), and there seems to be no change from the middle Volgian to the late Ryazanian (Fig. 3-4). The Valanginian and early Hauterivian are marked by strong fluctuations in the Zr/Al ratio, where maximum values reach 50 to 60. The succeeding Barremian reveals a relatively stable ratio of about 15.

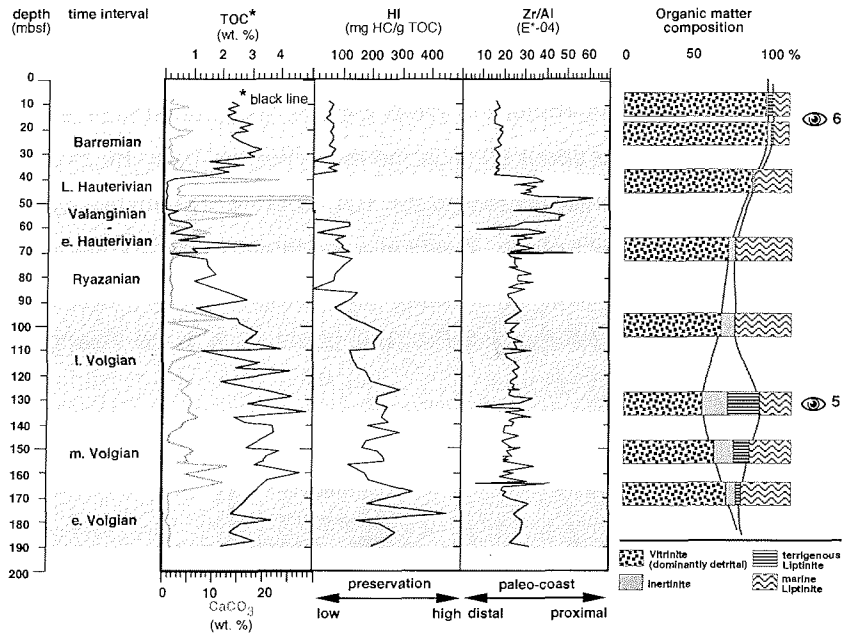

Fig. 3-5 Diagram showing TOC, $CaCO_3$, HI, Zr/Al ratio, and organic matter composition of core 6814/04-U-02 plotted against depth. Terms of organic matter preservation are displayed along with the HI value, and interpretations of the relative position to the paleo-coast are displayed with the Zr/Al ratio. The collective quantity of inertinite plus terrestrial liptinite is enveloped by solid lines, because they may be derived by wind. (👁 digital picture of OM composition, see Plate III in appendix)

3.4.2. Maceral composition

In core 13/1-U2 vitrinite makes up 10 to 60 % of the particulate organic matter (POM), and includes a moderate portion of detritus (appendix Pic. 1). There is a general decrease in the amount of vitrinite from base to top of the core almost parallel to the TOC content, except for the base late Volgian. As the counterpart to vitrinite the amount of liptodetrinite makes up 25 to 60 % of the POM (Fig. 3-3). Whereas terrigenous liptinite (5 to 40 %) and inertinite (1 to 10 %) are of minor importance, except for the late Volgian. The base late Volgian is marked by an increased amount of terrigenous liptinite, which makes up to 35 % POM, and produces high peaks in TOC and HI, respectively (Fig. 3-3, appendix Pic. 2).

The POM of core 6307/07-U-02 is dominated by vitrinite, and includes a relatively high proportion of detritus (Fig. 3-4). The general change in composition through time reveals a clear picture. The amount of vitrinite increases constantly from about 30 % in the early Volgian up to 80 % in the Valanginian, which is counter-parallel to the TOC content. The marine liptinite makes up the second major group, including a moderate to high proportion of detritus. It is clearly illustrated that its abundance declines steadily from about 60 % in the early Volgian (cf. Fig. 3-4, Pic. 3) to about 10 % in the Valanginian (cf. Fig. 3-4, Pic. 4).

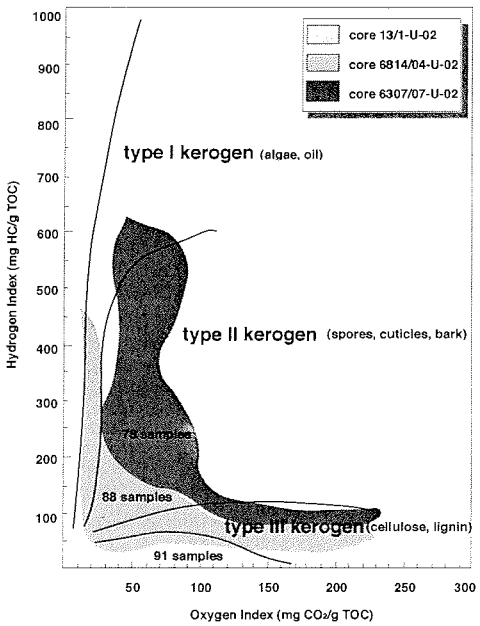

Fig. 3-6 Results of Rock-Eval pyrolysis from all 3 sediment cores plotted in a HI/OI van Krevelen-type diagram showing different types of OM (type I – IV kerogen) and their potential sources (c.f. Espitalié et al., 1977; Peters, 1986). Sample clusters were generalized by different fields of gray.

The amount of inertinite and terrigenous liptinite is generally much more important compared to core 13/1-U-02, and ranges from 5 to 20 % and 1 to 15 % of the POM, respectively. In particular, the amount of inertinite shows a symmetrical distribution with lowest values in the early Volgian and in the Valanginian and with a pronounced maximum at the base late Volgian. The

organic matter composition of core 6814/04-U2 is different from the others, because it is heavily dominated by vitrinite, which reaches up to 90 % of the POM (Fig. 3-5). The detrital fraction is also much larger compared to the other cores. Similar to core 6307/07-U-02 the amount of vitrinite is always negatively correlated to the TOC curve. Another difference is that vitrinite first decreases from about 60 % in the late early Volgian to its minimum in the early late Volgian (Fig. 3-5, Pic. 5). It does not increase again before the late Volgian (where the TOC content is highest) to reach about 90 % in the Barremian (Pic. 6). Marine liptinite is only a minor component (10 to 30 %), and has its maximum from the late Volgian to the late Ryazanian. Inertinite and terrigenous liptinite seem to correlate, and both increase mutually from 10 % in the late early Volgian to 30 % in the early late Volgian. Shortly thereafter inertinite and terrigenous liptinite decrease to insignificant amounts.

3.5. Discussion

3.5.1. Sources and preservation of organic matter

Determination of the origin and preservation of individual macerals provides information about the distance from their sources and the depositional conditions. To obtain this information we performed organic petrography supported by Rock-Eval data, and we discuss the applicability of $\delta^{13}C_{ORG}$ isotope data.

The organic matter of the Southeastern Passage (SEP) appears to be a mixture of marine and terrestrial organic matter, but the material presumably derived from marine sources is highly disintegrated. Hence, most of the detrital liptinite (cf. Fig. 3-3) is of uncertain origin, though we found a few indicators for a marine source, e.g. dinocysts and algae. However, due to poor preservation these relatively hydrogen-rich precursors now appear as the large amount of type III kerogen, as reflected in the HI/OI and S2/TOC diagrams (Fig. 3-6, 3-7). We found the relatively lipid-rich OM derived from terrestrial sources (spores

and pollen) is much better preserved than material from marine sources (Pic. 2). The macerals from cellulose and lignin-rich land-plants show a broad spectrum of maturation stages, from dark-brown vitrinite to light-gray primary fusinite.

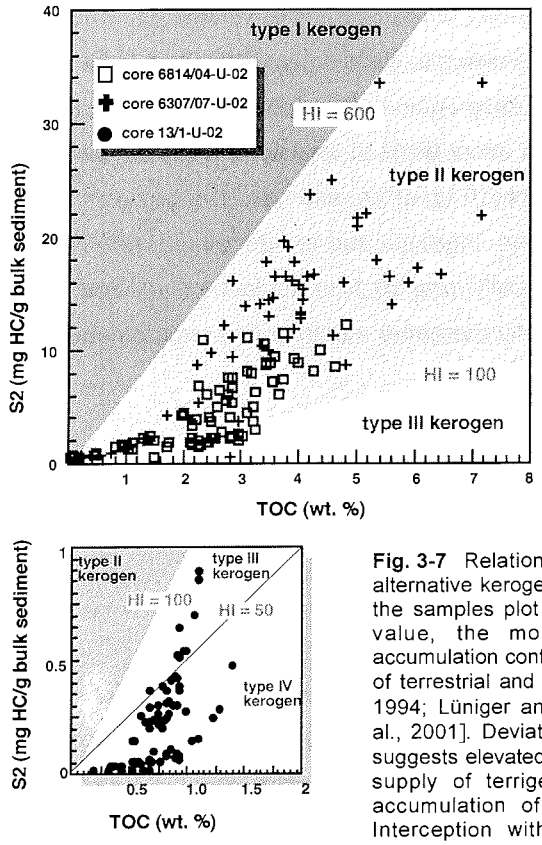

Fig. 3-7 Relationship between S2 and TOC for alternative kerogen type determination. The closer the samples plot along a line with a constant HI value, the more likely is organic carbon accumulation controlled by preservation and mixing of terrestrial and marine OM [e.g. Horsfield et al., 1994; Lüniger and Schwark, 2001; Tribovillard et al., 2001]. Deviations in the S2 or TOC direction suggests elevated primary production, or increased supply of terrigenous OM has influenced the accumulation of organic carbon, respectively. Interception with TOC axis may indicate the absorptive capacity of the mineral matrix [e.g. Langford and Blanc-Valleron, 1990], or the percentage of „dead" organic carbon [Cornford et al. 1998].

These macerals are considered as original type III and IV kerogen presented in the HI/OI and S2/TOC diagrams (Fig. 3-6, 3-7). In general, we observe a decrease of land-plant debris (vitrinite, including vitrodetrinite) from the base early Volgian to the early late Volgian (cf. Fig. 3-3) and a positive correlation with the TOC content. The Norwegian-Greenland-Seaway (NGS) shows a very different picture. The organic matter is clearly derived from both marine/aquatic

and terrestrial sources and the preservation is much better. We observe a general increase of land-plant debris (vitrinite, including vitrodetrinite) from the early Volgian to the early Barremian, although this course starts somewhat later in the northern NGS location (Fig. 3-5). However, most prominent is the high abundance of well-preserved liptinite fragments (≥ 10 μm) and liptodetrinite (≤ 5 – 10 μm), which reveal their marine sources (e.g. algae, dinocysts).

We found many physically intact algae at various depths (Pediastrum, Botryococcus, Tasmanites, and most important dinoflagellate cysts) that may be derived from estuarine, lagoonal and/or pelagic sources. Their relatively high preservation results in type II kerogen (Fig. 3-6, 3-7). Terrigenous liptinites are dominated by a variety of fairly to very well preserved spores and pollen (Pic. 3, Pic. 5), producing type II and II/III kerogen. Therefore, compared to the SEP a much wider spectrum of kerogen types appears in the HI/OI and S2/TOC diagrams (Fig. 6, 7). However, the most striking difference to the SEP is the negative relationship between TOC content and the amount of vitrinite.

Determination of OM sources can be supported by the application of $\delta^{13}C_{ORG}$ data [e.g. France-Lanord and Derry, 1994; Meyers, 1997; Schouten et al., 1997; Routh et al., 1999; Onstad et al., 2000; Van de Schootbrugge et al., 2000], but the isotopic signature of late Mesozoic sediments appears to be substantially different from modern sediments. As long as oceanic CO_2 is enriched in ^{13}C, sediments dominated by marine OM should produce higher, i.e. isotopically heavier, $\delta^{13}C_{ORG}$ values than sediments dominated by land-plant derived material. In contrast, we observed that our sediments rich in marine OM are characterized by $\delta^{13}C_{ORG}$ values from –25 to –30 ‰, whereas the sequences rich in terrestrial OM show values from –20 to –25 ‰. A similar inverted relationship is reported from various DSDP sites in the lower Cretaceous North Atlantic [e.g. Arthur and Dean, 1985; Dean et al., 1986] (Fig. 3-8).

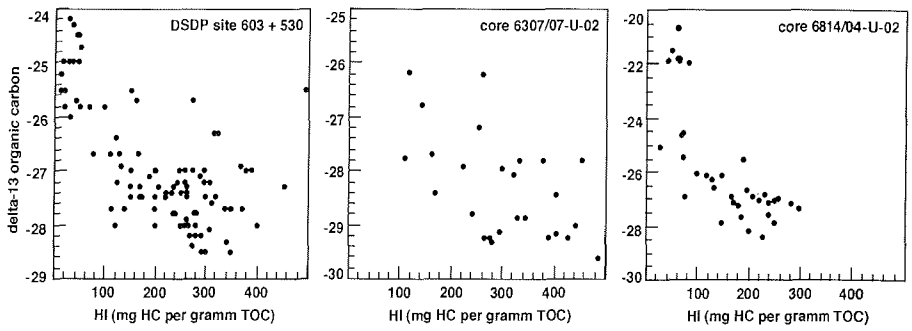

Fig. 3-8 Relationships between $\delta^{13}C_{ORG}$ and HI values of core 6814/04-U-02 and core 6307/07-U-02 (Fig. 8) demonstrate that hydrogen-rich organic matter is positively correlated with lighter (^{13}C depleted) values, and *vice versa*. This abnormal (different from modern) relationship is also reported from other Mesozoic sites, e.g. DSDP sites 367, 530 [Dean et al., 1986], and 603 [Arthur et al., 1985] which are summarized in Figure 8. This relationship seems to be stronger developed with increasing anoxia, and/or higher northern latitudes [Langrock et al., 2003a].

Several potential mechanisms were discussed to explain these unusual isotopic signatures in late Mesozoic sediments, such as diagenesis, increased atmospheric CO_2 partial pressure, and more exhaustive photosynthetic ^{13}C fractionation of marine phytoplankton [see Arthur et al., 1985; Dean et al., 1986; Meyers, 1997; Ehrbacher et al., 1999 and references therein). Rau et al. (1987) demonstrated a good correlation between low $\delta^{15}N$ and low $\delta^{13}C$ values in Cretaceous black shales, where the ^{15}N depletion is suggested as a result of periodically extensive denitrification by N_2-fixing bacteria set in largely anoxic or suboxic environments with slow deep-water turnover. This coincides with our interpretation of black shale formation of the Hekkingen Fm and Spekk Fm (see below).

3.5.2. Depositional environments

There are several processes that increase the amount of organic carbon that is preserved in the sedimentary record, e.g. anoxic bottom waters (= lack of bioturbation), reduced input of clastic material (= lack of dilution), high primary production (= benthic overload), high bulk accumulation rates (= rapid burial), and high supply of terrestrial organic matter [e.g. Müller and Suess, 1979;

Demaison and Moore, 1980; Stein, 1986; Arthur et al., 1987; DeGraciansky et al., 1987; Meyers, 1997]. To assess the depositional conditions we interpreted the pyrite size distribution [e.g. Wilkin et al., 1996, 1997], TOC-Fe-S relationships [e.g. Brumsack, 1988; Dean and Arthur, 1989; Lückge et al., 1996; Hofmann et al., 2000], and sedimentation rate/organic carbon relations [e.g. Stein, 1990].

location	time interval	pyrite as framboids (%)	mean diameter (μm)	size variability	interpretation
6814-04-U-02	Barremian	74	7,0	low	oxic - dysoxic (**)
	Valanginian - Hauterivian	7	8,0	low	oxic
	Volgian - Ryazanian	98	7,0	medium	anoxic - suboxic
6307-07-U-02	Valanginian - Hauterivian	no pyrite	no pyrite	no pyrite	oxic
	Volgian - Ryazanian	98	6,0	low	anoxic (*)
13-1-U-01	Late Volgian	88	13,0	high	oxic - dysoxic
	Early Volgian	86	12,0	high	oxic - dysoxic
Framvaren	Quaternary	80 - 85	5,8		oxic - dysoxic
Wallops Island	Quaternary	70 - 75	7,6		oxic - dysoxic (**)
Black Sea	Quaternary	95	5,1	low	anoxic (*)

Table 3-2 Pyrite size distribution inferred from reflected light microscopy (e.g. Wilkin et al., 1996, 1997). A high percentage, a low average diameter, and/or a low size variability of pyrite framboids suggest a formation under more anoxic conditions, predominantly within the water column. Modern surface sediments, e.g. from the Black Sea, can be related to the Volgian black shale sequences of core 6307/07-U-02 and 6814/04-U-02. Positive relationships to modern analogues are indicated by asterisks.

We found autochthonous pyrite framboids in all studied cores and almost all depths, except for the Valanginian and Hauterivian of core 6307/07-U-02. Autochthonous pyrite formation indicates anoxic conditions, but pyrite framboids that have formed within an anoxic water column, e.g. in the modern Black Sea, are typically smaller and less variable in size than those formed in the pore spaces of sediments underlying oxic and dysoxic water columns [e.g. Wilkin et al., 1996, 1997]. Our investigations clearly revealed that sediments with a high TOC content are dominated by pyrite framboids that are particularly small and less variable in size.

The Volgian and Ryazanian sediments of the NGS basins show that about 98 % of the total pyrite occurs as framboids (Table 3-2). Average diameters range from 6 μm to 7 μm with a low variability in size. This relatively uniform

size is obtained when pyrite is formed within the water column and sinks to the bottom by means of gravity, which suggests that at least a distinct layer of the water column was anoxic (e.g. Wilkin et al., 1996, 1997). The sediments of the succeeding Valanginian and Hauterivian of core 6814/04-U-02 reveal that only 7 % of the pyrite occurs as relatively uniform framboids, and 93 % is non-framboidal that has likely been formed below the sediment surface. During the identical time period no pyrite was formed in core 6307/07-U-02, indicating the absence of H_2S due to the lack of OM. In core 13/1-U-02 less than 88 % of the pyrite are framboids, and much of the framboids have formed huge aggregates filling the pore spaces in the sediment. The diameters of the framboids also differ from those in the other cores and show an average of 12 μm, ranging from 4 to 100 μm. This suggests a rather oxygenated water column, and that pyrite has formed predominantly in the sediment.

The TOC-Fe-S ternary diagrams (Fig. 3-9) display the limiting factors for pyrite formation to evaluate the depositional conditions [e.g. Berner and Raiswell, 1983; Berner, 1984; Brumsack, 1988; Dean and Arthur, 1989; Hofmann et al., 2000]. In the Skagerrak location most samples plot within a relatively narrow field, reflecting a low variability between the parameters (Fig. 3-9a).

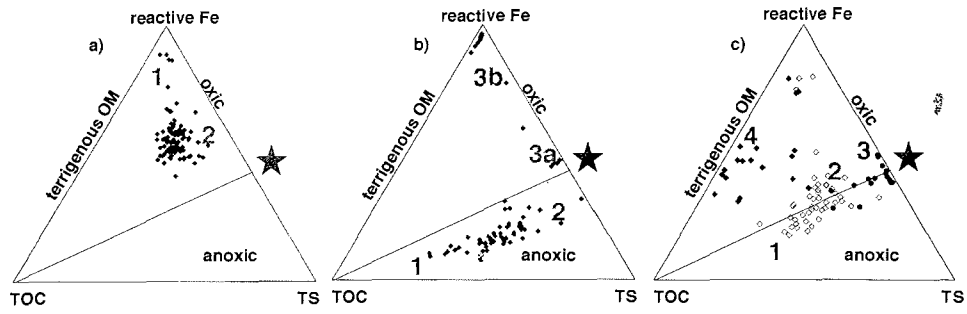

Fig. 3-9 TOC-Fe-S ternary diagram showing the limiting factors for pyrite formation [e.g. Brumsack, 1988; Dean and Arthur, 1989; Hofmann et al., 2000] for core 13/1-U-02 (a), core 6307/07-U-02 (b), and core 6814/04-U-02 (c). Formation of pyrite (FeS_2) is provided along the solid line. Below this line pyrite formation is limited by reactive iron, probably reflecting anoxic conditions. Above the line pyrite formation is limited by the absence or composition of OM, e.g. samples plot to the left if easy-to-metabolize compounds are absent. An evolutionary trend of changing depositional conditions is demonstrated by different numbers representing the early Volgian (1), the late Volgian (2), the Valanginian and Hauterivian (3), and the Barremian (4).

Pyrite formation was chiefly limited by the lack of labile hydrogen-rich organic matter, because sulfate is unlimited in marine environments. Hence, the sediments were likely deposited under relatively stable oxic conditions throughout the Volgian. The black shales of the Volgian and Ryazanian of core 6307/07-U-02 (Fig. 3-9b) plot below the "pyrite composition line" indicating limitations by reactive iron under oxygen-depleted conditions. There is a change along the line towards more oxic conditions, represented by the gray marl of the Valanginian (right flank), and the red marl of the succeeding Hauterivian (upper corner). The sediments of core 6814/04-U-02 are also characterized by distinct provinces. The general trend from more anoxic conditions in the Volgian to dysoxic conditions in the Ryazanian and oxic conditions in the Valanginian/Hauterivian is outlined in Figure 3-9c. The sediments of the Barremian, which follow a hiatus, plot in a different field (to the left) where the formation of pyrite is limited by the lack of labile organic matter (hydrogen-rich). These sediments are dominated by hydrogen-poor terrestrial OM, which seems to lessen the degree of decomposition by sulfate-reducing bacteria, and eventually decreases the availability of H_2S in the water column. This results in a decrease of pyrite framboids that crystallized in the water column (see pyrite size analysis above).

The stratigraphic framework presented in Mutterlose et al. (2003) reveals a very low sedimentation rate (SR) for all studied locations. The lack of dilution by clastic input is one of the prerequisites for accumulation of organic carbon-rich sediments. Low sedimentation rates may also indicate that high primary production was not the primary control on organic matter accumulation, at least not for the Norwegian-Greenland-Seaway examples. Therefore, we calculated initial (or decompacted) sedimentation rates (SR_0) to illustrate the relationship between marine organic carbon and sedimentation rate (after Stein, 1986b, 1990). We used a decompaction factor of x2 to x5 to account for the average porosity loss of clayey to silty sediments during diagenesis [e.g. Poelchau et al., 1997 and references therein]. Figure 3-10 shows the fields of potential deposition (open boxes) for each core. The Volgian to Ryazanian sediments of core 6307/07-U-02 (box 2) are hosted in the domain of anoxic depositional

conditions, which is reflected by high TOC contents and a low sedimentation rates.

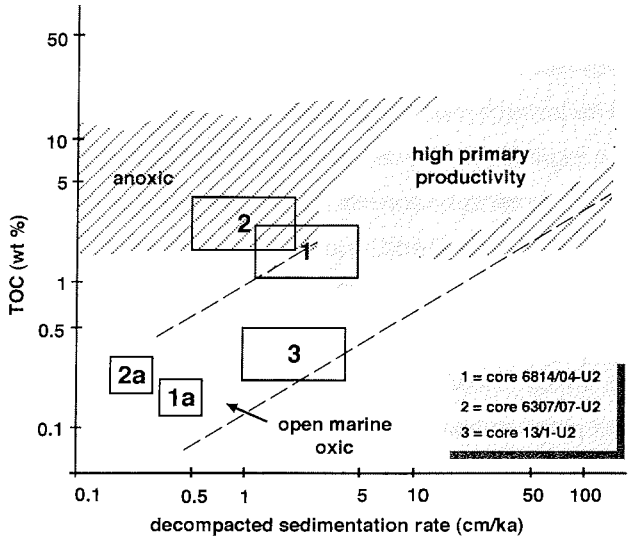

Fig. 3-10 Relationship between (marine) organic carbon content and decompacted sedimentation rates (modified after Stein, 1986b, 1990). Different fields of deposition (high productivity, anoxic, open-marine oxic) are based on results form Recent to Miocene sediments. Maximum sedimentation rates and minimum TOC data (and *vice versa*) were used to construct the open boxes which represent areas of potential deposition. The Volgian and Ryazanian sediments of the NGS (box 1 and 2) clearly show depositional conditions different to those in the SEP (box 3). Conditions in the NGS continuously changed to open-marine oxic in the Valanginian-Hauterivian (box 1a and 2a).

There is an overlap with the field of potential deposition of core 6814/04-U-02 (box 1) which is characterized by lower TOC contents and somewhat higher sedimentation rates compared to core 6307/07-U-02. The figure displays a border situation for core 6814/04-U-02 between anoxic, open-marine oxic and high primary productivity conditions. This coincides with the foregoing discussion, and may actually represent suboxic to dysoxic conditions in the middle Volgian, and more moderately dysoxic conditions in the Ryazanian. The Valanginian and Hauterivian of the NGS basins (box 1a and 2a) are characterized by much lower TOC contents compared to the sedimentation rates, hence, their fields of potential deposition fall in the "open-marine oxic"

domain. The field of potential deposition of core 13/1-U-02 (box 3) is situated in the "open marine oxic" domain, and supports the interpretations from the foregoing discussion.

We also calculated the paleoproductivity for the black-shale sequences based on estimated SR of 0.4 – 1.2 cm/ky for the early Volgian, and 1.2 – 1.9 cm/ky for the late Volgian. For oxic environments we used the equation (1) after Müller and Suess (1979) and Stein (1986b, 1990):

(1) $$PP = 5.31 * C * DBD^{0.71} * LSR^{0.07} * DEP^{0.45}$$

where PP is the primary productivity [$gC/cm^2/ka$], C the (marine) organic carbon content, DBD is the dry bulk density [g/cm^3], LSR the linear sedimentation rate [cm/ka], and DEP the water depth [m]. We assumed 200 m as an average water depth for this location. For estimating paleoproductivity in anoxic environments we used equation (2) after Bralower and Thierstein (1984):

(2) $$PP = 50 * C * LSR * DBD$$

where PP is the primary productivity [$gC/cm^2/ka$], C the (marine) organic carbon content, DBD is the dry bulk density [g/cm^3], and LSR the linear sedimentation rate [cm/ka]. Paleoproductivity values for the anoxic NGS basins range from about 4 to 20 $gC/cm^2/ka$, which is similar to the sediments with the highest organic carbon contents in the modern Black Sea [e.g. Izdar et al., 1983]. The Southeastern Passage, on the other hand, reveals about 30 to 40 $gC/cm^2/ka$ under oxic conditions, which is typical for open-marine environments [e.g. Stein, 1986].

An increased supply of terrestrial OM seems to be the primary control on organic carbon accumulation in the Southeastern Passage, because here we have a clear positive correlation between the TOC content and the amount of vitrinite. This seems plausible since the deposition occurred in an open-marine oxic environment. The complete opposite is documented in the Norwegian-

Greenland-Seaway, where an increased supply of terrestrial OM is unlikely to have had a major control on the organic carbon accumulation.

3.5.3. Paleoenvironmental change through time

There are different indicators to believe that the sediments were deposited on the shelf not far off the paleo-shore. First, the occurrence of well-preserved algae from fresh-water and brackish-water habitats along the NGS, such as Botryococcus and Tasmanites indicate the proximity to their sources. Some algae may possess a elevated buoyancy by emitting oil while they live (and so may have a larger distribution), but they will soon drop to the sea-floor and become exposed to biochemical disintegration after their relatively short life cycle. Second, there are occasionally vitrinites, vascular bundles, and clasts of bituminous coal that reach up to 1.5 mm in size (often with a high length/width ratio). Under normal hydrodynamic conditions (average current speeds, etc.) such large particles have a very limited lateral distribution [e.g. Lückge et al., 1996; Taylor et al, 1998]. Third, the abundance of terrigenous liptinites, e.g. whole spores, along the NGS indicates the proximity to the land. In particular, high diversity in type suggests proximity to a larger variety of land-plant sources, which should decrease with increasing distance from land. In that course, high diversity in size indicates that these particles were also not transported over long distances by wind or water with respect to gravity fractionation.

The increasing amount of detritus upwards in the section, which is derived from land-plants indicates a reduction of the organic particle size through time. Consequently, the ratio between vitrinite and vitrodetrinite becomes generally smaller, although the relative amount of these macerals increases. Contemporaneously, the Zr/Al ratio decreased (Fig. 3-4 and 3-5) suggesting that the grain size of the non-riverine mineral fraction decreased, reflecting the reduced influence of aeolian input [e.g. Hinrichs et al., 2001]. Assuming fractionation by gravity as the primary mechanism for sorting particles, it seems

that the distance between the core position and the coastline increased. However, in the northernmost location the change in the Zr/Al ratio is much less, which is probably due to a special paleogeographic setting with a consistent input of wind-derived clastic material. Black shale formation is often associated with rapid transgression of epicontinental seas, particularly during the early stages [e.g. Sheridan, 1987]. A first transgression pulse may have already occurred in the early Volgian, which could have initialized the formation of black shales. Lateral adjacent coastland including peat swamps may have been leached and increased the supply of nutrients and terrigenous organic matter to the sea margins, stimulating primary productivity that may have caused anoxia. But this theory is not supported by our results, because we illustrated that the black shale formation in the NGS was stimulated neither by a high sedimentation rate, a high terrigenous input, nor a high marine productivity. Deposition was likely hosted in an isolated anoxic basin with a stratified water-column, probably covered by a permanent halocline (Fig. 3-11). Primary production was low due to limited nutrient supply, the lack of upwelling water masses, and perhaps low Fe^{2+} input from the continents [see Boyd, 2000]. The inflow of oxygenated water masses and the vertical circulation was inhibited, thus promoting the preservation of organic matter similar to the "stagnation model" [e.g. Brumsack, 1980; De Graciansky et al., 1984; Nijenhuis et al., 1999]. Therefore, a transgression probably did not initiate, but rather "disturbed", the formation of black shales on a long-term scale. The hinterland became continuously flooded, vegetation withdrew, and the distance between the terrestrial sources and the depositional site increased. The amount of reworked terrestrial organic matter and the amount of detritus increased. Mutterlose et al. (2003) suggested a change from a more warm and humid climate in the Volgian to a more cool and arid climate in the Valanginian/Hauterivian for the Norwegian-Greenland-Seaway, which may be supported by the ongoing decay of land-plant material. But the momentous change was probably that oxygenated water masses started to enter the basins over ridges and sills, which probably destabilized the stratified water-column by increased vertical circulation and eventually diminished the intensity of anoxia.

This decreased the preservation of OM, and resulted in a fully oxygenated, more distal and sediment-starved basin in the Valanginian and Hauterivian. Even though primary production was probably enhanced during these conditions most of the marine organic matter was disintegrated before entering the sedimentary record.

3.6. Conclusions

The latest Jurassic to earliest Cretaceous time slice provided favorable conditions for the formation of black shales in the eastern Norwegian-Greenland-Seaway. In particular, the Volgian is characterized by immature sediments with high organic carbon contents and a fair to very good source rock generative potential.

Maceral analysis, Rock-Eval data, and $\delta^{13}C_{ORG}$ data revealed a variable mixture of terrigenous and marine organic matter, suggesting that deposition occurred in a shelf environment. The abundance of terrigenous liptinite, particularly sporinite, and algae derived from freshwater and brackish habitats indicates the proximity to the paleo-shore.

Pyrite size distribution, TOC-Fe-S and sedimentation rate/organic carbon relationships suggest that black shale formation occurred under suboxic to anoxic bottom water conditions and a continuous long-term change to more open-marine oxic conditions.

Changes from more hydrogen-rich organic matter in the early and middle Volgian to more "woody" and refractory organic matter in the Valanginian and Hauterivian is primarily a preservation effect controlled by the increase of bottom-water oxygenation.

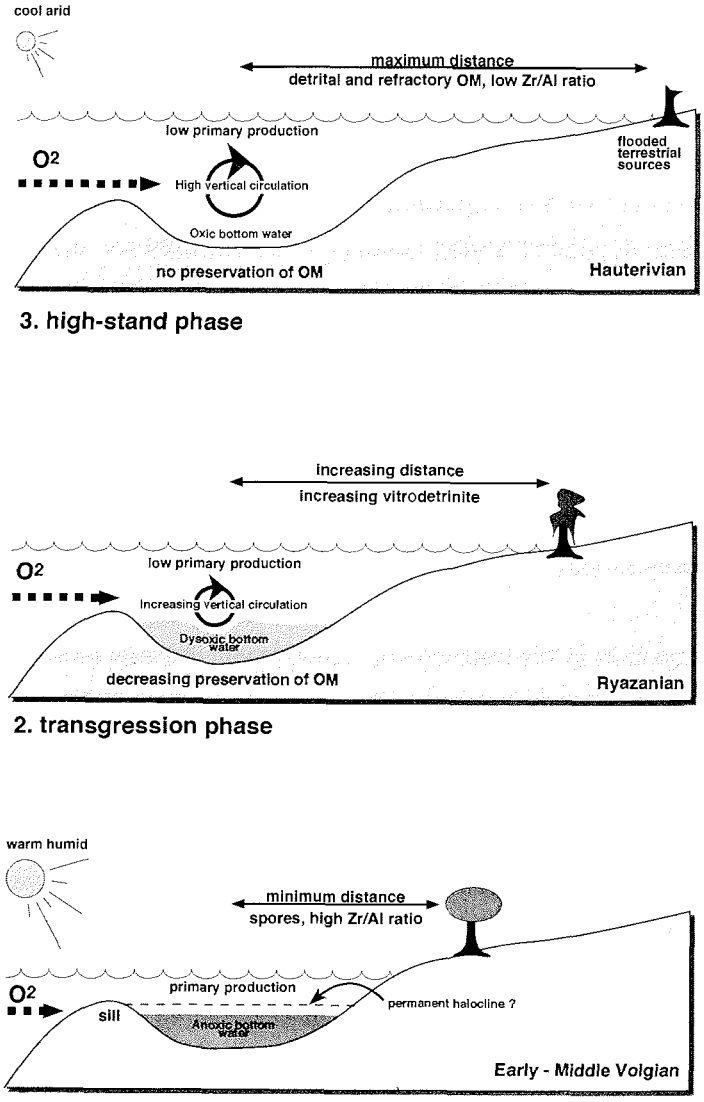

Fig. 3-11 Depositional model for the black shale formation in the eastern NGS. High preservation of OM is provided by oxygen deficiency, stratified water-column, and short transport distances (vertical and lateral). Advanced transgression increases transport distance and water depth, and allow more oxygenated water masses to enter the basin. This probably results in a decrease of anoxia, the reestablishment of benthic activity, the decrease of lipid-rich OM preservation, and eventually the termination of black shale formation.

The increasing amount of organic detritus derived from land-plants and the decreasing Zr/Al ratio suggest that the core positions moved farther from the paleo-shore, expanding the distance to the terrestrial sources. This may have occurred in terms of a transgression, probably caused by a sea-level rise.

The sediments from the southeastern passage to the Tethys realm (core 13/1-U-02) were deposited under conditions unfavorable for the formation of petroleum source rocks. Deposition occurred in an open-marine oxic environment with low organic carbon contents and low sedimentation rates. Accumulation of organic carbon was controlled by the input of terrestrial, particularly "woody", organic matter.

Acknowledgements

Financial support by the Deutsche Forschungsgemeinschaft (grant STE 412/13-1 and BR 775/10-1) is gratefully acknowledged. SINTEF Petroleum Research (Trondheim) kindly provided drilling core material and gave access to unpublished data. We thank U. Wand and S. Klein for technical assistance. We very much appreciate the critical comments of T. Wagner, U. Mann, J. Matthiessen, H. M. Weiss, M. Smelror, R. Littke, and two anonymous reviewers that helped to improve this contribution.

CHAPTER 4 Marine and Petroleum Geology (in press)

Origin of marine petroleum source rocks from the Late Jurassic to Early Cretaceous Norwegian Greenland Seaway – evidence for stagnation and upwelling

U. Langrock and R. Stein

Alfred Wegener Institute for Polar and Marine Research, Department of Geosciences, Columbusstrasse, 27568 Bremerhaven, Germany

Abstract

Forty samples were selected from Upper Jurassic to Lower Cretaceous black shales of IKU (Sintef Petroleum Research) sites 6307/07-U-02 and 6814/04-U-02, located on the mid-Norwegian shelf, for a detailed maceral analysis. The penetrated rocks include the *Spekk* and *Hekkingen* Formations, which represent major potential petroleum source rocks in the region. It was our first objective to reveal the type of organic material that is responsible for the source rock potential of these sediments. The results suggest that black shale formation has occurred in two different paleoceanographic settings; 1) in a "high-productive" and 2) an "anoxic/stagnant" environment. This conclusion is supported by inorganic and sedimentological data. In addition, sedimentation rates (SR) from recent biostratigraphic and sedimentological work on these sequences gave impulse for using accumulation rates to estimate the original organic carbon flux to the sediment. Organic carbon accumulation rates are relatively low but similar to mid-Cretaceous black shales from other ocean areas (average 10 – 300 mg/cm^2/ka). Supported by redox-sensitive Re/Mo ratios, SR/TOC relationships, and paleoproductivity estimates we suggest that the formation and preservation of organic carbon during black shale formation in the *Spekk Formation* has followed largely the conditions of the "stagnation model",

whereas the *Hekkingen Formation* is likely one possible example for the "productivity model".

4.1. Introduction

The geological understanding of the mid-Norwegian shelf (Fig. 4-1) has been enhanced by petroleum exploration and production operations during the 1980s and early 1990s and is summarized in drilling reports and subsequent papers, e.g. by Skarbø et al. (1988), Worsley et al. (1988), Hansen et al. (1991), Leith et al. (1990), Jongepier et al. (1996). Modern insights into plate tectonic evolution, structural development, sedimentology, paleoceanography, and geochemistry of strata of late Mesozoic age along the Norwegian shelf, including sediments of commercial importance, are owing to these investigations (e.g. Brekke et al., 1999; Smelror et al., 2001; Swientek and Ricken, 2001; Lipinski et al., 2003; Langrock et al., 2003b; Mutterlose et al., 2003). Fine-grained sediments of Late Jurassic to Early Cretaceous age occur along the eastern margin of the Norwegian-Greenland-Seaway and adjacent marginal seas (Smelror et al., 1994; Leith et al., 1990; Worsley et al., 1988; Århus et al., 1991; Wagner and Hölemann, 1995; Doré, 1991; Doré et al., 1997; Bugge et al., 2002; Mutterlose et al., 2003; Langrock et al., 2003). Drilling also recovered sediments that are exceptionally rich in organic carbon and provide moderate to very good source rock potential for liquid and gaseous petroleum. We investigated sediments from the mid-Norwegian shelf (Fig. 4-1) that represent major potential petroleum source rocks in the region. The cores are characterized by two major lithological units, including the *Spekk* and *Hekkingen* Formations (Fig. 4-2). A thick sequence of dark-colored, organic carbon-rich claystones (i.e. black shales) with subordinate silty or calcareous intercalation dominates the lower part of the cores. These are superceded by a younger overlying sequence of light-colored or reddish organic carbon-poor siltstones, marls and limestones. The transition between these two sedimentary units occurred gradually within a time interval of about 10 My during the Berriasian and Valanginian. The black shale sequences

of Late Jurassic age are represented by the *Spekk* Formation, which is a major source rock east of the Vøring Marginal High between 62° and 68° N (Fig. 4-1) and the time-equivalent *Hekkingen* Formation, which is an important source rock in the Nordland and Troms areas and extends into the central Barents Sea (e.g. Bugge et al., 1989, 2002; Worsley et al., 1994; Smelror et al., 1994, 1998, 2001).

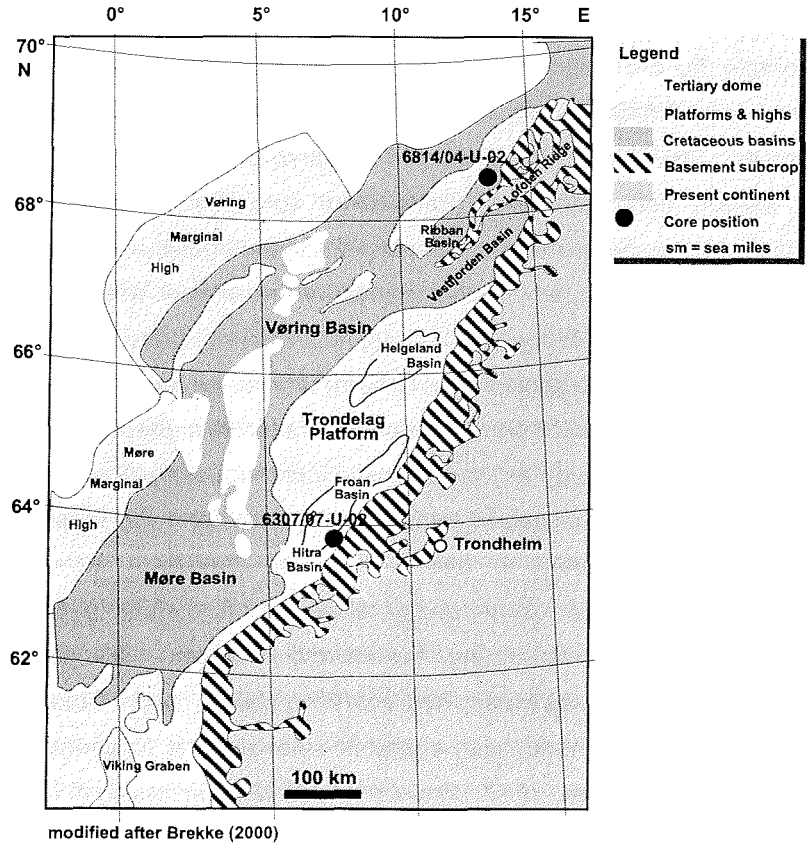

Fig. 4-1 Geographic section of the modern shelf region off mid-Norway, including principal sedimentary units and positions of drilling holes (modified after Brekke, 2000).

Both *Spekk* and *Hekkingen* Formations consist of immature to marginally mature sediments with high TOC contents relative to average shale (e.g. Wedepohl, 1971, 1991). A significant TOC decrease towards the top of both

formations, which is most severe during the Berriasian, is due to increased bottom water oxygenation that was likely caused by a rapid sea-level rise (e.g. Mutterlose et al., 2003; Langrock et al., in press). Variations within the formations are linked to 40-ky and 100-ky orbital-forced climate cycles (e.g. Swientek and Ricken, 2001; Swientek, 2002; Mutterlose et al., 2003) and are to some extent superimposed on local effects, such as silt dilution and increased primary production.

Paleogeographic turning points caused by either transgression or regression are favorable for the deposition of organic carbon-rich bituminous rock sequences (e.g. Bitterli, 1963), especially during the initial stage of such episodes (e.g. Sheridan, 1987). Collected research data suggest that most organic carbon accumulates in transitional (brackish) or alternating marine/freshwater regimes. Accumulation of particulate organic matter derived from terrestrial sources is subject to fractionation by wind or water, so that larger particles are usually deposited closer to the shore, e.g. in the estuaries.

Small-sized particulate organic matter (< 5μm) is hydrodynamically similar to the clay mineral fraction, which is highly capable of adsorbing dissolved organic carbon (DOC, < 0.8 to 0.4 μm) and metal ions to form organo-metal complexes. The conversion from the dissolved into the particulate form (by reasons of energy) is often attributed to changing water chemistry within the marine/freshwater transition zone and is especially important in view of petroleum source rock formation (e.g. Calvert and Pedersen, 1992; Meyers, 1997). The relationship between hydrocarbon source rocks and their depositional environment has been reported from several locations (e.g. Boussafir and Lallier-Vergès, 1997; Schulz et al., 2002). Two principal models for the causes of vast organic carbon accumulation have been under controversial discussion during the past three decades: (1) ocean wide episodes of "stagnation" in restricted stratified basin similar to the Black Sea, and (2) an increased primary production which causes oxygen minimum zones that impinge on the sea floor and thereby limit the remineralization of organic matter on the sea-floor [e.g. Pedersen and Calvert, 1990, Caplan and Bustin, 1999; Saelen et al., 2000; Nijenhuis et al., 2001; Röhl et al., 2001]. An

increased supply of terrigenous organic matter may also be an important mechanism for the accumulation of organic carbon-rich sediments in the marine realm [e.g. Stein et al., 1986]. The high northern paleolatitudes also received attention by scientists because most common information about formation of organic carbon-rich sediments was obtained largely from lower paleolatitudes, e.g. the Mid-Cretaceous Atlantic Ocean, but also the Tertiary Indian Ocean (e.g. Schlanger and Jenkyns, 1976; Stein et al., 1986; Brumsack and Thurow, 1987; Arthur et al., 1990; Bralower et al., 1994; Bralower and Thierstein, 1987; Siesser, 1995; Herrle et al., 2003). In higher latitudes climate changes should be more distinctively reflected in the sedimentary record than in the lower latitudes (e.g. Mutterlose et al., 2003), and the accumulation of organic carbon should be less diluted by carbonate sedimentation as it is found in the equatorial regions. Moreover, the source rock of the major oil provinces in the circum-Arctic Ocean are of Late Jurassic age (e.g. Leith et al., 1990), suggesting that formation of black shales with hydrocarbon potential are also most important (1) in true high paleolatitudes, (2) during the Jurassic-Cretaceous transition, and (3) during times of an exceptionally low sea-level compared, for example, to the mid-Cretaceous North Atlantic.

The primary objective of this paper is concerned with the origin of the organic carbon that has resulted in the source rock potential found in these immature Upper Jurassic and Lower Cretaceous sediments. Once the sources of the associated organic matter were determined from detailed microscopic analysis, mass accumulation rates of organic carbon and paleoproductivities were calculated and interpreted in relation to the depositional environment.

4.2. Data and procedures applied

Material was collected from two sediment cores drilled offshore mid-Norway during a shallow drilling campaign executed by Sintef Petroleum Research (former IKU) in the late 1980´s (Fig. 4-1) (e.g. Fjerdingstad et al., 1985; Århus et

al., 1987; Skarbø et al., 1988; Bugge et al., 1989; Hansen et al., 1991). Core 6307/07-U-02 was taken in the southern part of the Hitra Basin (off Smøla island, 63°27´54´´ N and 07°14´44´´ E) in a water depth of 290 m. Core 6814/04-U-02 was taken approximately 354 nautical miles (655 km) further to the NNE in the northern part of the Ribban Basin (near the Lofoten Islands, 68°09´45´´ N and 14°09´47´´ E) in a water depth of 233 m. Below a Quaternary cover, the cores immediately penetrate 104.80 m and 191.25 m, respectively, of shallow, WNW dipping Mesozoic strata that encompass the Kimmeridgian-Valanginian and Volgian-Barremian intervals (Fig. 4-2). The cores were sampled in irregular intervals of 1.5 – 2.0 meters, depending on the physical condition and the availability of the material, resulting in a time resolution of about 120 to 350 ky (cf. Mutterlose et al., 2003). Kerogen typing, determination of source rock generative potential and organic matter (OM) maturity were conducted according to Espitalié et al. (1977) and Peters (1986) using a Rock-Eval II (*plus S3 unit*). The hydrogen index (HI) was calculated from the amount of pyrolysable hydrocarbons (S2 value) based on the TOC content, and the oxygen index (OI) was calculated from the amount of associated carbon dioxide (S3 value) based on the TOC content. Indices were used in a HI/OI diagram to estimate kerogen types (I – IV), their potential sources and thermal maturity [cf. Espitalié et al, 1977; Peters, 1986].

The determination of the particulate organic matter (POM) was performed by means of maceral analysis. For this purpose 20 whole rock samples were collected from each sediment cores. The preparation of kerogen isolates was not necessary since the organic carbon content of the samples was relatively high (1 – 7 wt %). The small blocks of rock (3 – 4 cm^3) were orientated perpendicular to the bedding and fixed by a cold-setting epoxy-resin. After hardening they were successively ground and polished with diamond paste in multiple stages on an automatic unit to obtain optimal reflection properties. The macerals composition was determined by point-counting with a 25-point ocular grid using a Zeiss Axiophot microscope under incident and fluorescence light (395 – 440 nm). For statistical accuracy at least 200 macerals were counted in each sample. Macerals are distinguished into three main groups vitrinite,

inertinite and liptinite, including further subgroups and individual macerals according to the ICCP nomenclature described in Taylor et al. (1998). Vitrinites are cellulose and lignin-rich remains of higher land-plants, e.g. tissues of leaves or tree bark, and usually produce type II/III to III kerogen (cf. Espitalié et al., 1977; Peters, 1986; Horsfield et al., 1988). Inertinites may have similar sources as vitrinites but they have experienced distinct oxidative alteration, e.g. by wildfires or acidic environments. This results in a depletion of hydrogen and nitrogen and an enrichment of oxygen and carbon compounds which make them virtually inert to maturation processes (e.g. type IV kerogen during Rock-Eval pyrolysis). Liptinite is a collective term for all terrestrial and marine/aquatic organic matter which is rich in lipids and proteins, and that is characterized by distinct fluorescence properties. Terrestrial liptinites are derived from land-plant precursors (e.g. resins, waxes, cuticles, spores and pollen). Hence, for paleoenvironmental reconstruction and source rock characterization it is also important to discriminate the origin of the liptinite fraction of the organic matter.

4.3. Results

4.3.1. Base geochemical data

Core 6307/07-U-02 shows TOC contents between 0.1 and 7.0 wt. % that continuously decrease from the early Volgian to the late Ryazanian (Fig. 4-2). The decrease is particularly rapid through the Ryazanian. With the exception of a few fluctuations in the earliest Valanginian, the uppermost 20 meters of core 6307/07-U-02 are virtually barren of organic carbon. HI values show high variability between 200 to 600 [mg HC/g TOC] from the Lower Volgian to the uppermost Ryazanian. In the Valanginian values drop below 200 [mg HC/g TOC] and reach zero in the Hauterivian. TOC contents of core 6814/04-U-02 range from 0.1 to 4.8 wt. % and decrease similar to those in core 6307/07-U-02 (Fig. 4-2). Fluctuations in the lowermost Valanginian are also comparable to core 6307/07-U-02, and the succeeding Hauterivian is virtually barren of organic carbon. HI values range from 200 to 400 [mg HC/g TOC]

in the early Volgian and from 100 to 200 in the Ryazanian. The Valanginian is marked by values below 100 [mg HC/g TOC], whereas no values can be calculated in the Hauterivian because the TOC is too low.

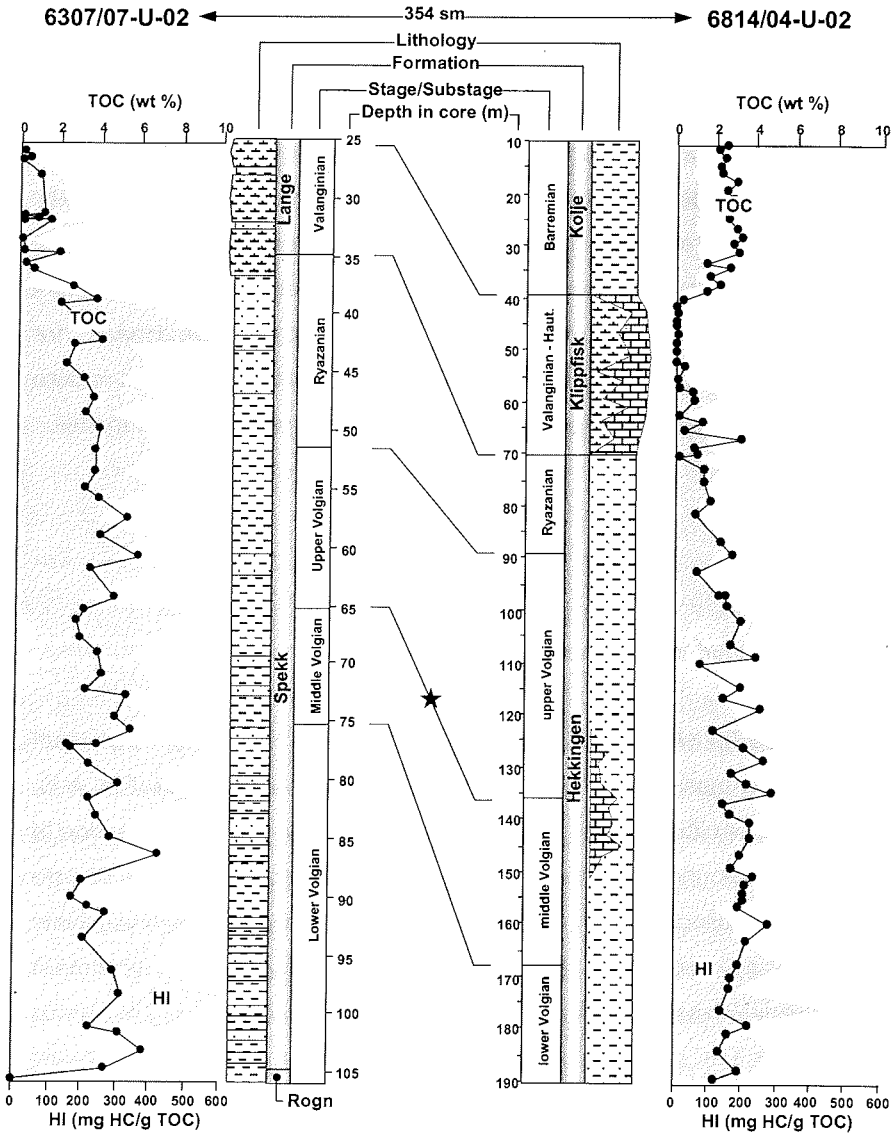

Fig. 4-2 Organic carbon content and Rock-Eval hydrogen index values of core 6307/07-U-02 and 6814/04-U-02. Essential differences were stressed-out by using identical scales. Time correlation, formations and lithology were collected from Brekke et al. (1999), Hansen et al. (1991), Smelror et al. (1994, 1998), Hardenbol et al. (1998), and Mutterlose et al. (2003).

4.3.2. Organic matter composition

The maceral composition of particulate organic matter (POM) was characterized on whole rock samples following largely the ICCP nomenclature described in Taylor et al. (1998) with the exception of funginite, which was introduced by Lyons (2000). A general overview of the organic matter composition is presented in Figure 4-3 and the total inventory, sources and optical properties observed are summarized in Table 4-1. In total, three maceral groups (vitrinite, inertinite, liptinite), twelve individual macerals and one microlithotype were identified under reflected white light and fluorescence light (picture gallery of microscopic photographs is available at www.pangaea.de/data).

Maceral Group	Maceral & Microlithotype*		Source	Reflected light	Fluorescence color	Form
Vitrinite	Telinite		woody tissues, primary	dark grey/medium gray	none	cellular/subrounded
	Vitrodetrinite		woody tissues, reworked	medium grey	none	cellular, brittle
Inertinite	Fusinite		woody tissues, charred	light grey	none	cellular, brittle
	Semifusinite		woody tissues, charred	grey (bronze hue)	none	cellular, brittle
	Funginite		fungal bodies	light grey/grey	none	cellular
	Inertodetrinite		woody tissues, charred	light grey/grey	none	brittle
	Semifusite*/Fusite*		coalified stems, twigs > 1mm	brownish grey/white	none	sub-cellular layers
Liptinite	terrigenous	Sporinite	land-plant spores	dull brown/translucent	yellow/orange/brown	whole spores
		Cutinite	land-plant cuticles	dull brown/translucent	yellow/orange/brown	
		Resinite	waxes, oils, fats, resins	dull brown/translucent	orange	amorphous
	marine-aquatic	Telalginite	freshwater/marine algae	dull brown/translucent	yellow	cellular, fragmented
		Lamalginite	freshwater/marine algae	dull brown/translucent	yellow/brown	thin bands
		Dinocysts	Dinoflaggelates	dull	green/yellow/brown	cellular, fragmented
	Liptodetrinite		marine-aquatic, various	dull	green/yellow	various disrupted

Table 4-1 General inventory of macerals, including their sources and optical properties, observed in the sediments. In total, three maceral groups (vitrinite, inertinite, liptinite), twelve individual macerals and one microlithotype were identified under reflected white light and fluorescence light.

Macerals of the vitrinite group are identified as dark gray to medium gray telinite (≥ 10 μm) and more light-colored vitrodetrinite (≤ 10 μm). None of the vitrinites show any fluorescence. Their shapes vary from sub-rounded and sub-angular particles to excellently preserved cellular tissues from land-plant leaves or bark. Most telinites are between 20 and 100 μm in size, some exceed 200 μm, and a few particles reach more than 500 μm with a length/width ratio of up to 10:1.

Particularly, in the Upper Volgian sequence from 6814/04-U-02, telinite particles smaller than about 40 μm tend to be more rounded and of lower maturity, whereas larger macerals tend to be more angular, structural better preserved and of higher maturity. Open cell-fillings consisting of admixtures of collinite (cf. Taylor et al., 1998) and mineral matter occur rarely and were not quantified. It was also observed that larger telinites (100 – 300 μm) with lower reflectivity are associated with much smaller macerals (10 – 50 μm) of the inertinite group and vice versa.

Macerals of the inertinite group are present as fusinite, semifusinite, funginite, and inertodetrinite. Although semifusinite is almost absent in core 6307/07-U-02, the macerals of the inertinite group are significantly more abundant (up to 20 %) compared to the core from 6814/04-U-02 (≤ 5 % of the POM) (Fig. 4-3). Generally, particles with higher reflectance and maturity are much more angular and vascular compared to other woody particles of lower maturity, i.e. telinite. Fusinite and semifusinite generally show very well preserved cell structures with curved edges, i.e. bogen structure and sieve-structure, and a broad spectrum of optical reflectivity. A combination of high structural integrity and various stages of fusinitization suggest that maturity was unlikely caused by coalification during diagenesis (i.e. rank fusinites), but rather by incomplete charring by wildfires (i.e. pyrofusinites) (Taylor et al., 1998).

Some pyrofusinites look like hair slides, almost white in reflected light and up to 100 μm in length. Semifusinites show optical reflection properties between those of vitrinite and fusinite, and they appear with a hue of bronze. These well preserved fragments often appear in clusters, or in partly fractured and shattered cellular bodies, but also as single particles up to 200 μm in size. Some medium-sized (50 to 80 μm) macerals are also found with a rectangular shape, lacking any cellular structure. Semifusinites are also often observed as scleres with sharp edges and spikes, forming a heap of ruins ("Trümmerfeld") that sometimes exceeds 200 μm in size. The shape of such heaps suggests that the pieces have broken apart from larger plant tissues in situ, hence, after their deposition as a result of compaction. Funginite, formerly addressed as sclerotinite, is rarely found and consists of very well preserved opaque cellular

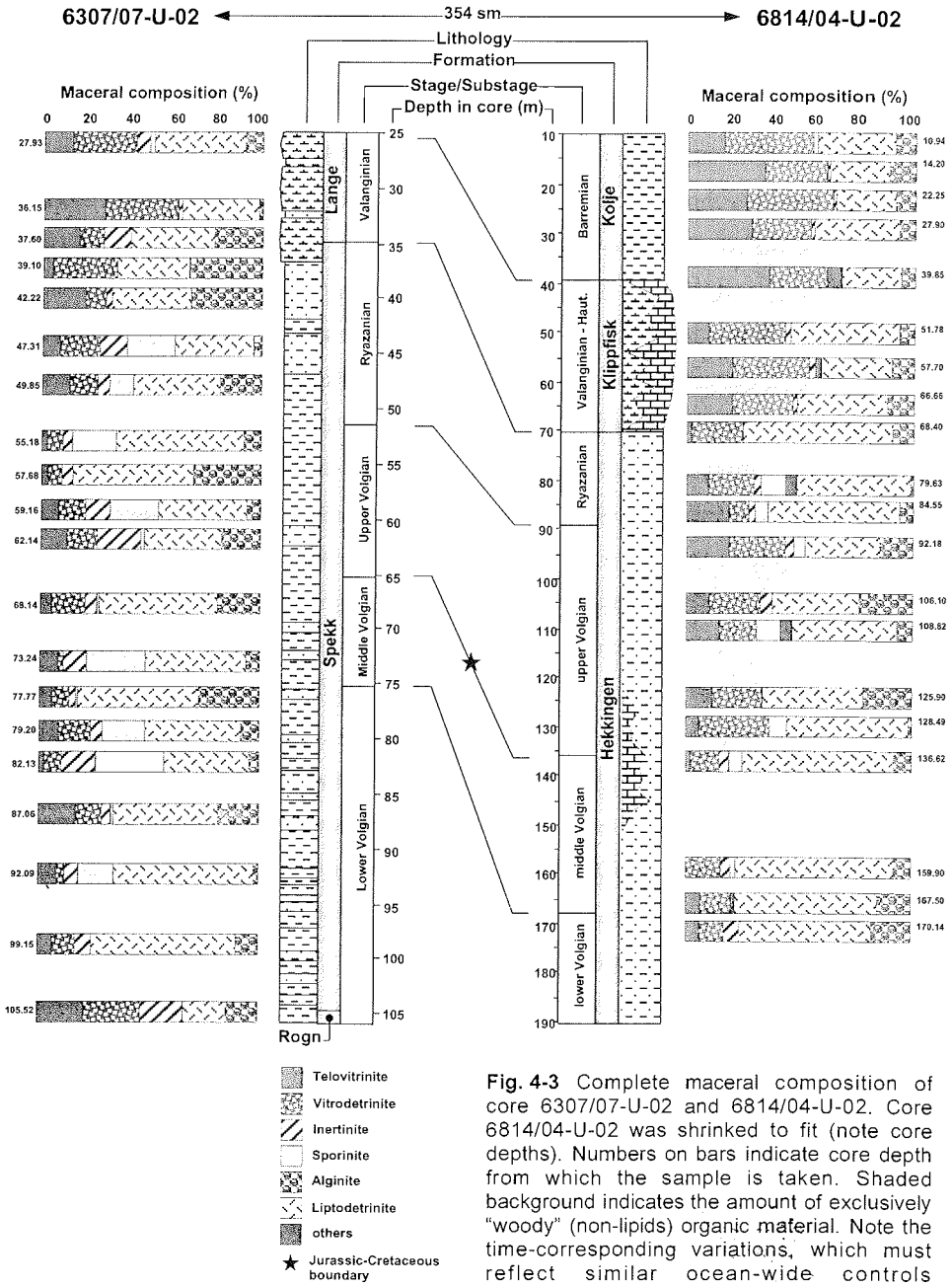

Fig. 4-3 Complete maceral composition of core 6307/07-U-02 and 6814/04-U-02. Core 6814/04-U-02 was shrinked to fit (note core depths). Numbers on bars indicate core depth from which the sample is taken. Shaded background indicates the amount of exclusively "woody" (non-lipids) organic material. Note the time-corresponding variations, which must reflect similar ocean-wide controls superimposed on regional effects.

bodies (from sclerotia) with regular cell structures and high reflectivity (cf. Lyons, 2000; Langrock et al., 2003a). There is a spectacular vascular bundle of 2 mm length and 0.2 mm width showing extremely well preserved cell structures and high reflectivity. It consists of different compressed layers of fusinite and likely reflects a part of a *fusite* microlithotype rather than a single plant tissue.

Macerals of the liptinite group must be distinguished into terrigenous and marine-aquatic liptinite. Sporinite is the most dominant and unmistakable terrigenous maceral and occurs in different morphologic types of microspores, ranging from about 10 to 200 μm in size. Individuals usually appear as collapsed spheres with relatively thick cell walls and single- or multi-layered exines. Larger forms with typical transected star ledges are rarely observed, whereas fractured exines of smaller forms are more common. Under fluorescence light sporinite shows a variety of colors from clear yellow to brown, reflecting different stages of biodegradation. Similar to inertinite the total amount of sporinite is much higher in the southerly core (max. 35 % POM) (see Fig. 4-3). Cutinite and resinite are abnormally rare in both cores and have been identified in only a few cases. Usually, cutinite originates from cuticular layers and cuticles and is probably the most resistant material produced by common land-plants (e.g. Taylor et al., 1998). Owing to its scarcity it was not usable for quantification, but this may have important paleoclimatic and paleogeographic implications. A determination between terpene resinite (originated from resins), or lipid resinite (originated from fats) was not successful. Generally, terrigenous liptinites (especially sporinite) become abruptly rare and then absent in the upper parts of the *Spekk* and *Hekkingen* Formations, probably reflecting the increasing distance to the paleo-shore (e.g. Littke et al., 1997; Langrock et al., 2003a, b; Mutterlose et al., 2003). The origin of marine liptinites is much more difficult to determine and has been subdivided into alginite (telalginite and lamalginite) and liptodetrinite. Visible entities of large colonial or thick-walled unicellular algae with a distinctive structure are termed telalginite. Four different types of telalginite were identified (in order of abundance): dinoflagellates (cysts), *Pila*, *Tasmanites*, and *Pediastrum*. Dinoflagellate cysts occur numerously throughout both cores in nearly equal quantities, except for

elevated abundance in the uppermost part of the *Spekk* Formation. These organic remnants of algae appear as chorate cysts with different types of single and branched processes and radiating spines. At least 5 different morphotypes were identified from 10 to 80 µm in diameter. The largest individuals show most severe marks of degradation, both physical and biochemical. The smallest individuals of less than 20 µm in size are more likely acritarchs rather than dinocysts because distinctive taxonomic indications are missing, e.g. the archaeopyle, and acritarchs usually develop smaller individuals (e.g. Williams, 1978). One species is most common in both cores and shows a spectacular bright green fluorescence color, reflecting their excellent preservation in physical and biochemical views. These individuals are about 10 µm in size with short single processes relative to their body and probably belong to the *Micrhystridium* lineage (e.g. Combaz, 1980). Algae of *Pila* type are usually compared to the modern *Botryococcus braunii*, which reproduce exclusively in freshwater habitats. These algae were observed occasionally but are generally more common in the southerly core. Degradation is sometimes at an advanced level but the original colonial structure can be distinguished in most cases. *Tasmanites* algae are compared to the modern analogue *Pachysphaera pelagica* and were observed at various depths in both cores, emitting an intensive yellow fluorescence color. The physical preservation is generally much better than that of *Pila* colonies, because *Tasmanites* is unicellular and has a more inflexible cell wall. They appear as flat thick-walled discs perpendicular to the bedding and reach 120 µm in length that may be about 80 µm in original diameter. Their original spherical form and characteristic numerous pore-canals, which penetrate the outer cell wall and leave small dimples on its surface, can be clearly identified when observed under reflected white light. In sediments deposited under more oxygenated conditions, particularly in the *Lange* and *Klippfisk* Formations, the formation of idiomorphic pyrite within some telalginites is a common process and reflects anoxic micro-environments below the sediment surface. Lamalginite, on the other hand, is less common in the sediments and appears as thin-walled filamentous algae of weak to medium yellow fluorescence color and a distinctive lamellar form parallel to the bedding.

Most macerals of the liptinite group are detrital (30 to 70 %) (Fig. 4-3), which is usually very difficult to address to a discrete biological source. However, that the majority of the liptodetrinite appears to be of marine-aquatic origin is a crucial point, particularly when calculating paleoproductivities. Our observations may suggest that terrigenous liptinites derived from the Norwegian coastland, i.e. dominantly spores, are much more resistant to physical disintegration than marine-aquatic organisms. The shape of most liptodetrinite macerals suggests that they have been derived from the fragile parts of marine organisms, such as most dinocysts and other algae. Supporting this, a large amount of liptodetrinite, though heavily crushed into pieces, has still higher fluorescence colors (shorter wavelength) than most intact terrigenous liptinite. Since the wavelength of fluorescing particles becomes longer with progressing biodegradation, i.e. more red colors when observed under the microscope, a land-plant source for liptodetrinite in our sediments is very unlikely. It has therefore mostly been classified as marine-aquatic organic matter.

4.3.3. Accumulation rates of organic carbon

It is difficult to interpret TOC data, particularly in coastal environments, because changes in the percent values of TOC may result from both organic and sedimentological changes (e.g. Stein et al., 1986). Therefore, we calculated mass accumulation rates of organic carbon to reflect the authentic organic carbon received by the sediment surface in units of mass per area and time, so avoiding effects of clastic dilution (cf. Thiede and Van Andel, 1975; Thiede et al., 1982). Physical properties of the sediment and stratigraphic control are imperative for calculating mass accumulation rates. Whereas bulk density and porosity are easily available, biostratigraphic control on black shale sequences of Late Mesozoic age are almost always a problem, particularly when dealing with very low sedimentation rates. Time control for the investigated cores was obtained largely from lithostratigraphic, palynological, and biostratigraphic studies [e.g. Skarbø et al., 1988; Hansen et al., 1991; Mutterlose et al., 2003;

Smelror, 1994; Smelror et al., 1998, 2001a; Vigran et al., 1998; Worsley et al., 1988]. Using the time scales of Hardenbol et al. (1998) the resulting linear sedimentation rates (LSR) are supported by a good correlation between biostratigraphic and astronomical dates (e.g. Berger et al., 1992; Oschmann, 1995; Swientek and Ricken, 2001), which is presented in Table 4-2.

Period	Linear sedimentation rate		
	(cm per 1000 years)		
Stage/substage	biostratigraphic		astronomical
	6307/07-U-02	6814/04-U-02	
Barremian	-	0,8	-
Hauterivian	0,3	0,3	-
Valanginian	0,3	0,3*	0,4*
Ryazanian	0,4	0,8	-
Late Volgian	0,5	1,5*	1,6*
Middle Volgian	0,3	0,8	-
Early Volgian	0,8**	0,6	0,8**

* peaks from spectral analysis investigated in core 6814/04-U-02 (after Swientek, 2002)

** peaks from spectral analysis investigated in core 6307/07-U-02 (after Swientek, 2002)

Table 4-2 Comparison between biostratigraphic and astronomical linear sedimentation rates (LSR) on the left and cyclicity-tuned LSR used in this paper (cf. Swientek and Ricken, 2001; Mutterlose et al., 2003).

It has to be considered, however, that pitfalls in the calculation of LSR may be caused by hiatuses in the Valanginian and Hauterivian, especially when the duration is uncertain. With the amount of marine organic matter obtained from maceral composition by kerogen microscopy, it was possible to calculate mass accumulation rates of marine organic carbon and eventually estimate paleoproductivities (see below). Mass accumulation rates of total organic carbon (MARTOC) in core 6307/07-U-02 show values that range from 60 to 80 mg/cm^2/ka in the Lower Volgian and drop to ≥ 40 mg/cm^2/ka in the Upper Volgian. From here values decrease upwards to ≥ 20 mg/cm^2/ka in the Ryazanian (Berriasian) and Lower Valanginian (Fig. 4-4).

The decrease towards the top of the core is a reflection of the TOC content and accelerated by the decreasing sedimentation rates. Based on the amount of marine organic matter (MOM) obtained from maceral analysis, accumulation rates of marine organic carbon (MARMOM) show a corresponding decrease from about 60 mg/cm^2/ka to ≥ 10 mg/cm^2/ka.

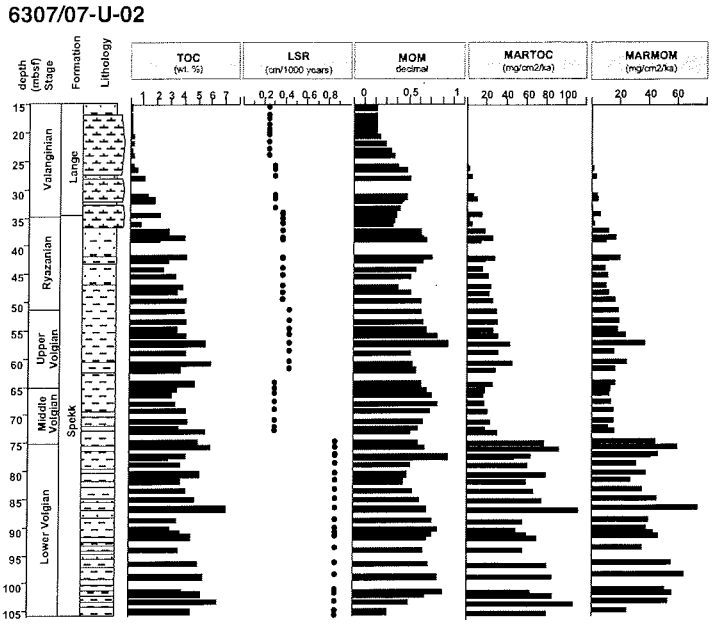

Fig. 4-4 Organic carbon content (Langrock et al., in press), corrected linear sedimentation rates (Mutterlose et al., 2003), marine organic matter (MOM) content (this paper), and mass accumulation rates of total organic carbon (MARTOC) and marine organic carbon (MARMOM) for core 6307/07-U-02.

Mass accumulation rates of total organic carbon (MARTOC) in core 6814/04-U-02 show values that increase from about 40 mg/cm^2/ka in the Lower Volgian to 100 - 150 mg/cm^2/ka in the Upper Volgian (Fig. 4-5). The decrease is also a reflection of the TOC content, resulting in a rapid decrease of MARTOC from ≥ 40 mg/cm^2/ka in the Ryazanian to ≥ 10 mg/cm^2/ka in the Valanginian and Hauterivian. Values from 40 to 60 mg/cm^2/ka are dominant throughout the succeeding Barremian. Based on the amount of marine organic matter (MOM) obtained from maceral analysis, accumulation rates of marine organic carbon (MARMOM) show corresponding values from about 20 to 80 mg/cm^2/ka with maximum values in the lower part of the Upper Volgian.

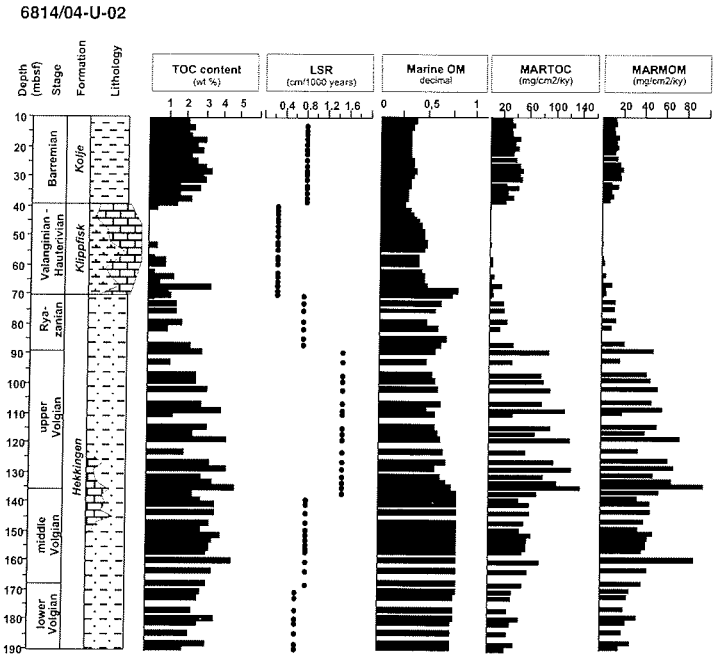

Fig. 4-5 Organic carbon content (Langrock et al., in press), corrected linear sedimentation rates (Mutterlose et al., 2003), marine organic matter (MOM) content (this paper), and mass accumulation rates of total organic carbon (MARTOC) and marine organic carbon (MARMOM) for core 6814/04-U-02.

4.4. Discussion

4.4.1. Organic facies types

The concept of organic facies types was previously developed by coal petrographers. They found that distinct coal macerals were generally deposited in distinct groups under similar chemical and physical conditions, and they defined organic facies types with special emphasis on its application in the oil industry (e.g. Jones, 1987; Taylor et al., 1998). Jones (1987) distinguished seven organic facies types (Table 4-3) only by the dominant type of organic matter, the atomic H/C ratio (at vitrinite reflectance $R_0 \pm 0.5$ %) and HI and OI values obtained from Rock-Eval pyrolysis. The organic facies types reflect a

decrease in the marine/aquatic and an increase in terrestrial/oxidized organic fraction of the sediment, documenting a successive reduction of the petroleum generative potential. According to the differentiation scheme of Jones (1987) shown in Table 4-3, we observed organic facies B to D in both cores, whereas organic facies A and AB are absent (Fig. 4-6, Fig. 4-7). Highest organic facies (B and BC) were found in the lower third of the cores and correspond to highest TOC and HI values and highest abundance of lipid-rich organic matter (cf. Fig. 4-3). In core 6307/07-U-02 organic facies BC is present throughout the Lower,

Organic facies	H/C (at R0 ±0.5 %)	Hydrogen Index (mg HC/g TOC)	Oxygen Index (mg CO_2/g TOC)	Dominant organic matter
A	≥ 1.45	≥ 850	≤ 30	algal, amorphous
AB	1.35 - 1.45	650 - 850	20 - 50	amorphous, minor terrestrial
B	1.15 - 1.35	400 - 650	30 - 80	amorphous, common terrestrial
BC	0.95 - 1.15	250 - 400	40 - 80	mixed, some oxidation
C	0.75 - 0.95	125 - 250	50 - 150	terrestrial, some oxidation
CD	0.60 - 0.75	50 - 125	40 - 150	oxidized, reworked
D	≤ 0.60	≤ 50	20 - 200	highly oxidized, reworked

Table 4-3 Classification scheme of organic facies types after Jones (1987)

Middle and Upper Volgianand in the Lower Berriasian (Fig. 4-6). Only two distinct periods in the Lower Volgian reveal organic facies B. In core 6814/04-U-02 (Fig. 4-7) the same period of time is characterized by a less constant facies distribution, as organic facies BC and C (Lower and Middle Volgian) is succeeded by organic facies C (Upper Volgian) and CD (Berriasian). A common feature of both cores is that the Klippfisk and Lange Formations of the Valanginian and especially the Hauterivian are dominated by organic facies CD and D.

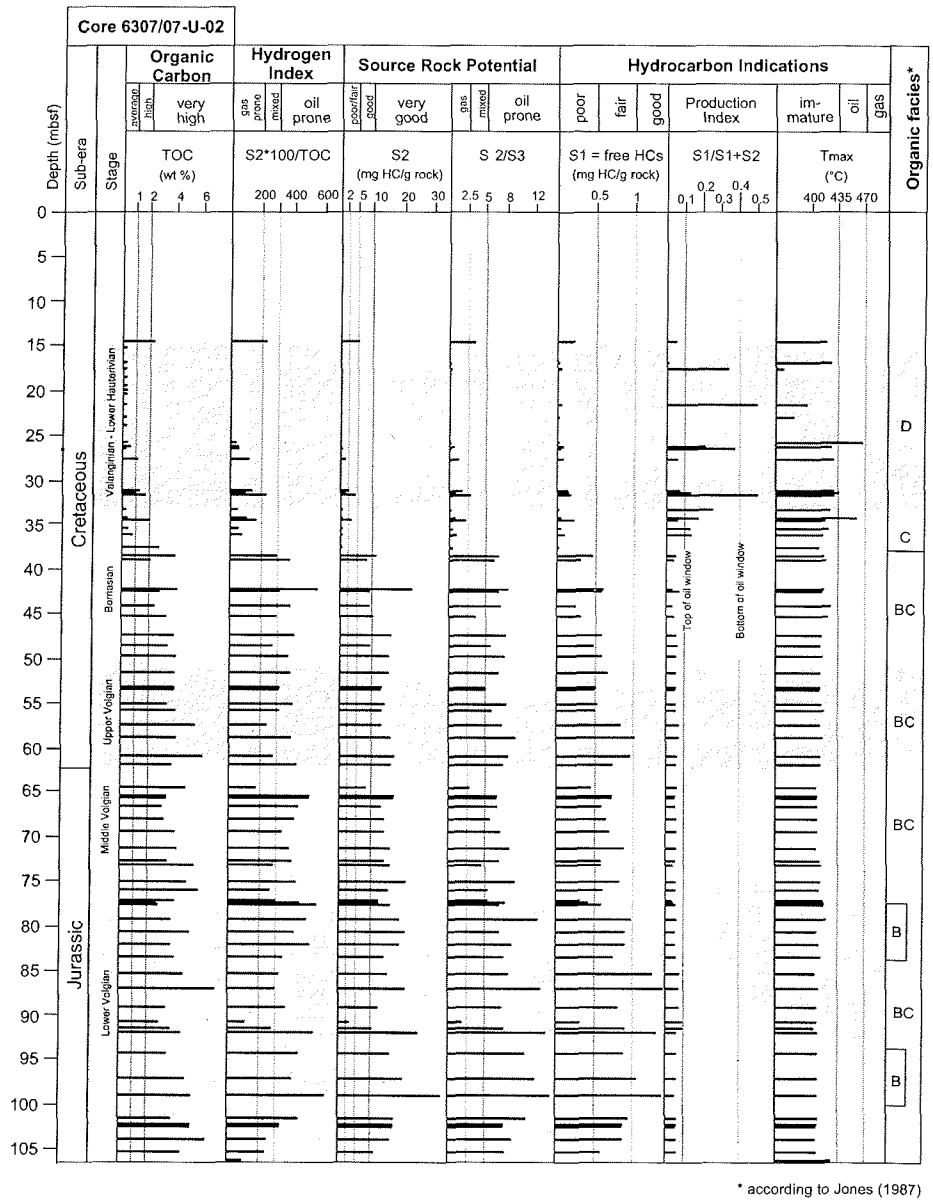

Fig. 4-6 Organic carbon, hydrogen index, source rock potential, and organic facies (after Jones, 1987) for core 6307/07-U-02. Note that production index and T_{MAX} are abnormally high in sequences of extremely low TOC that do neither reflect hydrocarbon generation nor passed maturity.

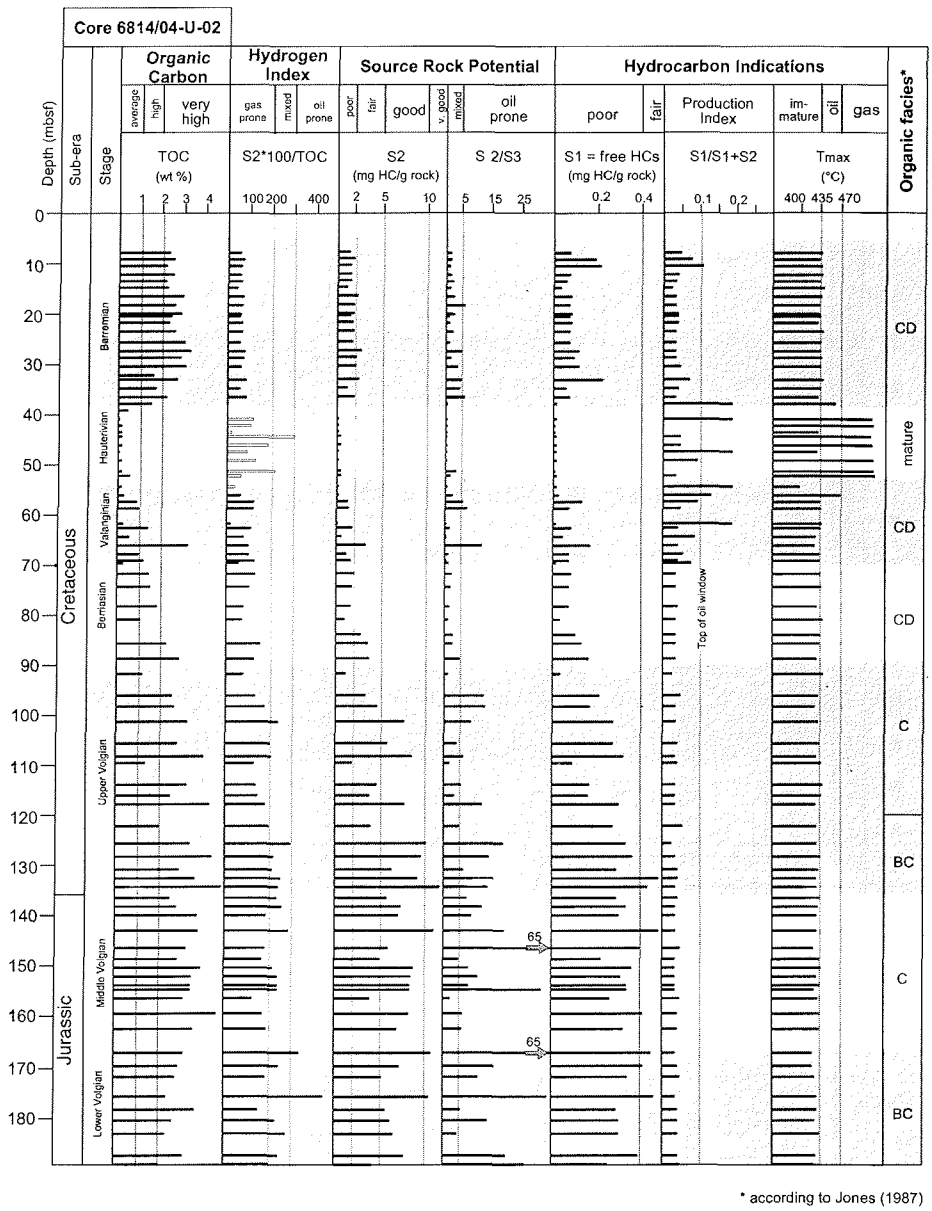

Fig. 4-7 Organic carbon, hydrogen index, source rock potential, and organic facies (after Jones, 1987) for core 6814/04-U-02. Note that production index and T_{MAX} may be abnormally high in sequences of extremely low TOC that do neither reflect hydrocarbon generation nor passed maturity.

4.4.2. Source rock potential and paleoenvironment

The *Spekk* Formation of core 6307/07-U-02 has crucial prerequisites to be a black-shale in the sense of Tissot and Welte (1984) because the sediments are rich in organic carbon compared to average shale (Fig. 4-6) (Wedepol, 1971, 1991). High preservation of lipid-rich organic matter is reflected by HI values from 300 to 600 [mg HC/g TOC] providing very good potential for oil generation. Indications of hydrocarbons generated from the kerogens, reflected by the S2 value, are good in the lower parts of the *Spekk* Formation and decrease towards the top similar to the source rock potential. Production index (PI) and T_{MAX} values indicate that the organic matter is immature (T_{MAX} < 435°C) and has not yet reached the onset top of the oil-window (PI < 0.1). Organic carbon content and source rock potential decrease during the Upper Berriasian and the Valanginian and reach almost zero during the Hauterivian. Here, the residual amount of organic matter consists of refractory material (inert and almost exclusively terrestrial) as a result of oxidative fractionation. As a consequence, T_{MAX} and PI values rise and give the false evidence of hydrocarbon generation. The previous classification of organic facies (Jones, 1987) coincides with these results and reflects the increasing dominance of highly oxidized and reworked organic matter (refractory OM). Even though the *Hekkingen* Formation consists of organic carbon-rich sediments with TOC values higher than 2 % by weight (Fig. 4-7), average values are lower by about 1 % compared to the *Spekk* Formation (cf. Fig. 4-6). The lower potential for a source rock becomes even clearer considering the HI values, which range only from 100 to 300 [mg HC/g TOC] and indicate a much lesser degree of preservation of lipid-rich OM. As a result, the sediments have only a good to fair potential for generating oil and mixed oil/gas products.

Similar to core 6307/07-U-02 (cf. Fig. 4-6) the source rock potential becomes subsequently poor and more gas-prone during the Berriasian and Valanginian. Free hydrocarbons (S1 value) are much less abundant and may have already been released during late diagenesis. This is most likely due to the pre-mature level of the organic matter as indicated by the T_{MAX} (≈ 435°C) values. The

distribution of organic facies types according to Jones (1987) in the *Hekkingen* Formation is a reflection of the source rock potential. The subsequent Barremian of core 6814/04-U-02 (Fig. 4-7), which is not documented in core 6307/07-U-02, is a period with less variations in organic carbon and HI values. Even though the TOC content is very high (> 2 %), the potential is poor for generating mixed oil/gas products because the input and/or preservation of lipid-rich organic matter. The resulting HI is less than 100 and the amount of S2 hydrocarbons are also quite low. Therefore, this sequence has been addressed to organic facies CD.

A high source rock potential (subsequently abbreviated as SRP) is often found in immature sediments relatively rich in organic carbon with a high preservation of lipid-rich organic matter (OM) (e.g. Tissot and Welte, 1984). Such sediments are predominantly found in shallow-marine environments because they provide essential nutrients, high input rates of lipid-rich OM from marine (primary production) and terrestrial sources, and relatively short travel time through the water column. In contrast to many upwelling areas, a significant proportion of lipid-rich organic matter from terrestrial sources, such as sporinite and resinite, may contribute to a high petroleum potential of sediments formed in epicontinental seas and shelf basins. For this reason the exclusive use of organic-geochemical approaches for determining OM sources in near-shore environments may produce contradictory results (e.g. Fahl and Stein, 1999). For adequate quantification the "extracted" information, e.g. obtained from biomarker analysis, is often difficult to interpret without invoking other parameters, e.g. from palynological studies or organic petrography (maceral analysis). Provided that macerals can be distinguished by characteristic properties (good physical preservation), petrographic analysis of organic matter gives a clear association between organic particles and their biological sources. Because time-resolution of maceral data is usually low as a result of expansive preparation, a combination of organic-geochemical, inorganic-geochemical and petrographic analysis has been successfully applied in recent works (e.g. Kim et al., 1999; Boucsein, 2000; Caplan and Bustin, 2001; Wagner, 2002; Langrock et al., 2003a,b). The most significant macerals

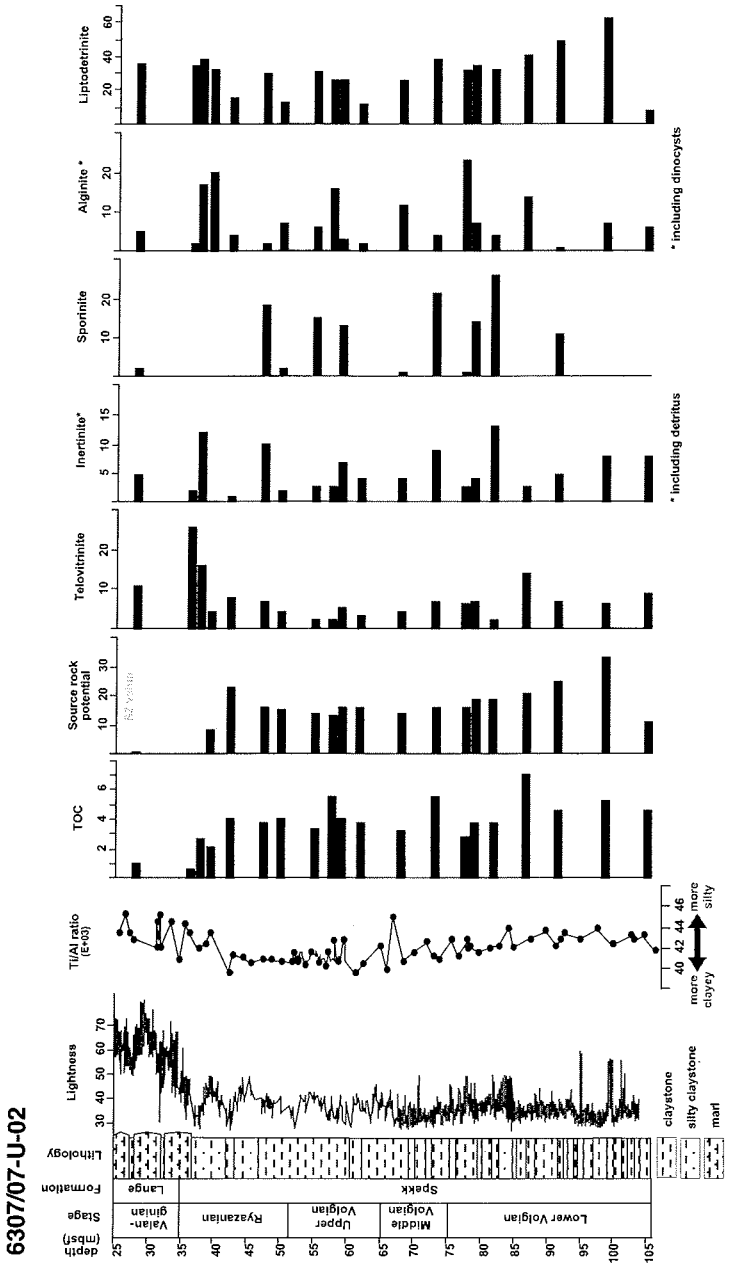

Fig. 4-8 Relationship between source rock potential and selected macerals/maceral groups of core 6307/07-U-02, considering sprectrophotometric L* values (Swientek, 2002) and Ti/Al ratios (cf. Lipinski et al., 2003).

obtained from petrographic analysis were compared to the SRP and supported by sedimentological and inorganic-geochemical data illustrated in Figure 4-8 and 4-9.

The L* value (obtained from photospectrometry) returns the lightness of a sediment as a kind of gray value, which is primarily affected by the fossil and mineral assemblages (cf. Swientek, 2002). Swientek (2002) clearly demonstrates that low L* values, especially the dark color of black shales, do not reflect high organic carbon contents but the abundance of pyrite. On the other hand, increased L* values indicate more sandy and/or calcareous intercalation, which may indeed be associated with a reduced (diluted) TOC content. Figures 4-8 and 4-9 display remarkable, relatively invariable L* values with a mean of about 30 % for the entire Volgian and Ryazanian section. This reflects the abundance of pyrite within the dark-colored, organic-carbon-rich sequences of both cores. Pyrite size distribution has shown that sediments of the Spekk Formation were deposited under more anoxic conditions compared to the Hekkingen Formation (e.g. Langrock et al., 2003b). An increase of L* by more than 20 in the Valanginian-Hauterivian section clearly documents the formation of more light-colored carbonates and marls under more open-marine oxic conditions (e.g. Mutterlose et al., 2003). Even though pyrite formation is favored by the availability of H_2S from anaerobic bacterial utilization of lipid-rich OM, no correlation exists between L* values and the abundance of liptinite.

A more consistent picture can be obtained from the Ti/Al ratio (cf. Lipinski et al., 2003). Almost exclusively derived from the continents, titanium is a heavy metal associated with the SiO_2 (quartz) mineral fraction, whereas aluminum is predominantly found in clay minerals. One way to interpret Ti/Al ratios is that an increasing ratio indicates an increasing proportion of silt and sand. Usually, an increase in mineral grain size indicates an elevated transport energy, which may be associated to higher sedimentation rates. Whether these have positive effects or negative effects (clastic dilution) on the organic carbon accumulation depends largely on the dimension of increase and the general sediment fraction. Since river discharge is climate-controlled by weathering of the hinterland, the Ti/Al ratio may also increase when the input of Al^{3+} from river

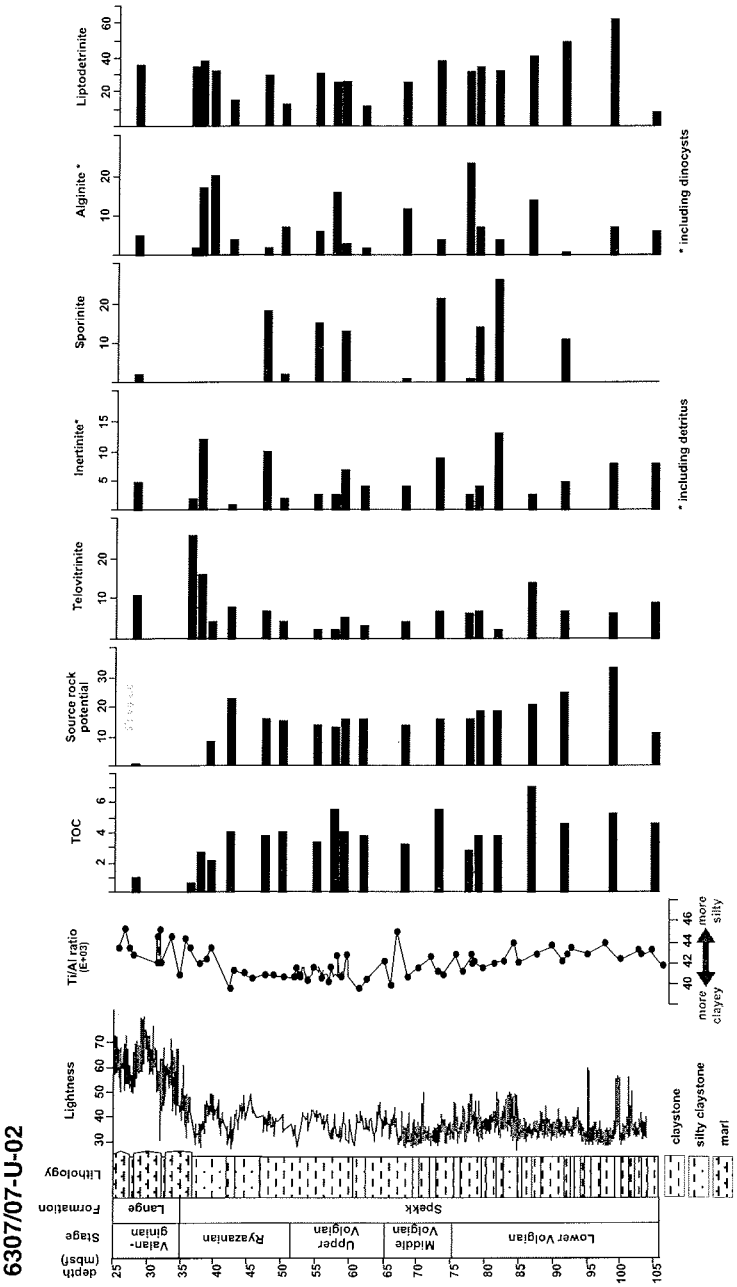

Fig. 4-9 Relationship between source rock potential and selected macerals/maceral groups of core 6814/04-U-02, considering sprectrophotometric L* values (Swientek, 2002) and Ti/Al ratios (cf. Lipinski et al., 2003).

discharge is extremely reduced, e.g. during arid climate periods. Also, the input of Ti^{4+} may become enhanced by (desert-) winds. Such a climate has been suggested for the Valanginian-Hauterivian periods (e.g. Podlaha et al., 1998; Mutterlose and Kessels, 2000; Price et al., 2000; Mutterlose et al., 2003), documented in Figures 4-4 and 4-5. Ti/Al ratios are much higher in core 6814/04-U-02 compared to core 6307/07-U-02, indicating that the sediment is generally much more silty (coarser), which likely results in a dilution of the SRP. In the northern core position, low Ti/Al ratios correspond largely to a high TOC content and high SRP (see arrows). This suggests that organic carbon accumulation and preservation of organic matter with elevated SRP is highest in more fine-grained, argillaceous sediments (low Ti/Al ratio). It may therefore be concluded that more coarse-grained, siliceous sediments (high Ti/Al ratio) reflect dilution of the organic carbon content and the SRP. A less obvious relationship between high TOC values and low Ti/Al ratios is observed in the southern core position. However, the southern core reveals a positive correlation between SRP and Ti/Al ratios on a long-term scale. Hence, it seems that more coarse-grained clastic incursions have a negative influence on the SRP in core 6814/04-U-02 but a rather positive influence in core 6307/07-U-02. This becomes more evident when the SRP is compared to individual macerals. In core 6307/07-U-02, high conformity exists between the SRP and the amount of liptodetrinite, whereas no relationship seems apparent to alginite and sporinite (Fig. 4-8). However, organic petrography has shown that most of the liptodetrinite has been produced from the physical breakdown of different algae. Hence, the correlation between SRP and algae is established indirectly over liptodetrinite. The relationship between SRP and more coarse-grained clastic incursions (see above) is now given more sense by the association with lipid-rich detritus. More silty incursions may reflect higher energy transport and may lead to a higher degree of physical disintegration of algae. The increase of sedimentation rate seems to have no negative effects on the organic carbon content by means of dilution. In the case of core 6814/04-U-02 the SRP is best reflected by the abundance of alginite, which is expected for petroleum source rocks (Fig. 4-9). Based on the above information the SRP and the TOC content

are highest during phases of more fine-grained, less energetic clastic sedimentation. This coincides with the results obtained from maceral analysis because the degree of physical disintegration of algae is lower during more "muddy" sedimentation. Hence, the SRP in this area of deposition seems to originate primarily from preservation of non-detrital, primary alginite (including dinocysts). Sporinite and liptodetrinite have different patterns of occurrence, but contributions may not be excluded.

4.4.3. Sporinite paucity

One of the most important observations related to paleoclimatic changes is the striking paucity of sporinite from the Middle Ryazanian to the Hauterivian and Barremian in both cores (Fig. 4-8, 4-9; cf. Fig. 4-3). A minor paucity is also apparent during the lowermost Volgian. Sporinite originates from the outer cell walls (exines and perines) of spores and pollen and is composed of sporonin (or sporopollenin). This substance is biochemically very resistant and insoluble, but is readily attacked by oxygen under dry conditions, especially in calcareous environments (e.g. Taylor et al., 1998). Keil et al. (1994) found that pollen grains were completely degraded within 10,000 years in the presence of oxygen in the sediment, but were highly preserved for at least 100,000 years under anoxic conditions. A change from anoxic/dysoxic, sapropelic environments in the Volgian to more oxic, calcareous environments in the Valanginian-Hauterivian has been documented for the cores investigated by Lipinski et al. (2003) and Langrock et al. (in press). It may therefore be concluded that biochemical preservation of sporinite is much more affected by the redox conditions of the sediment surface than by the conditions of transportation. Particularly in non-upwelling shelf environments with relatively low sedimentation rates, the travel time of particulate matter in the water may be several orders of magnitude shorter than its residence in the upper sediment layers (e.g. Erlenkeuser, 1980).

In general, marine and brackish sediments are characterized by much smaller amounts of sporinite than sediments formed in freshwater environments

(e.g. Taylor et al., 1998). The abundance of sporinite and other terrigenous liptinites are therefore often used to indicate proximity to the paleo-coast (e.g. Littke et al., 1997). The relatively high abundance and diversity of sporinite of the studied cores, especially in the Spekk Formation (Fig. 4-8), suggest that their positions were generally close to the paleo-coast and may reflect a high level of vegetation, which is usually associated with a more warm and humid climate. Although the paucity of sporinite starts very abruptly, it may be correlated to a rapid sea-level rise and a change from a more warm-humid to a more cold-arid climate that commenced in the Ryazanian and reached its maximum in the Valanginian and Hauterivian (e.g. Podlaha et al., 1998; Price et al., 2000; Mutterlose et al., 2003). A similar paucity of sporinite is also reported from the terrestrial Katharina seam of the Ruhr Carboniferous, which is likely a consequence of severe oxidative degradation by a marine roof succeeding the peat surface. It is therefore suggested that the paucity of sporinite was caused by a combination of (1) increasing distance to the source region, (2) complete oxidation by a rapid marine transgression, and/or (3) a more cool and arid climate.

4.4.4. Depositional environment – stagnation vs. productivity

Calculating the rate at which organic carbon was produced by primary organisms in the photic zone of an ancient ocean is still a puzzling task. A variety of indicators, or proxies, for primary productivity have been suggested, such as accumulation rates of organic carbon, biogenic carbonate, opal flux, and trace elements (e.g. Diester-Haass, 1978; Müller and Suess, 1979; Bralower and Thierstein, 1984; Sarnthein et al., 1987; Stein et al., 1989a, b; Siesser, 1995; Berger and Wefer, 2002; Diester-Haass and Zahn, 2002). The percentage of organic carbon that becomes preserved in the sediment is highly variable and depends on several parameters. In an oxic open-ocean environment with water depths of more than about 1000 meters organic carbon may be so efficiently oxidized that less than 0,1 % may eventually become

incorporated in the sediment (e.g. Brummer and Van Eijden, 1992). For this purpose Stein et al. (1986) proposed equation (1) based on Müller and Suess (1979) for calculating paleoproductivity (PP) in open-marine oxic environments. For details and limits of use of equation (1) see Stein et al. (1986). On the other hand, sediment data largely obtained from the modern anoxic Black Sea show that about 2 % of the organic carbon produced in the surface waters becomes preserved in the sediment. This led Bralower and Thierstein (1986) to suggest equation (2) for calculating paleoproductivities (PP) in general anoxic environments (e.g. Stein, 1991), where PP is the paleoproductivity, C (MOM) is the percentage of marine organic carbon, WBD is the wet bulk density, PO the porosity, LSR the linear sedimentation rate, and DEP is the estimated water depth.

(1) $$PP_{oxic} = 5.31 \bullet (MOM \bullet (WBD - 1.026 * PO/100))^{0.71} \bullet LSR^{0.07} * DEP^{0.45}$$

(2) $$PP_{anoxic} = 50 \bullet C * (WBD - 1.026 * PO/100) * LSR$$

In order to distinguish between oxic and anoxic environments the organic carbon/sedimentation rate relationship is often used (cf. Müller and Suess, 1979; Stein, 1991). However, based on new LSR data presented in Mutterlose et al. (2003) and Swientek (2002) our differentiation has been improved (Fig. 4-10). Moreover, Lipinski et al. (2003) have demonstrated that redox-sensitive rhenium and molybdenum, in particular the Re/Mo ratio, in the investigated cores may allow to distinguish between anoxic, suboxic, and more oxic water conditions (Fig. 4-11, Fig. 4-12). They showed that depositional conditions in core 6814/04-U-02 were much less anoxic compared to core 6307/07-U-02, which coincides with the results presented in the TOC/SR diagram. It was therefore necessary to calculated PP after both equations (1 and 2) to reveal the most reasonable range of paleoproductivity values according to the conditions in the water column.

In the lower black shale sequence of core 6307/07-U-02 (from about 75 m to 105 m depth, Fig. 4-2) surface water productivity may have reached 20 – 30 $gC/m^2/y$ when using equation (2) (Fig. 4-11). Values are much lower than

average productivities estimated for modern coastal environments (50 - 150 gC/m²/y) (e.g. Pinet, 1992; Tissot and Welte, 1984), anoxic sediments from the Quaternary Sea of Japan (120 – 150 gC/m²/y) (e.g. Stein, 1991), and even for sediments (TOC ≥ 4 wt%) from the modern Black Sea (50 – 90 gC/m²/y) (e.g. Shimkus and Trimonis, 1974; Izdar et al., 1987; Calvert and Vogel, 1987).

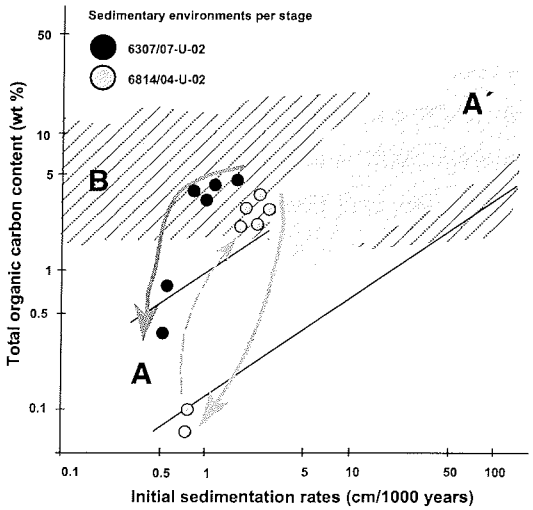

Fig. 4-10 Relationship between (marine) organic carbon content and decompacted sedimentation rates per stage (modified after Stein, 1990, 1991), where different fields of deposition (A=open-marine oxic, A´=high productivity, B=anoxic) are based on results form Recent to Miocene sediments. Each of the circles represent one stage, e.g. the Valanginian. Starting from two different environments the arrows indicate continuous pathways of changes in environmental conditions from the early Volgian to the Hauterivian. Dashed arrow indicates an immediate change of the environment from the Hauterivian to the Barremian in core 6814/04-U-02 back to conditions that once prevailed in the Volgian.

However, our results are much more comparable to the general trend of mid-Cretaceous black shales (e.g. Bralower and Thierstein, 1987), which show exceptionally low average PP_{anoxic} values from 10 to 100 gC/m²/y. This is also a strong indication that the organic carbon accumulation is primarily due to preservation under anoxic conditions, and that anoxia was unlikely to be caused by high productivity, such as may occur in upwelling areas (Thiede and Van Andel, 1977, Demaison and Moore, 1980; Brumsack, 1980, 1987). As a consequence, paleoproductivities calculated after equation (1) are not appropriate for core 6307/07-U-02. Using equation (2) surface water productivity during black shale formation in core 6814/04-U-02 may have reached 10 to 30 gC/m²/y (Fig. 4-12), which is comparable to the other core. But TOC/SR relationship (cf. Fig. 4-10) and Re/Mo ratios indicate that the black shales were unlikely to have been deposited in an anoxic environment, but

rather in a much more dysoxic environment (Fig. 4-12). Therefore, paleoproductivities calculated after equation (1) appear more realistic. Assuming these conditions, surface water productivity calculated for sediments ≥ 2 wt.% TOC may now reach 200 to 350 gC/m²/y, which fall in the range of values for modern upwelling areas (250 – 300 gC/m²/y) (e.g. Pinet, 1992; Romankevich, 1984; Tissot and Welte, 1984). It has to be considered, however, that deep-water conditions were not oxic but rather dysoxic in core 6814/04-U-02, so that PP values may be somewhat overestimated. The result show similarities to average paleoproductivities of marginal upwelling sites off NW-Africa (100 – 300 gC/m²/y) (e.g. Stein et al., 1989a; Stein, 1991).

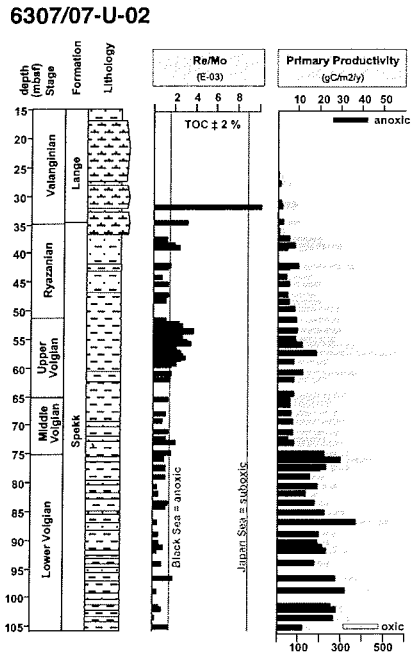

Fig. 4-11 Re/Mo ratios (Lipinski et al., 2003) to discriminate anoxic from dysoxic or oxic environments and paleoproductivity estimates for both oxic (gray) and anoxic (black) conditions for core 6307/07-U-02.

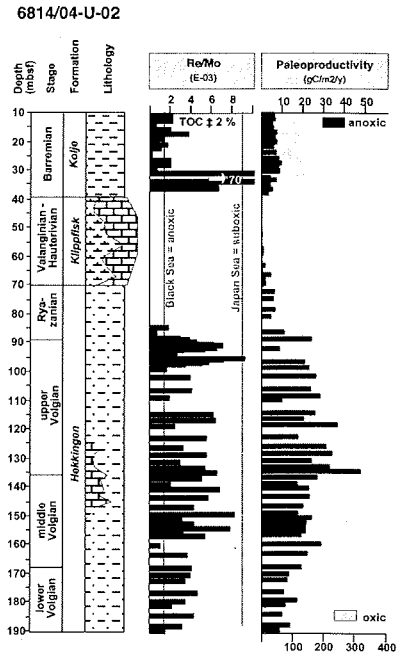

Fig. 4-12 Re/Mo ratios (Lipinski et al., 2003) to discriminate anoxic from dysoxic or oxic environments and paleoproductivity estimates for both oxic (gray) and anoxic (black) conditions for core 6814/04-U-02.

The results suggest that organic carbon accumulation has been primarily enhanced by an elevated downflux of organic carbon in a high-productive

environment (e.g. Pedersen and Calvert, 1990). However, the paleoceanographic position was likely more exposed than restricted (Fig. 4-13), which probably resulted in higher sedimentation rates (higher Ti/Al ratios), higher clastic dilution (lower TOC) and lesser preservation of the lipid-rich OM (lower SRP).

4.5. Summary

Conclusions drawn from all previous microscopic, geochemical, and sedimentological results suggest that oceanographic positions for the cores at the time of sediment deposition, were situated in the margin of the nascent Norwegian Sea (Fig. 4-13). The organic matter in the Ribban Basin site is derived from both marine and terrestrial sources, and the relatively high abundance of recycled "woody" material may reflect a higher degree of oxygenation and a more energetic and/or longer transport from their sources on land. Although the source rock potential is considerably lower (organic facies BC and C), compared to the Hitra Basin site, its variation through time is reflected by the variations in the amount of primary algae, with some uncertain contributions from recycled marine organic matter. This suggests that primary production in the surface water has probably a distinct control on organic carbon accumulation. Since Re/Mo ratios and TOC/SR relationships support a more dysoxic, open-marine environment, estimated surface water productivities are relatively high. The influence of coastal upwelling under oxic to dysoxic deep-water conditions at this site is therefore very likely. This environment results in lower preservation of marine OM, enrichment in refractory OM, and a much lower source rock potential. Large comparability exists to the late Cenozoic ODP site 658 from the marginal upwelling off NW-Africa, suggesting that black shale formation in the Ribban Basin site followed a modification of the "productivity model". The sediments from the Hitra Basin site are characterized by higher amounts of marine and lipid-rich terrigenous organic matter compared to the Ribban Basin site. A high source rock potential (organic facies B and BC)

is positively correlated with the amount of recycled marine organic matter. Supported by low Re/Mo ratios and TOC/SR relationships, the black shales were likely formed in an anoxic, probably stratified basin with low sedimentation rates.

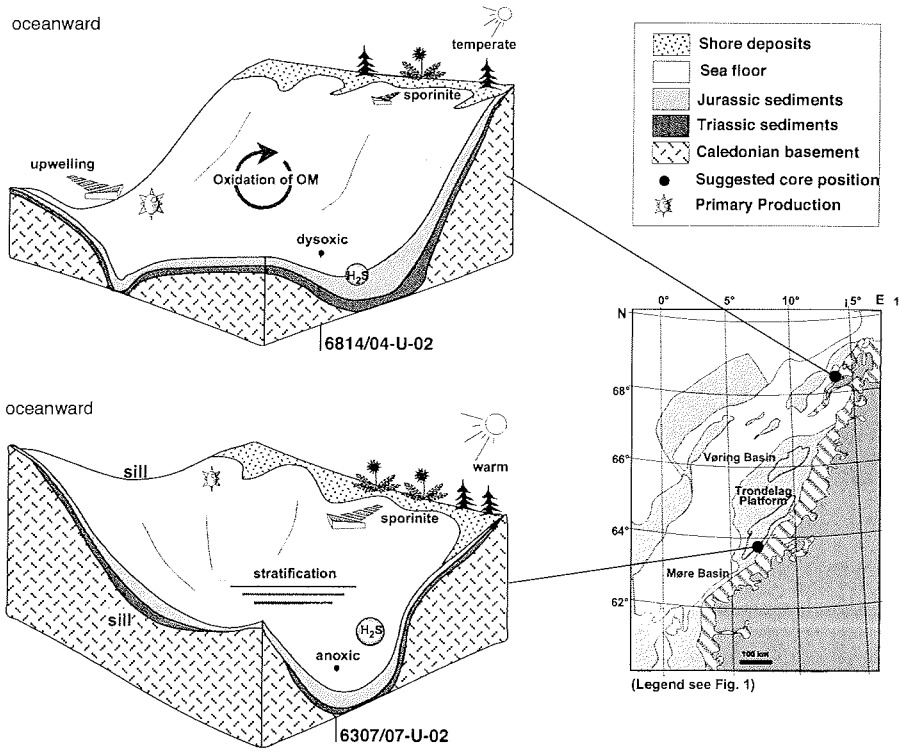

Fig. 4-13 Model for two principally different environments during black shale formation concluded from multiple evidence, suggesting conditions similar to the "stagnation model" for core 6307/07-U-02 and conditions according to the "productivity model" for core 6814/04-U-02. The model does not account for sea-level changes that affect both cores contemporaneously (see Fig. 2, 7).

Therefore, surface water productivity was estimated to be very low compared to modern coastal environments, which is reported from different Cretaceous black shales. Paleoproductivity values are lower than low-productivity areas in the modern Black Sea, but are similar to the nascent Indian Ocean during the

Eocene. Hence, the Hitra Basin site is believed to represent black shale formation following to the "stagnation model".

Acknowledgements

Sintef Petroleum Research (Trondheim) provided all core material and is thanked for their kind co-operation. Steven Hay and one anonymous reviewer are gratefully acknowledged for their comments that helped to improve this contribution. This work was supported financially by the German Science Foundation (grant STE 412/13-1).

5. Summary and outlook

The organic matter in four sediment cores from the Norwegian shelf (near Skagerrak, Trøndelag Platform, Lofoten Islands, south-central Barents Sea) was investigated in order to determine ***origin***, ***transport***, ***accumulation***, and ***preservation*** of organic carbon in the nascent Norwegian-Greenland-Seaway. Each of the sediment cores contain organic carbon-rich sequences, which follow different local and orbital parameters; but all document a significant paleoceanographic long-term change that affected the entire seaway during the Jurassic-Cretaceous transition. One principal objective of this study is also to emphasize the importance of organic petrography and geochemistry in combination with inorganic-geochemical, isotopic, and sedimentological data to find proxies for paleoenvironmental reconstruction.

The transition between the Late Jurassic and the Early Cretaceous provided favorable conditions for the accumulation and preservation of organic carbon along the continental margins of the young and shallow seaway between Norway and Greenland and in the Barents Sea. Because the Scandinavian continental shelf endured as an almost intact unit during previous tectonic episodes in the region, the cores taken along its passive margin reflect more or less the original meridional transect from the northwestern Tethys into the Barents Sea.

The **origin** of the organic matter was well determined by microscopic analysis and supported by data obtained from Rock-Eval pyrolysis and elemental and carbon isotope analysis. As a typical characteristic of shelf sediments the organic matter is derived from both terrestrial and marine sources. A highly variable composition through time reflect regional (tectonic-forced) and/or climatic (orbital-forced) changes in the paleoenvironment. The assemblage of distinct macerals from various sources, with respect to their preservation, may improve to localize and enclose the depositional environment, just like a multi-parameter "positioning system".

For example, the combination of excellently preserved freshwater algae, coal fragments, and vascular particles of higher land plants in the Barents Sea points to a muddy lake or estuarine environment. But the occurrence of marine algae, low sedimentation rates and high trace metal enrichments strongly suggest a formation in a seawater environment. Consequently, a near-shore, probably lagoonal, low-salinity, stagnant and strictly anoxic position has been suggested for a sequence in core 7430/10-U-01. A change in organic matter composition over a specific period of time may have different reasons. In the case of the mid-Norwegian sediments from the Ribban and Hitra Basins, an increasing amount of refractory material reflects a higher efficiency of oxidative fractionation to the debit of the more labile, lipid-rich organic matter and the petroleum potential of the sediments. Additionally, the decreasing particle size is pointing towards an increasing distance to the paleo-coast owing to the proposed rising sea-level.

The conditions of **transportation** are reflected in the sedimentary facies and also in the associated organic matter. On its way from the continental sources to the marginal oceans by wind and water, the organic matter receives different marks, which probably contain information about the regimes passed through. Changes in fluorescence color of lipid-rich organic matter towards longer wavelengths may indicate a longer exposure to oxidative charge, e.g. a longer distance from their sources. Larger particles derived from land plants are more likely transported by water than by wind, but an unbroken leaf may float over hundreds of miles off the shelf, whereas a small heavy ash particle may reach the sea-floor in a matter of days.

This study revealed that along the eastern margins of the nascent NGS fine-grained sediments are preferentially associated with lower sedimentation rates, higher organic carbon contents, higher preservation of lipid-rich organic matter, and (as a result) higher petroleum potential. This is because most organic particles (including bacteria) are hydrodynamically equivalent to the clay and silt fraction. On the other hand, the physical breakdown of lipid-rich OM (represented by the amount of liptodetrinite) seems to play a crucial role in the

formation of petroleum potential in the core from the Hitra Basin on the Trøndelag Platform. Physical disintegration may increase the particle surface by a few orders of magnitude, so probably improving aerobic bacterial activity by a certain degree. Passing a high-standing pycnocline down into anoxic bottom waters may cause decease and incorporation of these bacteria in the sediment, which may contribute to the high petroleum potential found in core 6307/07-U-02.

The **accumulation** rate of organic carbon reflects the authentic organic carbon flux to the sea floor in units of mass per area and time. Avoiding effects of clastic dilution by incorporating the sedimentation rate, it gives a more realistic picture than interpreting mere organic carbon contents. The rate of organic carbon received by the sediment surface is generally low in the investigated sites, reflecting a reduced input from the photic zone and also from the continent. Low accumulation rates of organic carbon are also reported from many mid-Cretaceous black shales formed under oxygen-depleted conditions. Reduced input of terrestrial material through rivers may indicate a lower level of vegetation in the hinterland and/or reduced river activity, which both may be caused by a cooler climate. The postulated low sea-level during this period supports this theory. A seasonal ice cover upon a shallow epicontinental sea caused by reduced salinity, such as in the modern Baltic Sea, may be a possible situation for some core sites along the NGS. This would also probably explain the abundance of well-preserved freshwater algae in the paleo-Barents Sea. However, individual accumulation rates of organic carbon at each site are primarily controlled by the local paleoceanographic framework, such as proximity to coast and rivers, sedimentary facies, water depth, sea floor morphology, and resulting current systems.

Mass accumulation rates of bulk organic carbon in the two mid-Norwegian sites are in a similar range from about 50 to 150 mg/cm^2/ka. However, interpretation of other parameters suggests that black shale formation in the Ribban Basin has likely occurred under more oxic/dysoxic conditions compared to the Hitra Basin, which is supposed as a typical anoxic basin. Hence,

estimations of paleoproductivity point towards an upwelling position for core 6814/04-U-02, which would also fit in the picture obtained from organic petrography.

The **preservation** of organic carbon is particularly good to very good in the lower and middle Volgian (latest Cretaceous) sections, except for core 13/1-U-02, but this is a concept used in different ways. For the sedimentologist, the *preserved* fraction of the organic matter relative to the *recycled* fraction is often defined via the TOC content, which is quite high in the investigated sediment cores and increases towards higher latitudes from about 1 % to more than 30 % by weight. From the petrographic point of view, the organic matter is well preserved when the textures of a large amount of biological precursors are still visible. From a geochemical point of view, organic carbon is well-preserved when high amounts of hydrogen-rich organic matter "survived" or "failed" severe biochemical destruction, so probably generating high petroleum potential during maturation. In general, preservation of organic matter in marine sediments may be enhanced by two principal mechanisms. Oxygen is hereby the ubiquitous source of direct and indirect organic matter destruction and the fate of all living things.

Removing the organic matter quickly from oxidative systems is one possibility, e.g. by rapid burial. This may be in turn realized by two different processes. A higher flux rate of clastic material, which is very common close to deltas and the continental slope, prevents the organic matter from disintegration, but it dilutes the bulk organic carbon signal. On the other hand, higher flux rates of terrestrial material may provoke less bacterial activity, promote preservation, and bulk content of organic carbon. This would result in two sediments with distinct differences in sedimentary and organic facies, but the potential for black shale formation would be indeed low. A modification of the former process seems to be reflected in core 6814/04-U-02 from the Ribban Basin, where a higher flux of inorganic material resulted in a reduced organic carbon content but has still preserved a significant amount of hydrocarbon potential. The latter process is observed in core 13/1-U-02 from the Skagerrak

site, showing a close relationship between the amount of terrestrial "woody" organic matter and the organic carbon accumulation rate.

The second principal mechanism for OM preservation is anoxia. Anoxia emerges when the demand for oxygen by aerobic bacteria exceeds the supply. In this case utilization of organic matter is taken over by anaerobic bacteria using largely SO_4^{2-} as their oxygen source. These bacteria return H_2S as a by-product, which is toxic to most species and may also have a snowballing effect on the water column. Despite that remineralization of OM by anaerobic bacteria may be less efficient, the most important consequence seems to be the desolation of benthic life. However, anoxic bottom waters may be generated by two general means. Provided that renewal of water masses is inhibited, e.g. by a stratified water column in an isolated basin, anoxia may occupy a persistent part of the bottom-water that may reach up into the photic zone. These "stagnant" conditions are suggested during black shale formation at the locations represented by core 6307/07-U-02 from the Hitra Basin and core 7430/10-U-01 from the Barents Sea. Anoxia may also emerge right below the photic zone, e.g. in the high-productive surface waters of upwelling areas. When this oxygen minimum zone impinges on the seafloor, e.g. on the continental slope, a momentary anoxic to dysoxic bottom water is established that may have similar effects on the benthic. Since the oxygen depletion in this position may be less severe and permanent compared to a silled anoxic puddle, it has been suggested for black shale formation at the location represented by core 6814/04-U-02 from the Ribban Basin.

For the first time, high-resolution analysis was applied to small intervals of the sediments from the Hitra Basin, Ribban Basin, and the Barents Sea that are supposed to encompass the Jurassic-Cretaceous transition. Figure 5-1 illustrates variations of the hydrocarbon potential (S2 value) obtained from Rock-Eval pyrolysis for sections 53 to 59 meters in core 6307/07-U-02, 88 to 96 meters in core 6814/04-U-02, and 49.97 to 50.81 meters in core 7430/10-U-01 (zoomed out sections). All sections show a similar trend of S2 values with a pronounced long-term minimum close to the Jurassic-Cretaceous boundary

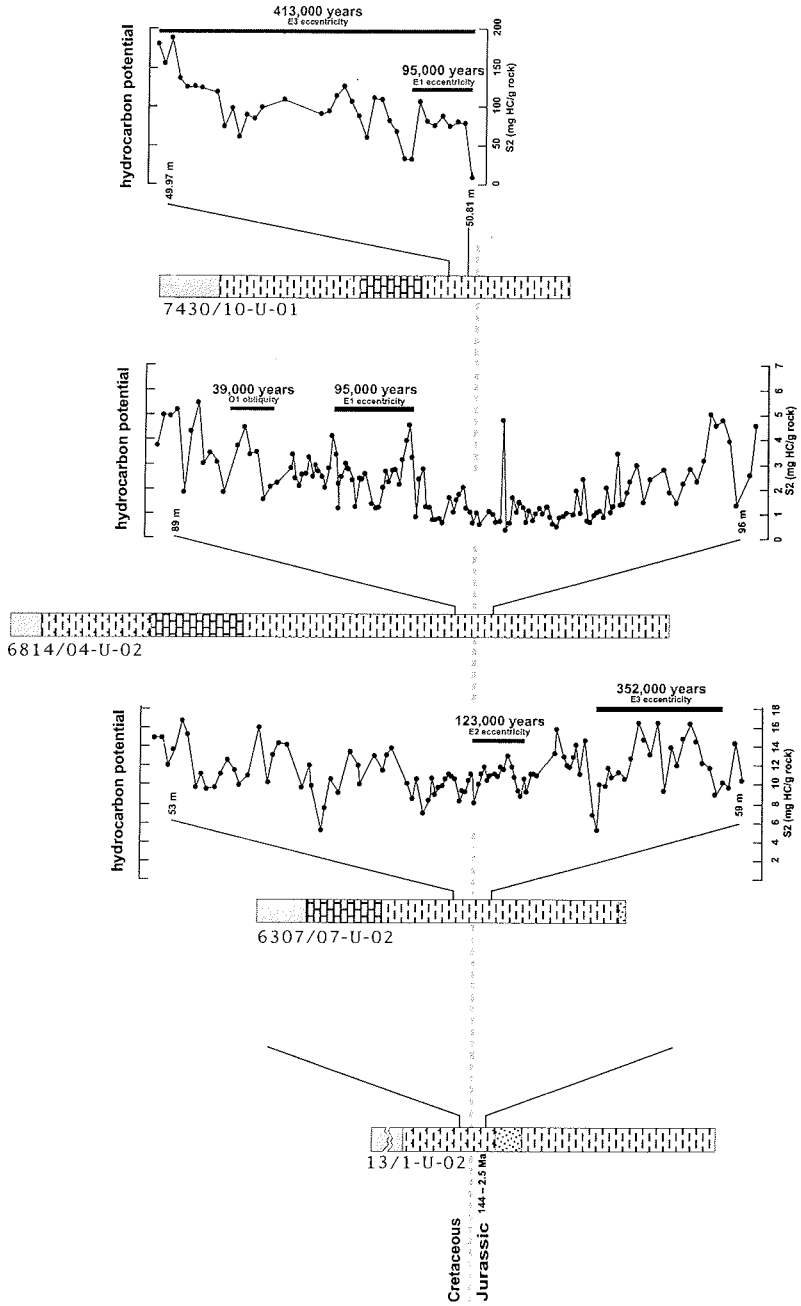

Fig. 5-1 Results from high-resolution analysis applied to the cores investigated during this study, allowing access to orbital-forced climate cycles. Correlation with other parameters, such as trace metal enrichments, stable isotopes, organic matter, and biomarkers may be subject of upcoming studies.

(dashed line). High-resolution analysis also increased the chance to unmask variations that respond to climate changes, i.e. to detect Milankovitch cycles. Based on sedimentation rate estimates and cyclicity analysis made by Swientek (2002), various cycles, such as a distinct eccentricity, were identified in the high-resolution sections (Fig. 5-1).

To unravel the fate of organic material, considering the complexity of all processes that play important roles in the global carbon cycle, is still a big challenge and crucial to the understanding of continent-ocean interactions. With respect to very low sedimentation rates and the age of these sediments, the results are very promising and may be both incitement and basis for further studies. Particularly the combination of organic-geochemical/organic-petrographic studies and the analysis of fossil biomolecules, or biomarkers, seems to be a very reasonable aim in view of determining the origin of organic matter in marine sediments. This study is a decent contribution to the insight of black shale formation by presenting unusual examples from high northern paleolatitudes during the Jurassic-Cretaceous transition.

6. References

ARTHUR, M.A., SCHLANGER, S.O., & JENKYNS, H.C. (1987): The Cenomanian-Turonian oceanic anoxic event, II. Palaeoceanographic controls on organic-matter production and preservation. In: BROOKS J & FLEET A (Eds.), Marine Petroleum Source Rocks. Geological Society Special Publication 26: 401–420.

ARTHUR, M.A., DEAN, W.E., & CLAYPOOL, G.E. (1985): Anomalous ^{13}C enrichment in modern marine organic carbon, *Nature*, 315, 216–218.

BARRON, E.J., HARRISON, C.G.A., SLOAN, J.L. & HAY, W.W. (1981): Paleogeography, 180 million years ago to the present. *Eclogae Geol. Helv.* 74: 443-470.

BERGER, A., IMBRIE, J., HAYS, J., KUKLA, G.T. & SALTZMAN, B. (Eds., 1984): Milankovitch and Climate: Understanding the Response to Astronomical Forcing, NATO ASI Series, 126, Parts 1 + 2, D. Reidel, Dordrecht.

BERGER, W.H. AND WEFER, G. (2002): On the reconstruction of upwelling history: Namibia upwelling in context. Marine Geology 180: 3-28.

BERGER, A. (1977): Support for the astronomical theory of climate change. Nature, 269: 44-45.

BERNER, R. A. (1984): Sedimentary pyrite formation: An update. Geochimica et Cosmochimica Acta 48: 605 – 615.

BERNER, R.A. & RAISWELL, R. (1983): Burial of organic carbon and pyrite sulfur in sediments over Phanerozoic time: a new theory. Geochimica et Cosmochimica Acta 47: 855 – 862.

BITTERLI, P. (1963): Aspects of the genesis of bituminous rock sequences. Geologie en Mijnbouw, 42, 6: 183-201.

BOUCSEIN, B. (2000): Organic carbon in Late Quaternary sediments: Responses to paleoenvironmental chenges in the Laptev and Kara seas (Arctic Ocean), PhD thesis, Alfred Wegener Institute for Polar and Marine Research, Berichte zur Polarforschung 365, 103 pp.

BOUSSAFIR, M. AND LALLIER-VERGÈS, E. (1997): Accumulation of organic matter in the Kimmeridge Clay Formation (KCF): an update fossilisation model for marine petroleum source-rocks, Marine and Petroleum Geology 14: 75-83.

BOYD, P.W., WATSON, A.J., LAW, C.S., ABRAHAM, E.R., TRULL, T., MURDOCH, R., BAKKER, D.C.E., BOWIE, A.R., BUESSELER, K.O., CHANG, H., CHARETTE, M., CROOT, P., DOWNING, K., FREW, R., GALL, M., HADFIELD, M., HALL, J., HARVEY, M., JAMESON, G., LAROCHE, J., LIDDICOAT, M., LING, R., MALDONADO, M.T., MCCAY, R.M., NODDER, S., PICKMERE, S., PRIDMORE, R., RINTOUL, S., SAFI, K., SUTTON, P., STRZEPEK, R., TANNEBERGER, K., TURNER, S., WAITE, A. & ZELDIS, J. (2000): A mesoscale phytoplankton bloom in the polar Southern Ocean stimulated by iron fertilization, Nature 407: 695–702.

BRALOWER, T.J. & THIERSTEIN, H.R. (1987): Organic carbon and metal acumulation rates in Holocene and mid-Cretaceous sediments: paleoceanographic significance. In: BROOKS, J. & FLEET, A. (Eds.): Marine Petroleum Source Rocks. Geological Society Special Publication 26: 345–369.

BREKKE, H.D. (2000): The Tectonic evolution of the Norwegian Sea continental margin with emphasis on the Vøring and Møre basins. Geol. Soc. Spec. Publ. 167: 327-378.

BREKKE, H.D., DAHLGREN, S., NYLAND, B., & MAGNUS, C. (1999): The prospectivity of the Vøring and Møre basins on the Norwegian Sea continental margin. In: FLEET, A.J. & BOLDY, S.A.R. (Eds): Petroleum Geology of Northwest Europe. Proceedings of the 5th Conference: 261–274.

BRUMMER, G.J.A. AND VAN EIJDEN, A.J.M. (1992): "Blue-ocean" paleoproductivity estimates from pelagig carbonate mass accumlation rates. In: G.J. van der Zwaan, F.J. Jorissen and W.J. Zachariasse (Eds.), Approaches to Paleoproductivity Reconstructions. Marine Micropaleontology, 19: 99-117.

BRUMSACK, H.-J. (1980): Geochemistry of Creataceous black shales from the Atlantic Ocean. Chemical Geology 31: 1–25.

BRUMSACK, H.J. (1987): The inorganic geochemistry of Cretaceous black shales (DSDP Leg 41) in comparison to modern upwelling sediments from the Gulf of California. In: SUMMERHAYES, C.P. & SHACKLETON, N.J. (Eds.): North Atlantic Palaeoceanography, Geological Society Special Publication 21: 447–462.

BRUMSACK, H.J. (1989): Geochemistry of Recent TOC-rich sediment from the Gulf of California and the Black Sea, Geologische Rundschau 78: 851-882.

BRUMSACK, H.-J. AND THUROW, J. (1986): The Geochemical facies of black shales from the Cenomanian/Turonian boundary event (CTBE), Mitt. Geol.-Paläont. Inst. Univ. Hamburg, SCOPE/UNEP Sonderband, 60: 247-265.

BUGGE, T., ELVEBAKK, G., BAKKE, S., FANAVOLL, S., LIPPARD, S., LEITH, T.L., MANGERUD, G., MÖLLER, N., NILSSON, I., RØMULD, A., SCHOU, L., VIGRAN, J.O., WEISS, H.M. & ÅRHUS, N. (Eds., 1989): Shallow drilling Barents Sea 1988. Trondheim, Norway: IKU report: 309 p.

BUGGE, T., ELVEBAKK, G., FANAVOLL, S., MANGERUD, G., SMELROR, M., WEISS, H.M., GJELBERG, .J, KRISTENSEN, S.E. & NILSEN, K. (2002): Shallow stratigraphic drilling applied in hydrocarbon exploration of the Nordkap Basin, Barents Sea. Marine and Petroleum Geology 19: 13-37.

BUSTIN, R.M. & BARNES, M.A. (1988): Determining levels of organic diagenesis in sediments and fossil fuels. Diagenesis, Geoscience Canada Reprint Series 12: 205–226.

CALVERT, S.E. (1987): Oceanographic controls on the accumulation of organic matter in marine sediments. In: BROOKS, J. & FLEET, A. (Eds.): Marine Petroleum Source Rocks. Geological Society Special Publication 26: 137–151.

CALVERT, S.E. & PEDERSEN, T.F. (1992): Organic Carbon Accumulation and Preservation in Marine Sediments: How important is anoxia? In: WHELAN, J.K. & FARRINGTON, J.W. (Eds.): *Organic Matter: Productivity, Accumulation, and Preservation in Recent and Ancient Sediments*, Columbia University Press: 533 p.

CALVERT, S.E. & VOGEL, J.S. (1987): Carbon accumulation rates and the origin of the Holocene sapropel in the Black Sea. Geology 15: 918–921.

CAPLAN, M.L. & BUSTIN, R.M. (1998): Paleoceanographic controls on geochemical characteristics or organic-rich Exshaw mudrocks: role of enhanced primary production, Organic Geochemistry 30: 161–188.

CAPLAN, M.L. AND BUSTIN, R.M., 2001. Paleoenvironmental and paleoceanographic controls on black, laminated mudrock deposits: examples from Devonian-Carboniferous strata, Alberta, Canada. Sedimentary Geology, 145: 45-72.

COMBAZ, A. (1980): Les kerogenes vus au microscope. Kerogens seen under a microscope. In: Durand, B., Kerogen; insoluble organic matter from sedimentary rocks. Ed. Technip, Paris (France): 55-112.

COPLEN, T.B. (1995): Reporting of stable carbon, hydrogen, and oxygen isotopic abundances. In: IAEA-TECDOC-825, IAEA, Vienna. Reference and intercomparison materials for stable isotopes of light elements: 31-34.

CORNFORD, C., GARDNER, P. & BURGESS, C. (1998): Geochemical truths in large data sets. I: Geochemical screening data, Organic Geochemistry 29: 519–530.

DE GRACIANSKY, P.C., BROSSE, E., DEROO, G., HERBIN, J.P., MONTADERT, L., MÜLLER, C., SIGAL, J. & SCHAAF, A. (1987): Organic-rich sediments and paleoenvironmental reconstructions of the Cretaceous North Atlantic. In: BROOKS, J. & FLEET, A. (Eds.): Marine Petroleum Source Rocks. Geological Society Special Publication 26: 317–344.

DE GRACIANSKY, P.C., DEROO, G., HERBIN, J.P., MONTADERT, L., MÜLLER, C., SCHAAF, A. & SIGAL, J. (1984): Ocean-wide stagnation episode in the late Cretaceous, *Nature* 308: 346–349.

DEAN, W.E. & ARTHUR, M.A. (1989): Iron-sulfur-carbon relationships in organic-carbon-rich sequences: Cretaceous western interior seaway. American Journal of Science 289: 708–743.

DEAN, W.E. & ARTHUR, M.A. (1999): Sensitivity of the North Atlantic Basin to cyclic climatic forcing during the Early Cretaceous. Journal of Foraminiferal Research 29: 465–486.

DEAN, W.E., ARTHUR, M.A. & CLAYPOOL, G.E. (1986): Depletion of ^{13}C in Cretaceous Marine Organic Matter: Source, Diagenetic, or Environmental Signal? Marine Geology 70: 119–157.

DEAN, W.E. & GARDNER, J.M. (1994): Geochemical evidence for enhanced preservation of organic matter in the oxygen minimum zone of the continental margin of northern California during the late Pleistocene. Paleoceanography 9: 47–61.

DEGENS, E.T., BEHRENDT, M. ET AL. (1968): Metabolic fractionation of carbon isotopes in marine plankton-II: Data on samples collected off the coasts of Peru and Ecuador. Deep-Sea Research 15: 11–20.

DEMAISON, G.J. & MOORE, G.T. (1980): Anoxic environments and oil source bed genesis. Organic Geochemistry 2: 9–31.

DIESTER-HAASS, L. AND ZAHN, R. (2001): Paleoproductivity increase at the Eocene-Oligocene climatic transition: ODP/DSDP sites 763 and 592, Paleogeography, Paleoclimatology, Paleoecology 172: 153-170.

DIESTER-HAASS, L. (1978): Sediments as indicators of upwelling. In: R. Boje and M. Tomczak (eds.), Upwelling Ecosystems. Springer, Berlin, pp. 261-281.

DORÉ, A.G. (1991): The structural foundation and evolution of Mesozoic seaways between Europe and the Arctic. In: CHANNEL, J.E.T., WINTERER, E.L. & JANSA, L.F. (Eds.): Paleogeography and paleoceanography of the Tethys. Paleogeography, Paleoclimatology, Paleoecology 87: 441–492

DORÉ, A.G., LUNDIN, E.R., BIRKELAND, Ø., ELIASSEN, P.E., & JENSEN, L.N. (1997): The NE Atlantic margin: implications of late Mesozoic and Cenozoic events for hydrocarbon prospectivity, Petroleum Geoscience: 2, 117–131.

DOTT, R.H. JR. & BATTEN, R.L. (1981): Evolution of the Earth, McGraw Hill, New York, 113 p.

DYPVIK, H. & ATTREP, M. JR. (1999): Geochemical signals of the late Jurassic, marine Mjølnir impact, Meteorites & Planetary Science 34: 393–406.

DYPVIK, H. & FERRELL, R.E. JR. (1998): Clay mineral alteration associated with a meteorite impact in the marine environment (Barents Sea), Clay Minerals 33: 51–64.

DYPVIK, H. & HARRIS, N.B. (2001): Geochemical facies analysis of fine-grained siliciclastic using Th/U, Zr/Rb and (Zr+Rb)/Sr ratios, *Chemical Geology* 181: 131-146.

DYPVIK, H., GUDLAUGSSON, S.T., TSIKALAS, F., ATTREP, M. JR., FERRELL, R.E. JR., KRINSLEY, D.H., MØRK, A., FALEIDE, J.I. & NAGY, J. (1996): Mjølnir structure: An impact crater in the Barents Sea. Geology 24: 779–782.

ENGLEMAN, E.E., JACKSON, L.L. & NORTON, D.R. (1985): Determination of carbonate in geological materials by coulometric titration. Chemical Geology 53: 125-128.

ERBACHER, J., HUBER, B.T., NORRIS, R.D. & MARKEY, M. (2001): Increased thermohaline stratification as a possible cause for an ocean anoxic event in the Cretaceous period. Nature 409: 325-327.

ERLENKEUSER, H. (1980): 14C age and vertical mixing of deep-sea sediments, Earth and Planetary Science Letters, 47, (3): 319-326.

ESPITALIÉ, J., LAPORTE, J.L., MADEC, M., MARQUIS, F., LEPLAT, P., PAULET, J. & BOUTEFEU, A. (1977): Source rock characterization method for petroleum exploration. Proceedings of the 9th Annual Offshore Technology Conference 3: 439–443.

FAHL, K. AND STEIN, R. (1999. Biomarkers as organic-carbon-source and environmental indicators in the Late Quaternary Arctic Ocean: Problems and Perspectives. Marine Chemistry, 63: 293-309.

FJERDINGSTAD, V., ÅRHUS, N., BUGGE, T., ELVEBAKK, G., FANAVOLL, S., HELGESEN, I.K., LEITH, T.L., SCHOU, L., SÆTTEM, J., AND VIGRAN, J.O., 1985. Shallow drilling Barents Sea, IKU report, Trondheim, Norway, 124 pp.

FRANCE-LANORD, C. & DERRY, L.A. (1994): $\delta^{13}C$ of organic carbon in the Bengal Fan: Source evolution and transport of C3 and C4 plant carbon to marine sediments. Geochimica et Cosmochimica Acta 58: 4809–4814.

FRY, B., BRAND, W., MERSCH, F.J., THOLKE, K. & GARRITT, R. (1992): Automated analysis system for coupled $\delta^{13}C$ and $\delta^{15}N$ measurements. Analytical Chemistry 64: 288–291.

FUECHTBAUER, H. (Ed., 1988): Sedimente und Sedimentgesteine, Sediment-Petrologie Teil II, 4. Auflage, Stuttgart: Schweizerbart, 1141 p.

GRADSTEIN, F.M., AGTERBERG, F.P., OGG, J.G., HARDENBOL, J., VAN VEEN, P., THIERRY, J. & HUANG, Z. (1995): A Triassic, Jurassic and Cretaceous time scale. In: BERGGREN, W.A., KENT, D.V., AUBRY, M.P. & HARDENBOL, J. (Eds.): Geochronology, timescales and global stratigraphic correlation. SEPM Special Publication 54: 95-126.

GUDLAUGSSON, S.T. (1993): Large impact crater in the Barents Sea. Geology 21: 291–294.

HALLAM, A. (1987): Mesozoic organic-rich shales. In: BROOKS, J. & FLEET, A. (Eds.): Marine Petroleum Source Rocks. Geological Society Special Publication 26: 251–269.

HALLAM, A. & WIGNALL, P.B. (1999): Mass extinctions and sea-level changes. Earth Science Reviews 48: 217–250.

HANSEN, J.W., BAKKE, S., FANAVOLL, H., LØSETH, H., MØRK, A., MØRK, M.B.E., RISE, L., SMELROR, M., VERDENIUS, J.G., VIGRAN, J.O. & WEISS, H.M. (1991): Shallow drilling Nordland VI and VII 1991, Trondheim, IKU-Report : 390 p.

HAQ, B.U., HARDENBOL, J. & VAIL, P.R. (1988) : Mesozoic and Cenozoic chronostratigraphy and cycles of sea-level change. In: WILGUS, C.K., HASTINGS, B.S., KENDALL, C.G.ST.C., POSAMENTIER, H.W., ROSS, C.A. & VAN WAGONER, C. (Eds.): Sea level Changes: An Integrated Approach. Soc Econ Petrol Min Spec Publ 42: 71–108.

HARDENBOL, J., THIERRY, J., FARLEY, M.B., JACQUIN, T., DE GRACIANSKY, P.C., VAIL, P.R. (1998): Mesozoic and Cenozoic sequence chronostratigraphic framework of European basins. In: DE GRACIANSKY, P.C., HARDENBOL, J., THIERRY, J. & VAIL, P.R. (Eds.): Mesozoic and Cenozoic Sequence Stratigraphy of European Basins, Soc Sed Geol Spec Publ 60: 7–14.

HAY, W.W. (1995): Cretaceous Paleoceanography. Geologica Carpathica 46: 257–266.

HAY, W.W. (1998): Detrital sediment fluxes from the continent to the oceans, Chemical Geology 145: 287–323.

HAY, W.W., DE CONTO, R.M., WOLD, C.N., WILSON, K.M., VOGT, S., SCHULTZ, M., WOLD-ROSSBY, A., DULLO, W.-C., RONOV, A.B., BALUKHOVSKY, A.N. & SÖDING, E. (1999): Alternative global Cretaceous paleogeography. In: BARRERA, E. & JOHNSON, C.C. (Eds.): Evolution of the Cretaceous ocean-climate system. Geological Society of America 332: 1-47.

HERRLE, J.O., PROSS, J., FRIEDRICH, O., KÖSSLER, P. AND HEMLEBEN, C. (2003): Forcing mechanisms for mid-Cretaceous black shale formtion: evidence from the Upper Aptian and Lower Albian of the Vocontian Basin (SE France), Paleogeography, Paleoclimatology, Paleoecology 190: 399-426.

HINRICHS, J., SCHNETGER, B., SCHALE, H. & BRUMSACK, H.-J. (2001): A high resolution study of NE Atlantic sediments at station Bengal: geochemistry and early diagenesis of Heinrich layers, *Marine Geology* 177: 79–92.

HOCHULI, P.A., COLIN, J.P., VIGRAN, J.O. (1989): Triassic biostratigraphy of the Barents Sea area. *In* Collinson, J.D. (ed.), *Correlation in Hydrocarbon Exploration, Norwegian Petroleum Society*, Graham & Trotman, 131-153.

HOFMANN, P., RICKEN, W., SCHWARK, L. & LEYTHAEUSER, D. (2000): Carbon-sulfur-iron relationships and $\delta^{13}C$ of organic matter for late Albian sedimentary rocks from the North Atlantic Ocean: paleoceanographic implications, *Palaeoceanography, Palaeoclimatology, Palaeoecology* 163: 97–113.

HÖLEMANN, J.A. & HENRICH, R. (1994): Allochthonous versus autochthonous organic matter in Cenozoic sediments of the Norwegian Sea: Evidence for the onset of glaciations in the northern hemisphere. Marine Geology 121: 87-103.

HOLTVOETH J., WAGNER, T., HORSFIELD, B., SCHUBERT, C.J. & WAND, U. (2001): Late Quaternary supply of terrigenous organic matter to the Congo Deep Sea Fan (ODP Site 1075): Implications for equatorial African paleoclimate. Geo-Marine-Letters 21: 23–33.

HORSFIELD, B., YORDY, K.L., & CRELLING, J.C. (1988): Determining the petroleum-generating potential of coal using organic geochemistry and organic petrology. In: MATTAVELLI, L. & NOVELLI, L. (Eds.): Advances in organic geochemistry 1987; Part I, Organic geochemistry in petroleum exploration; proceedings of the 13th international meeting on organic geochemistry, Organic Geochemistry 13: 121–129.

HORSFIELD, B., CURRY, D.J., BOHACS, K., LITTKE, R., RULLKÖTTER, J., SCHENK, H.J., RADKE, M., SCHAEFER, R.G., CARROLL, A.R., ISAKSEN, G. & WITTE, E.G. (1994): Organic Geochemistry of freshwater and alkaline lacustrine sediments in the Green River Formation of the Washakie Basin, Wyoming, USA, Organic Geochemistry 22: 415–440.

HUFFMAN, E.W.D.JR. (1977): Performances on a new automatic carbon dioxide coulometer, *Microchemical Journal* 22: 567-573.

IZDAR, E., KONUK, T., ITTEKKOT, V., KEMPE, S. & DEGENS, E.T. (1983): Particle flux in the Black Sea: Nature of the organic matter, in DEGENS, E.T. ET AL. (eds.), Particle Flux in the Ocean, Mitt. Geol. Pal. Inst., Hamburg University, Vol. 62, p. 1 – 18.

JOHANSEN, S.E., OSTISTY, B.K., BIRKELAND, Ø., FEDOROVSKY, Y.F., MARTIROSJAN, V.N., BRUUN CHRISTENSEN, O., CHEREDEEV, S.I., IGNATENKO, E.A. & MARGULIS, L.S. (1990): Hydrocarbon potential in the Barents Sea region; play distribution and potential. In: VORREN, T.O., BERGSAGER, E., DAHL-STAMNES, Ø.A., HOLTER, E., JOHANSEN, B., LIE, E. & LUND, T.B. (Eds.): Arctic Geology and Petroleum Potential – proceedings of the Norwegian Petroleum Society conference. Norwegian Petroleum Society (NPF) Special Publication 2: 273-320

JONES, R.W. (1987): Organic Facies. In: Welte, D.H. (ed.). Advances in Petroleum Geochemistry 2: 1-89.

JONGEPIER, K., MACLEOD, K.G. & WING, S.L. (Eds.) (1996): Triassic to early Cretaceous stratigraphic and structural development of the northeastern Møre Basin margin, off Mid-Norway, Norsk Geologisk Tidsskrift, 76, p. 199 – 214.

KEIL, R.G., HU, F.S., TSAMAKIS, E.C., HEDGED, J.I. (1994): Pollen in marine sediments as an indicator of oxidation of organic matter. Nature, 369, No. 6482: 639-641.

KIM, J., WAGNER, T., BACHMANN, M., AND KUSS, J. (1999): Organic facies and thermal maturity of Late Aptian to Early Cenomanian shelf deposits, Northern Sinai (Egypt). Int. J. Coal Geology, 39: 251-278.

LANGFORD, F.F. & BLANC-VALLERON, M.M. (1990): Interpreting rock-eval-pyrolysis data using graphs of pyrolysable hydrocarbons vs. total organic carbon, AAPG Bulletin 74, 799 – 804.

LANGROCK, U. & STEIN, R. (2001): Organic matter preservation and paleoenvironmental implications for Lower Cretaceous marine sapropels from the Norwegian and Barents Sea shelf, European Union of Geosciences – EUG XI, Journal of Conference Abstracts 6: 196-197

LANGROCK, U., STEIN, R., LIPINSKI, M. & BRUMSACK, H.-J. (2003 a): Paleoenvironment and sea-level change in the early Cretaceous Barents Sea – implications from near-shore marine sapropels, Geo-marine letters, 23 (1): 34-42, DOI 10.1007/s00367-003-0122-5.

LANGROCK, U., STEIN, R., LIPINSKI, M. & BRUMSACK, H.-J. (2003 b): Late Jurassic to Early Cretaceous black shale formation and paleoenvironment in high northern latitudes – examples from the Norwegian-Greenland-Seaway, Paleoceanography, DOI: 10.1029/2002PA000867.

LANGROCK, U. AND STEIN, R. (in press): Origin of marine petroleum source rocks from the Late Jurassic to Early Cretaceous Norwegian Greenland Seaway – evidence for stagnation and upwelling. Marine and Petroleum Geology.

LARSEN, R.M., FJÆRAN, T. & SKARPNES, O. (1990): Hydrocarbon potential of the Norwegian Barents Sea based on recent well results. In: VORREN, T.O., BERGSAGER, E., DAHL-STAMNES, Ø.A., HOLTER, E., JOHANSEN, B., LIE, E. & LUND, T.B. (Eds.): Arctic Geology and Petroleum Potential – proceedings of the Norwegian Petroleum Society conference. Norwegian Petroleum Society (NPF) Special Publication 2: 321-331

LARSON, R.L. (1991a): Latest pulse of Earth: evidence for a mid-Cretaceous superplume. Geology 19, 547-550.

LARSON, R.L. (1991b): Geological consequences of superplumes. Geology 19, 963-966

LEITH, T.L., WEISS, H.M., MØRK, A., ÅRHUS, N., ELVEBAKK, G., EMBRY, A.F., BROOKS, P.W., STEWARD, K.R., PCHELINA, T.M., BRØ, E.G., VERBA, M.L., DANYUSHEVSKAYA, A. & BORISOV, A.V. (1990): Mesozoic hydrocarbon source-rocks of the Arctic region, In: VORREN, T.O., BERGSAGER, E., DAHL-STAMNES, Ø.A., HOLTER, E., JOHANSEN, B., LIE, E. & LUND, T.B. (Eds.): Arctic Geology and Petroleum Potential – proceedings of the Norwegian Petroleum Society conference. Norwegian Petroleum Society (NPF) Special Publication 2: 1-25

LEVENTHAL, J. S. (1983): An interpretation of carbon and sulfur relationships in Black Sea sediments as indicators of environments of deposition. Geochimica et Cosmochimica Acta, 47: 133 – 137.

LIPINSKI, M., WARNING, B. AND BRUMSACK, H.-J. (2003): Trace metal signatures of Jurassic/Cretaceous black shales from the Norwegian Shelf and the Barents Sea, Paleogeography, Paleoclimatology, Paleoecology 190: 459-475.

LIPPARD, S. & ROKOENGEN, K. (1989): *Report 21.3460.00/01.89 Shallow drilling Farsund Subbasin 1988/89: Bedrock mapping and evaluation of potential coring sites*, 47 pp., IKU Trondheim.

LITTKE, R. (1993): Deposition, diagenesis, and weathering of organic matter-rich sediments. Lecture Notes in Earth Science, 47: 216 pp.

LITTKE, R., BAKER, D.R. & RULLKÖTTER, J. (1997): Deposition of Petroleum Source Rocks. In: WELTE, H.D., HORSFIELD, B. & BAKER, D.R. (Eds.): Petroleum and Basin Evolution, Insights from Petroleum Geochemistry. Geology and Basin Modeling, Berlin Heidelberg New York: Springer, 273–333

LUECKGE, A.B., LALLIER-VERGÈS, M. & LITTKE, R. (1996): Comparative study of organic matter preservation in immature sediments along the continental margins of Peru and Oman. Part I: Results of petrographical and bulk geochemical data. Organic Geochemistry, 24 (4): 437 – 451.

LÜNIGER, G. & SCHWARK, L. (2002): Characterization of sedimentary organic matter by bulk and molecular geochemical proxies: an example from an Oligocene maar-type Lake Enspel, Germany, *Sedimentary Geology*, 148, 1-2: 275 – 288.

LUNDIN, E. AND DORÉ, A.G. (2001): Mid-Cenozoic post-breakup deformation in the "passive" margins bordering the Norwegian-Greenland Sea. *Marine and Petroleum Geology*,

LYONS, P.C. (2000): Funginite and secretinite – two new macerals of the inertinite maceral group, *International Journal of Coal Geology*, 44, 95 – 98.

MEYERS, P.A. (1997): Organic geochemical proxies of paleoceanographic, paleolimnologic, and paleoclimatic processes. Organic Geochemistry 27: 213-250.

MILTNER, A. & EMEIS, K.-C. (2000): Origin and transport of terrestrial organic matter from the Oder lagoon to the Arkona Basin, Southern Baltic Sea, Organic Geochemistry 31, 57-66.

MØRK, A. & SMELROR, M. (1999): Correlation and non-correlation for high order circum-Arctic Mesozoic Sequences, Manuscript.

MÖSLE, B., COLLINSON, M.E., FINCH, P., STANKIEWICZ, B.A., SCOTT, A.C. & WILSON, R. (1998): Factors influencing the preservation of plant cuticles: a comparison of morphology and chemical composition of modern and fossil examples, Organic Geochemistry 29, issue 5-7, 1369-1380.

MÜLLER, P.J. & SUESS, E. (1979): Productivity, sedimentation rate, and sedimentary organic matter in the oceans - I. Organic carbon preservation. Deep-Sea Research, 26(a): 1347 – 1362.

MÜLLER, P.J., SCHNEIDER, R. & RUHLAND, G. (1994): Late Quaternary $_{P}CO_2$ variations in the Angola Current: Evidence from organic carbon $\partial^{13}C$ and alkenone temperatures. Carbon Cycling in the Glacial Ocean: Constraints on the Ocean`s Role in Global Change. NATO ASI Series, 117: 343 – 366.

MUTTERLOSE, J. & KESSELS, K. (2000): Early Cretaceous calcareous nannofossils from high latitudes: implications for palaeobiogeography and

palaeoclimate. Palaeoceanography, Palaeoclimatology, Palaeoecology, 160: 347 – 372.

MUTTERLOSE, J., BRUMSACK, H.-J., FLOEGEL, S., HAY, W.W., KLEIN, C., LANGROCK, U., LIPINSKI, M., RICKEN, W., SOEDING, E., STEIN, R. & SWIENTEK, O. (2003): The Norwegian-Greenland Seaway: a key area for understanding Late Jurassic to Early Cretaceous paleoenvironments, *Paleoceanography*, Vol. 18 (1): DOI 10.1029/2001PA000625.

NIJENHUIS, I.A., BOSCH, H.-J., SINNINGHE DAMSTÉ, J.S., BRUMSACK, H.-J. & DE LANGE, G.J. (1999): Organic matter and trace element rich sapropels and black shales: a geochemical comparison, Earth and Planetary Science Letters 169, pp. 277 – 290.

NIJENHUIS, I.A., BECKER, J. & DE LANGE, G.J. (2001): Geochemistry of coeval marine sediments in Mediterranean ODP cores and a land section: implications for sapropel formation models, Paleogeography, Paleoclimatology, Paleoecology 165, pp. 97 – 112.

ONSTAD, D.G., CANFIELD, D.E., QUAY, P.D. & HEDGES, J. (2000): Sources of particulate organic matter in rivers from the continental USA: Lignin phenol and stable isotope composition, Geochimica et Cosmochimica Acta, Vol. 64, 20, pp. 3539 – 3546.

OSCHMANN, W., ROESSLER, J., AND HÜSSNER, H. (1995): Manipulations of insolation data (from Berger and Loutre, 1991) for the simulation of "realistic geological situations". Zbl. Geol. Paläont., I (1/2): 317-335.

PEDERSEN, T.F. & CALVERT, S.E. (1990): Anoxia versus Productivity: What Controls the Formation of organic carbon-rich sediments and sedimentary rocks? AAPG Bull., 74 (4): 454 – 466.

PETERS, K.E. (1986): Guidelines for Evaluating Petroleum Source Rock Using Programmed Pyrolysis, *AAPG Bulletin*, 70, 3, 318–329.

PINET, P.R., 1992. Oceanography. West Publ., St. Paul, MN, 571 pp.

PODLAHA, O.G., MUTTERLOSE, J. & VEIZER, J. (1998): Preservation of $\delta^{18}O$ and $\delta^{13}C$ in belemnite rostra from the Jurassic/Early Cretaceous successions. Am. J. Sci., 298: 324 – 347.

POELCHAU, H.S., BAKER, D.R., HANTSCHEL, TH., HORSFIELD, B. & WYGRALA, B. (1997): Basin simulation and the design of the conceptual basin model, in Petroleum and Basin Evolution, edited by D.H. WELTE ET AL., Springer Verlag Berlin Heidelberg.

PRICE, G.D., RUFFELL, A.H., JONES, C.E., KALIN, R.M. & MUTTERLOSE, J. (2000): Isotopic evidence for temperature variation during the Early Cretaceous (late Ryazanian – mid Hauterivian). Geological Society of London 155: 335–343.

RAU, G.H., ARTHUR, M.A., & DEAN, W.E. (1987): 15N/14N variations in Cretaceous Atlantic sedimentary sequences: implications for past changes in marine nitrogen biogeochemistry. EPSL, 82: 269-279.

RAISWELL, R. & BERNER, R.A. (1986): Pyrite and organic matter in Phanerozoic normal marine shales. Geochimica et Cosmochimica Acta, 50: 1967–1976.

RILEY, L.A. & TYSON, R.V. (1980): Palynofacies and paleoenvironment of the Kimmerigdian sediments of the northern North Sea. *In*: Christopher, R.A. (ed.), Proceedings of the eleventh annual meeting of the American Association of stratigraphic palynologists., Palynology 4: 249 pp.

RÖHL, H.-J., SCHMID-RÖHL, A., OSCHMANN, W., FRIMMEL, A. & SCHWARK, L. (2001): The Posidonia Shale (Lower Toarcian) of SW-Germany: an oxygen-depleted ecosystem controlled by sea level and paleoclimate, Paleogeography, Paleoclimatology, Paleoecology 165, pp. 27 – 52.

ROKOENGEN, K., LIPPARD, S., MORGENSEN, R. & RISE, L. (1988): *Rep. 24.1486/01/88 Nearshore bedrock mapping 62° - 57°30´ N*, 62 pp., IKU Trondheim.

ROMANKEVICH, E.A. (1984): Geochemistry of organic matter in the ocean. Springer Verlag, Berlin, Germany, 334 pp.

ROUTH, J., MCDONALD, T.J. & GROSSMAN, E.L. (1999): Sedimentary organic matter sources and depositional environment in the Yegua formation (Brazos County, Texas). *Organic Geochemistry*, 30, 1437 – 1453.

RULLKÖTTER J., MUKHOPADHYAY, P.K. ET AL. (1984): Geochemistry and petrography of organic matter in Cretaceous sediments from the Southeastern Gulf of Mexico, Deep Sea Drilling Project hole 535 - preliminary results. Initial Reports of the Deep Sea Drilling Project, 77: 489 – 493.

SÆLEN, G., TYSON, R.V., TELNÆS, N. & TALBOT, M.R. (2000): Contrasting watermass conditions during deposition of the Whitby Mudstone (Lower Jurassic) and Kimmeridge Clay (Upper Jurassic) formations, United Kingdom. *Palaeogeography, Palaeoclimatology, Palaeoecology*, 163, 163–196.

SARNTHEIN, M., WINN, K., AND ZAHN, R. (1987): Paleoproductivity of oceanic upwelling and the effect of atmospheric CO_2 and climatic change during deglaciation times. In: Berger, W.H. and Labeyrie, C. (eds.), Abrupt Climatic Changes. Reidel, Dordrecht, pp. 311-337.

SCHLANGER, S.O. & JENKYNS, H.C. (1976): Cretaceous Oceanic Anoxic Events: Causes and consequences. Geologie en Mijnbouw 55: 179–184.

SCHLANGER, S.O., ARTHUR, M.A., JENKYNS, H.C. & SCHOLLE, P.A. (1987): The Cenomanian-Turonian oceanic anoxic event, I. Stratigraphy and distribution of organic carbon-rich beds and the marine $\delta^{13}C$ excursion. In: BROOKS, J. & FLEET, A. (Eds.): Marine Petroleum Source Rocks. Geological Society Special Publication, 26: 371 – 399.

SCHOUTEN, S., SCHOELL, M., RIJPSTRA, W.I.C., SINNINGHE DAMSTÉ, J.S. & DE LEEUW, J.W. (1997): A molecular stable carbon isotope study of organic matter in immature Miocene Monterey sediments, Pismo basin, Geochimica et Cosmochimica Acta, Vol. 61, 10, pp. 2065 – 2082.

SCHUBERT, C.J. & STEIN, R. (1996): Deposition of organic carbon in Arctic Ocean sediments: terrigenous supply vs. marine productivity. Organic Geochemistry, 24 (4): 421 – 436.

SCHULZ, H.-M., SACHSENHOFER, R.F., BECHTEL, A., POLESNY, H., AND WAGNER, L. (2002): The origin of hydrocarbon source rocks in the Austrian Molasse Basin (Eocene-Ologocene transition), Marine and Petroleum Geology 19: 683-709.

SHERIDAN, R.E. (1987): Pulsation tectonics as the control of North Atlantic paleoceanography. In: SUMMERHAYES, C.P. & SHACKLETON, N.J. (Eds.):

North Atlantic Paleoceanography. Geological Society Special Publication 21: 255–275.

SHIMKUS, K.M. AND TRIMONIS, E.S. (1974): Modern sedimentation in the Black Sea. In: Degend, E.T. and Ross, D.A. (eds.), The Black Sea – Geology, Chemistry, and Biology, AAPG Memoirs 20: 249-278.

SIESSER, W.G. (1995): Paleoproductivity of the Indian Ocean during the Tertiary period. Global and Planetary Change 11, 71-88.

SINNINGHE DAMSTÉ, J.S. & KÖSTER, J. (1998): An euxinic southern North Atlantic Ocean during the Cenomanian/Turonian oceanic anoxic event. Earth and Planetary Science Letters 158: 165–173.

SKARBØ, O., BAKKE, S., JACOBSEN, T., KROGSTAD, W., LUNDSCHIEN, B., MYHR, M. B., RISE, L., SCHOU, L., SMELROR, M., VERDENIUS, J.D., VIGRAN, J. & ÅRHUS, N. (1988): Shallow drilling off Møre-Trøndelag 1988, 283 pp., IKU-Report, Trondheim, Norway.

SMELROR, M. (1994): Jurassic stratigraphy of the Western Barents Sea region: A review. Geobios 17: 441–451.

SMELROR, M., JACOBSEN, T., RISE, L., SKABØ, O., VERDENIUS J.D. & VIGRAN, J. O. (1994): Jurassic to Cretaceous stratigraphy of shallow cores on the Møre Basin margin, Mid-Norway, Norsk Geologisk Tidsskrift, 74, p. 89 – 107.

SMELROR, M., MØRK, A., MONTEIL, E., RUTLEDGE, D. & LEEREVELD, H. (1998): The Klippfisk Formation - a new lithostratigraphic unit of Lower Cretaceous platform carbonates on the Western Barents Shelf, *Polar Research*, 17, 181–202.

SMELROR, M., DYPVIK., H., & MØRK, A. (2001a): Cretaceous boundary beds of the Barents Sea possibly induced by the Mjølnir Impact. *In:* BUFFETAUT, E. & KOEBERL, C. (Eds.): Geological and Biological Effects of Impact Events, Impact Studies, Springer Verlag p. 69 – 82.

SMELROR, M., MØRK, A., MØRK, M.B.E., WEISS. H.M. & LØSETH, H. (2001b): Middle Jurassic-Lower Cretaceous transgressive-regressive sequences and facies distribution off Troms, northern Norway. In: MARTINSEN, O.J. & DREYER, T. (Eds.): Sedimentary Environments

Offshore Norway – Paleozoic to Recent. NPF Special Publication 10: 211–232.

SMITH, A.H.V. (1962): The palaeoecology of Carboniferous peats based on the miospores and petrography of bituminous coals, *Proceedings of Yorkshire Geological Society*, 33, 423-474.

STEIN, R. (1990): Organic carbon content/sedimentation rate relationship and its paleoenvironmental significance for marine sediments. Geo-Marine Letters 10: 37-44.

STEIN, R. (1991): Accumulation of organic carbon in marine sediments, in *Lecture Notes in Earth Sciences*, 34, edited by S. BHATTACHARJI ET AL., 217 pp., Springer Verlag, Berlin, Heidelberg, New York.

STEIN, R., RULLKÖTTER, J. & WELTE, D.H. (1986): Accumulation of organic-carbon-rich sediments in the late Jurassic and Cretaceous Atlantic Ocean - A synthesis. Chemical Geology 56: 1–32.

STEIN, R., RULLKÖTTER, J. & WELTE, D.H. (1989a): Changes in paleoenvironments in the Atlantic Ocean during Cretaceous times: results from black shales studies. Geologische Rundschau, 78 (3): 883 – 901.

STEIN, R., TEN HAVEN, H.L., LITTKE, R., RULLKÖTTER, J., AND WELTE, D.H. (1989b): Accumulation of organic carbon at upwelling Site 658 and non-upwelling Sites 657 and 659: implications for the reconstruction of paleoenvironments in the eastern subtropical Atlantic through late Cenozoic times. In: Ruddiman, W. Sarnthein, M., et al., Proc. ODP Sci. Results, 108: 361-385.

STORVOLL, V., BJORLYKKE, K., KARLSEN, D., & SAIGAL, G. (2002). Porosity preservation in reservoir sandstones due to grain-coating illite; a study of the Jurassic Garn Formation from the Kristin and Lavran fields, offshore mid-Norway. Marine and Petroleum Geology, Vol. 19, No. 6: 767-781.

STREET, C. & BROWN, P.R. (2000): Paleobiogeography of Early Cretaceous (Berriasian-Barremian) calcareous nannoplankton. Marine Micropaleontology 39: 265-291.

SWIENTEK, O. AND RICKEN, W. (2001): Hochauflösende Klimazyklen in Sedimenten der borealen Unterkreide. In: Gaupp, R. and van der Klauw, S. (eds.), Sedimente 2001 conference abstract, Schriftenreihe der Deutschen Geologischen Gesellschaft, 13: 91-92.

SWIENTEK, O. (2002): The Greenland Norwegian Seaway: climatic and cyclic evolution of Late Jurassic-Early Cretaceous sediments, PhD thesis, Mathematisch-Naturwissenschaftliche Fakultät der Universität zu Köln, pp. 119.

TAYLOR, G.H., TEICHMÜLLER, M., DAVIES, A., DIESSEL, C.F.K., LITTKE, R. & ROBERT, P. (Eds.) (1998): Organic Petrology. Berlin: Gebrüder Bornträger, 704 pp..

THIEDE, J. & VAN ANDEL, T.H. (1977): The Paleoenvironment of anaerobic sediments in the Late Mesozoic South Atlantic Ocean. Earth and Planetary Science Letters, 33: 301 – 309.

THIEDE, J. (1980): Paleo-oceanography, margin stratigraphy, and paleophysiography of the Tertiary North Atlantic and Norwegian-Greenland Seas, Philosophical Transactions of the Royal Society, London, Series A., 294: 177-185.

THUROW, J., BRUMSACK, H.-J., RULLKÖTTER, J., LITTKE, R. & MEYERS, P.A. (1992): The Cenomanian/Turonian Boundary Event in the Indian Ocean - a Key to Understand the Global Picture. Geophysical Monograph, 70: 253 – 273.

TISSOT, B.P. & WELTE, D.H. (Eds.) (1984): *Petroleum Formation and Occurrence*, 699 pp., Springer Verlag, New York.

TRIBOVILLARD, N., BIALKOWSKI, A., TYSON, R.V., LALLIER-VERGÈS, E., AND DECONINCK, J.-F. (2001): Organic facies variation in the late Kimmeridgian of the Boulonnais area (northernmost France), Marine and Petroleum Geology, 18, p. 371-389.

TSIKALAS, F., GUDLAUGSSON, S.T. & FALEIDE, J.I. (1998): Collapse, infilling, and postimpact deformation at the Mjølnir impact structure, Barents Sea. Geological Society of America Bulletin 110 (5): 537-552

TWICHELL, S.C., MEYERS, P.A. & DIESTER-HAASS, L. (2002): Significance of high C/N ratios in organic carbon-rich Neogene sediments under the Benguela Current upwelling system. Organic Geochemistry 33: 715-722.

TYSON, R.V. & PEARSON, T.H. (Eds.) (1991): Modern and ancient continental shelf anoxia, *Geol. Soc. Spec. Publ.*, Vol. 58, 470 pp.

VAN ANDEL, T.H., HEATH, G.R. & MOORE, T.C. (1975): Cenozoic History and Paleoceanography of the Central Equatorial Pacific Ocean. Geol. Soc. Am., Memoir 143.

VAN DE SCHOOTBRUGGE, B., FÖLLMI, K.B., BULOT, L.G. & BURNS, S.J. (2000): Paleoceanographic changes during the early Cretaceous (Valanginian-Hauterivian): evidence from oxygen and carbon stable isotopes. Earth and Planetary Science Letters 181: 15–31.

VIGRAN, J.O., MANGERUD, G., MØRK, A., BUGGE, T., AND WEITSCHAT, W. (1998): Biostratigraphy and sequence stratigraphy of the lower and middle Triassic deposits from the Svalis Dome, Central Barents Sea, Norway, Palynology, 22: 89-141.

WAGNER, T. (2002): Late Cretaceous to early Quaternary organic sedimentation in the eastern Equatorial Atlantic, Paleogeography, Paleoclimatology, Paleoecology 179, pp. 113 – 147.

WAGNER, T. & HÖLEMANN, J.A. (1995): Deposition of organic matter in the Norwegian-Greenland-Sea during the Past 2.7 Million years. Quaternary Research, 44: 355 – 366.

WAPLES, D.W. (Ed.) (1981): *Organic Geochemistry for Exploration Geologists, Burgess Publication Company*, 151 pp., Minnesota.

WAPLES, D.W. & SLOAN, J.R. (1980): Carbon and nitrogen diagenesis in deep sea sediments. Geochimica et Cosmochimica Acta 44 (10): 1463-1470.

WEDEPOHL, K.H. (1970): Environmental influences on the chemical composition of shales and clays. In: AHRENS, L.H., PRESS, F., RUNCORN, S.K. & UREY, H.C. (Eds.): Physics and Chemistry of the Earth. Oxford: Pergamon, 307-333.

WEDEPOHL, K.H. (1991): The composition of the upper Earth´s crust and the natural cycles of selected metals. Natural Resources. In: Marian, E. (ed.), Metals and their compounds in the environment. VHC, Weinheim, pp. 3-17.

WEISSERT, H. & MOHR, H. (1996): Late Jurassic climate and its impact on carbon cycling. Palaeogeography, palaeoclimatology, palaeoecology, 122: 27 – 43.

WEISSERT, H., LINI, A., FÖLLMI, K.B. & KUHN, O. (1998): Correlation of Early Cretaceous carbon isotope stratigraphy and platform drowning events: a possible link? Paleogeography, Palaeoclimatology, Palaeoecology, 137: 189 – 203.

WESTERHAUSEN, L., POYNTER, J., EGLINTON, G., ERLENKEUSER, H. & SARNTHEIN, M. (1993): Marine and terrigenous origin of organic matter in modern sediments of the equatorial East Atlantic: the $\delta^{13}C$ and molecular record, *Deep-Sea Research I*, 40, 1087–1121.

WILKIN, R.T., BARNES, H.L. & BRANTLEY S.L. (1996): The size distribution of framboidal pyrite in modern sediments: An indicator of redox conditions. Geochimica et Cosmochimica Acta 60 (20): 3897–3912.

WILKIN, R.T., ARTHUR, M.A. & DEAN, W.E. (1997): History of water-column anoxia in the Black Sea indicated by pyrite framboid size distributions. Earth and Planetary Sciences Letters 148: 517–525.

WILLIAMS, G.L. (1978): Dinoflaggelates, acritarchs and tasmanitids: 293 – 326. In: HAQ, B.U. & BOERSMA, A. (Eds.): Introduction to marine micropalaeontology. Elsevier, New York, 376 pp.

WORSLEY, D., JOHANSEN, R. & KRISTENSEN, S.E. (1988): The Mesozoic and Cenozoic succession of Tromsøflaket. In: DALLAND, A., WORSLEY, D. & OFSTAD, K. (Eds.): A lithostratigraphic scheme for the Mesozoic and Cenozoic succession offshore mid- and northern Norway. Norwegian Petroleum Directorate Bulletin 4: 42–65.

ZIEGLER, P.A. (1988): Evolution of the Arctic-North Atlantic and the western Tethys. AAPG Memoir 43, 198 pp.

ÅRHUS, N. (1991): The transition from deposition of condensed carbonates to dark claystones in the Lower Cretaceous succession of the southwestern Barents Sea. Norsk Geologisk Tidsskrift, 71: 259–263.

ÅRHUS, N., BUGGE, T., ELVEBAKK, G., FJERDINGSTAD, V., LEITH, T.L., MØRK, A., RENDALL, H., SKARBØ, O. & WEISS, H.M. (Eds., 1987): Shallow drilling Elf Aquitaine/Norsk Hydro/Statoil Barents Sea. IKU-Report: 50 p.

ÅRHUS, N., KELLY, S.R.A., COLLINS, J.S.H. & SANDY, M.R. (1990): Systematic paleontology and biostratigraphy of two early Cretaceous condensed sections from the Barents Sea. Polar Research 8: 165-194.

Acknowledgements

First I would like to spend credits to my supervisor Professor Dr. Ruediger Stein (AWI) who initiated this project and gave impulse to its forthcoming. His consistent care, scholarship, and counsel helped very much to carry out this work.

I also thank Professor Dr. Rüdiger Henrich (University of Bremen) very much for taking over the second expertise on my dissertation.

My dear friend and colleague PD Dr. Tomas Wagner (University of Bremen) taught me basic knowledge in the field of organic petrography. Our meetings were essential to my understanding of all those "Biofussel" in the sediments. Thank you so much!

Professor W.W. Hay (Colorado State University, USA) needs also to be thanked for his critical review of the abstract and introduction chapters.

Working with my fellows at the Alfred Wegener Institute for Polar and Marine Research in Bremerhaven was both profit and pleasure. Among those I would especially thank my friends Daniel Birgel, Bettina Boucsein, Claudia Didié, Klaus Dittmers, Christian Hass, Jens Hefter, Matthias Kraus, Jens Matthiessen, and Frank Schoster. I enjoyed very much being part of the band named "Packhalle 10" and I really wished that we had more time for playing together. Thanks to you all!

The staff of Sintef Petroleum Research (Norway), in particular Atle Mørk, Hermann M. Weiss, and Ute Mann, need special thanks because they provided access to core material, confidential drilling reports, and helpful support at any time. Thank you for your cooperation.

I suppose that producing analytical data would have been less comfortable without technical help from Rita Fröhlking, Beate Hollmann, Martina Siebold, and Walter Luttmer. I must also thank the staff of ICG-4 at Research Center Jülich for technical support on the Rock-Eval-2 as well as Simone Klein and Diane Lord for their laboratory assistance.

This work also benefits very much from the excellent cooperation among the members of the INCREASE project, in particular my research colleagues Marcus Lipinski (ICBM Oldenburg), Christian Klein (University of Bochum), Oliver Swientek (Shell AG) and Sascha Floegel (Geomar).

Financial support was granted by the Deutsche Forschungsgemeinschaft (DFG) from April 1999 to March 2001 (project Ste 412/13-1).

I also appreciate very much the support from the Department of Geosciences at the Alfred Wegener Institute for Polar and Marine Research throughout the past four years, which was represented by Professor Dr. Dieter K. Fütterer.

Last but not least I must be very grateful for endurance, understanding, and support given to me by my wife Sandra and our family. I guess that without you this work would have never come to an end. THANK YOU!

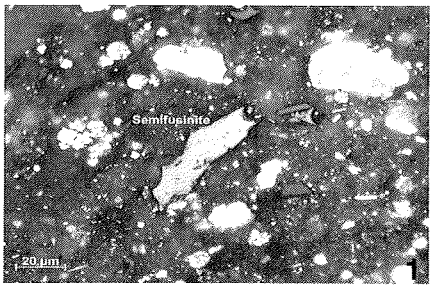
Semifusinite
20 µm
1

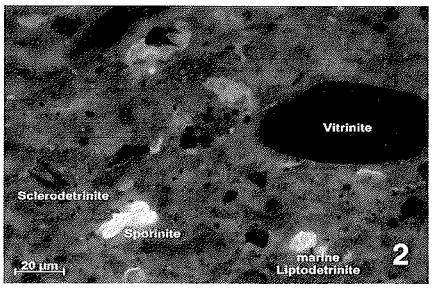
Vitrinite
Sclerodetrinite
Sporinite
marine
Liptodetrinite
20 µm
2

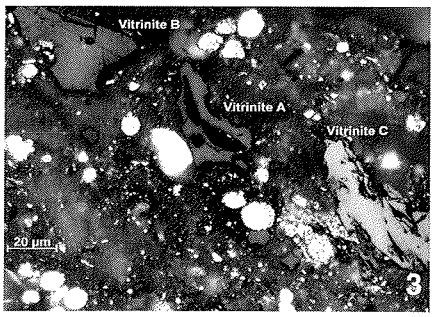
Vitrinite B
Vitrinite A
Vitrinite C
20 µm
3

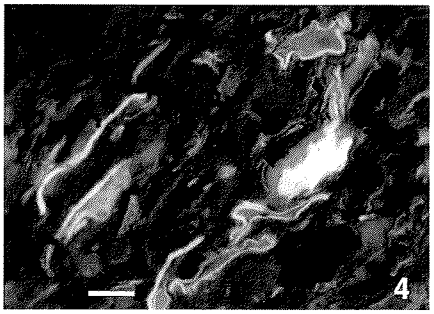
4

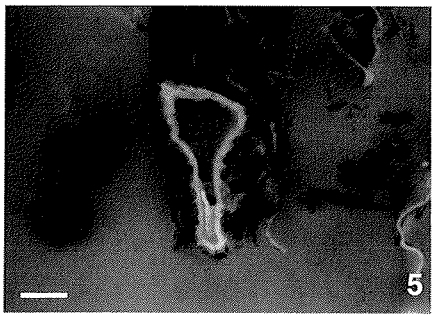
5

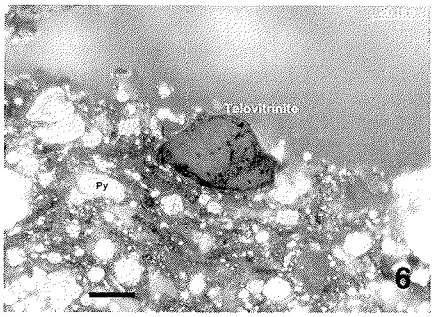
Telovitrinite
Py
6

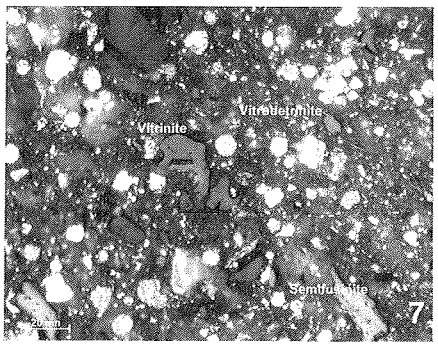
Vitrodetrinite
Vitrinite
Semifusinite
7

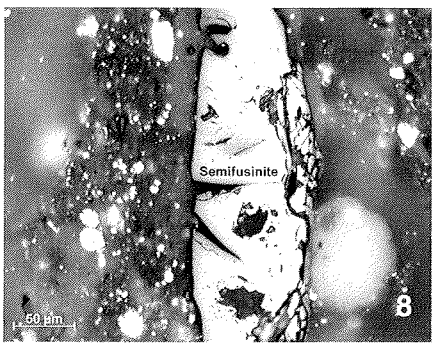
Semifusinite
50 µm
8

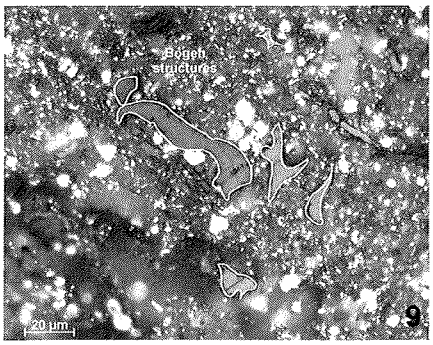

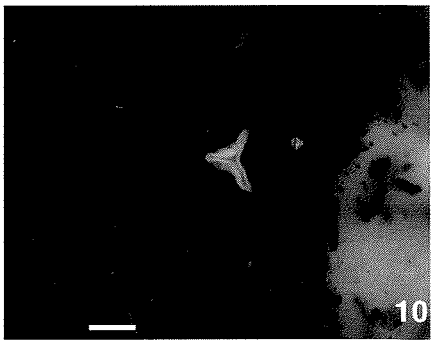

Plate I Core 13/1-U-02

All pictures were taken with a Zeiss AxioCam® digital video camera (maximum resolution 3600 x 3600 pixel) mounted on a Zeiss Axiophot light microscope using reflected white light (RWL) and ultraviolet light (UV). Depth is given in meters below sea-floor, i.e. core depth, and reflects also the sample number given in data tables.

Fig. 1 Depth: 125.50 m, Semifusinite, pyrite, detritus, RWL, 500 x magnification
Fig. 2 Depth: 125.50 m, Vitrinite, pyrite, detritus, FL, 500 x magnification
Fig. 3 Depth: 125.50 m, Vitrinites, various maturity, RWL, 500 x magnification
Fig. 4 Depth: 141.50 m, Sporinite (or alginite) fragments, thin-walled, FL,scale bar equals 20 µm
Fig. 5 Depth: 141.50 m, Sporinite (exines), FL, 500 x magnification, scale bar equals 20 µm
Fig. 6 Depth: 157.00 m, Vitrinite (sub-rounded), silty matrix, RWL, scale bar equals 20 µm
Fig. 7 Depth: 157.00 m, Vitrinite, vitrodetrinite, semifusinite, RWL, 500 x magnification
Fig. 8 Depth: 177.25 m, Semifusinite (500 x 100 µm), RWL, 200 x magnification
Fig. 9 Depth: 192.47 m, Vitrinite (angular), "Bogen-structure", RWL, 500 x magnification
Fig. 10 Depth: 207.25 m, Sporinite (spore), FL, scale bar equals 20 µm

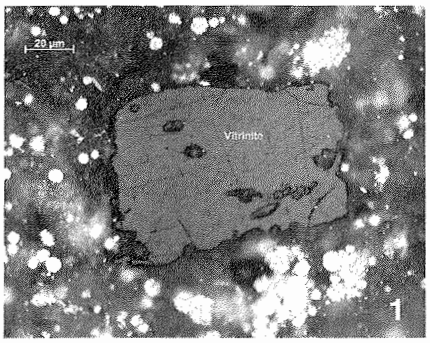
20 µm
Vitrinite
1

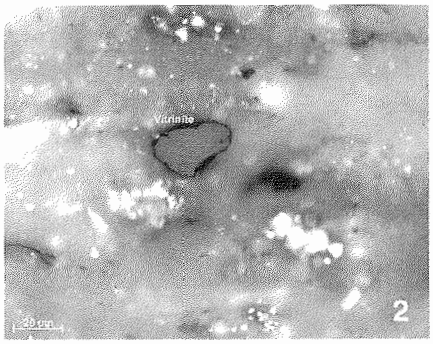
Vitrinite
2

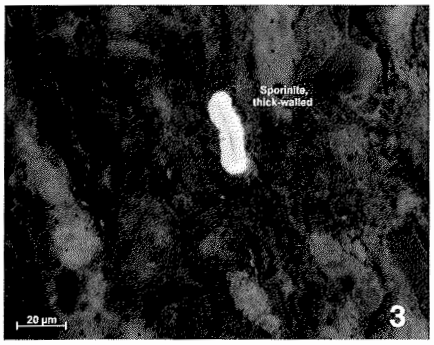
Sporinite,
thick-walled
20 µm
3

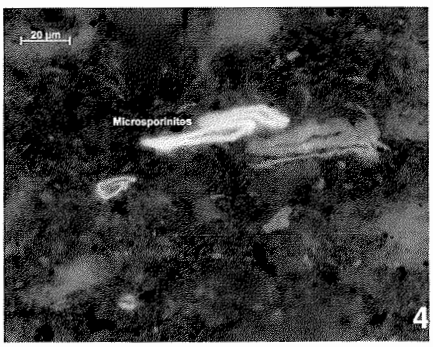
20 µm
Microsporinites
4

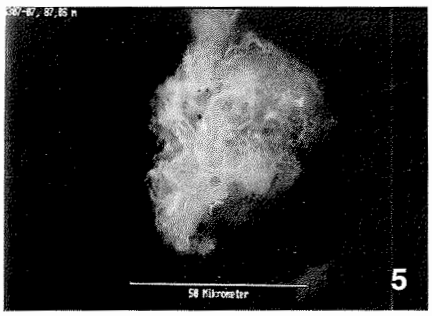
50 Nikrometer
5

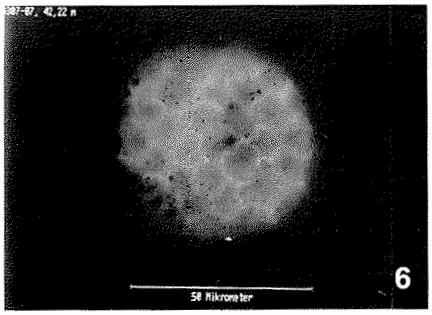
50 Nikrometer
6

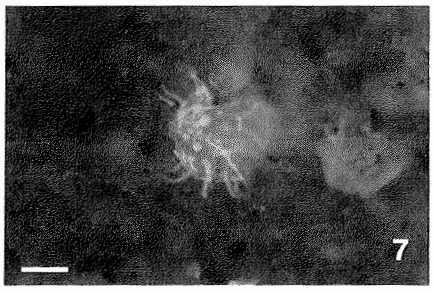
7

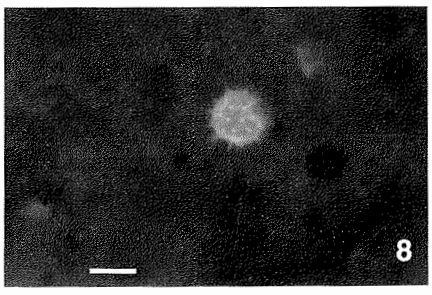
8


9

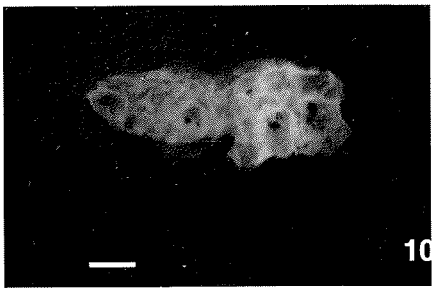
10


11

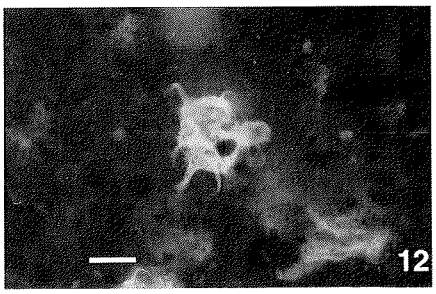
12

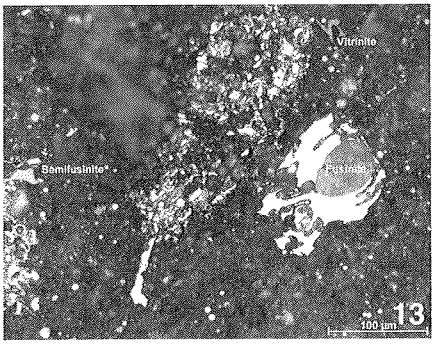
Vitrinite
Semifusinite*
Fusinite
100 µm
13

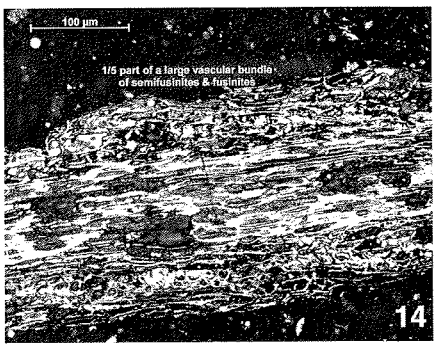
100 µm
1/5 part of a large vascular bundle
of semifusinites & fusinites
14

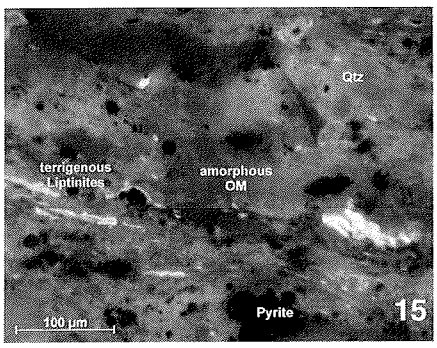
Qtz
terrigenous
Liptinites
amorphous
OM
Pyrite
100 µm
15

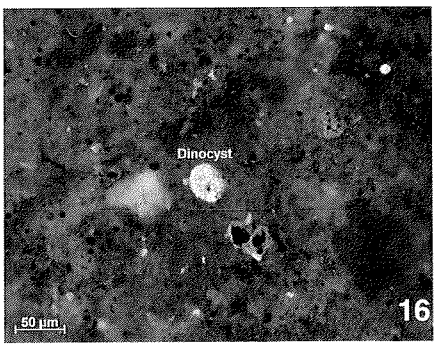
Dinocyst
50 µm
16

Plate II Core 6307/07-U-02

All pictures were taken with a Zeiss AxioCam® digital video camera (maximum resolution 3600 x 3600 pixel) mounted on a Zeiss Axiophot light microscope using reflected white light (RWL) and ultraviolet light (UV). Depth is given in meters below sea-floor, i.e. core depth, and reflects also the sample number given in data tables.

Fig. 1 Depth: 87.06 m, Vitrinite (100μm), sub-angular, pyrite, RWL, 500 x magnification
Fig. 2 Depth: 27.93 m, Vitrinite, rounded, silty-sandy matrix, RWL, 500 x magnification
Fig. 3 Depth: 62.14 m, Sporinite (microspore), thick-walled, FL, 500 x magnification
Fig. 4 Depth: 62.14 m, Sporinites (various), well-preserved, FL, 500 x magnification
Fig. 5 Depth: 87.06 m, Telalginite, degraded, colonial (*Botryococcus*?), FL, 500 x magnification
Fig. 6 Depth: 42.22 m, Telalginite, *Pediastrum*(?), FL, 500 x magnification
Fig. 7 Depth: 37.60 m, Telalginite, Dinoflagellate cysts, degraded, FL, scale bar equals 10 μm
Fig. 8 Depth: 42.22 m, Dinocyst or acritarch, FL, scale bar equals 10 μm
Fig. 9 Depth: 42.22 m, Sporinite, FL, 500 x magnification, scale bar equals 20 μm
Fig. 10 Depth: 63.36 m, Telalginite/Liptodetrinite, colonial, FL, 500 x magnification, scale bar equals 20 μm
Fig. 11 Depth: 87.06 m, Liptodetrinite, Dinocyst fragment, FL, 500 x magnification, scale bar equals 20 μm
Fig. 12 Depth: 99.15 m, 2 dinoflagellate cysts, well-preserved, FL, 500 x magnification, scale bar equals 20 μm
Fig. 13 Depth: 87.06 m, Vitrinite (100μm), sub-angular, pyrite, RWL, 500 x magnification
Fig. 14 Depth: 87.06 m, Semifusinite and fusinite (white), shattered, RWL, 200 x magnification
Fig. 15 Depth: 80.00 m, Fusite (microlithotype), 2000 μm, coal fragment, RWL, 200 x magnification
Fig. 16 Depth: 60.00 m, Dinoflagellate cysts and liptodetritus, FL, 200 x magnification

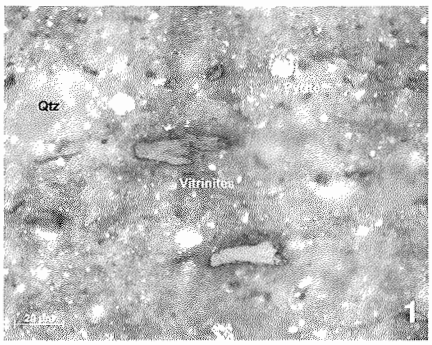
Qtz
Vitrinites
1

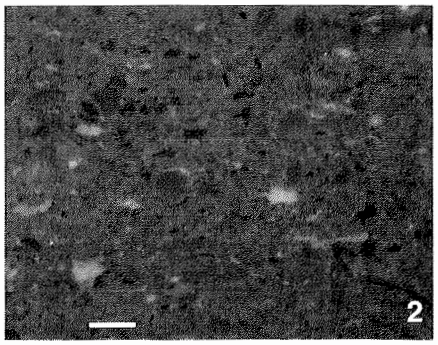
2

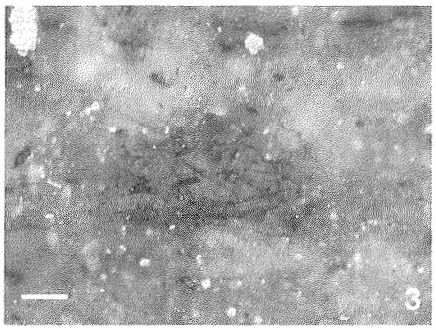
3

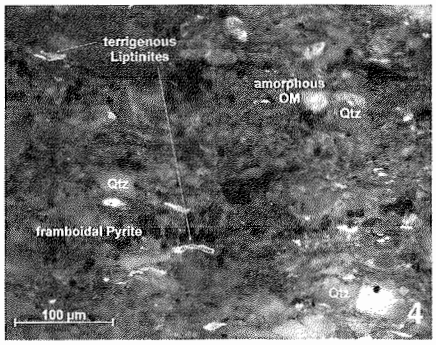
terrigenous
Liptinites
amorphous
OM
Qtz
Qtz
framboidal Pyrite
Qtz
100 µm
4

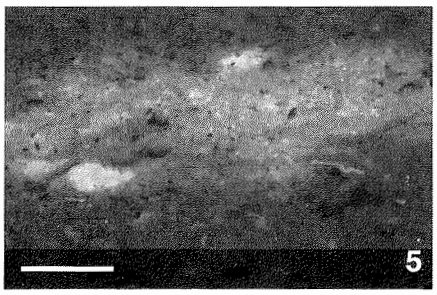
5

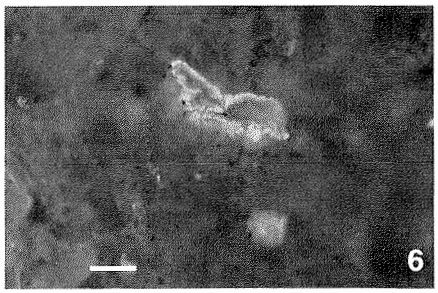
6

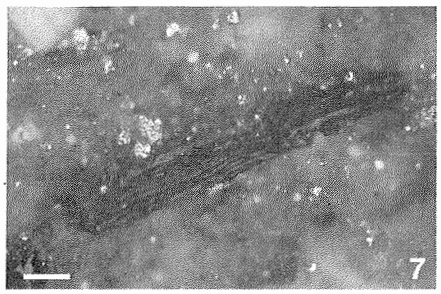
7

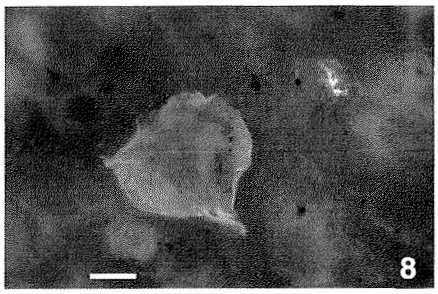
8

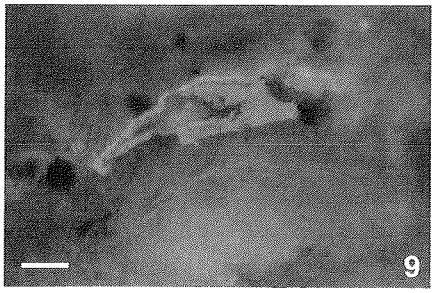
9

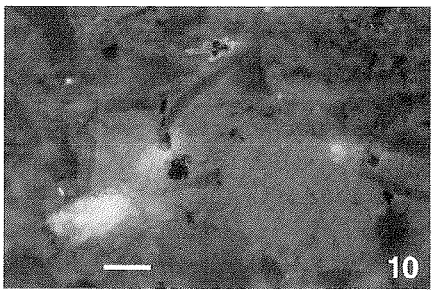
10

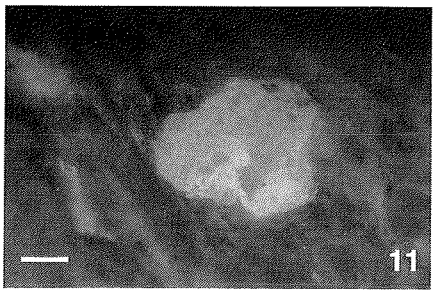
11

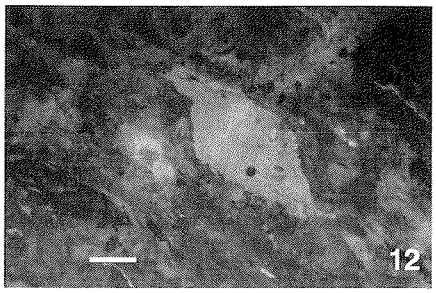
12

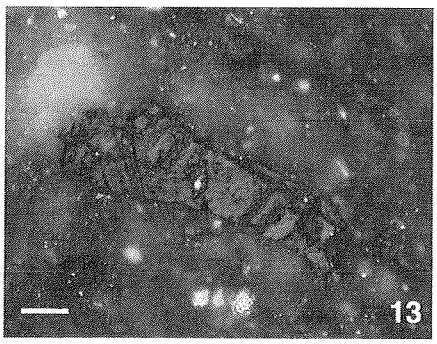
13

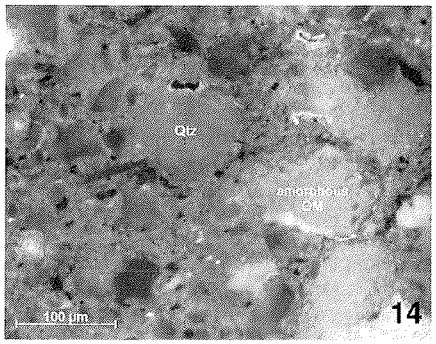
Qtz
amorphous OM
100 µm
14

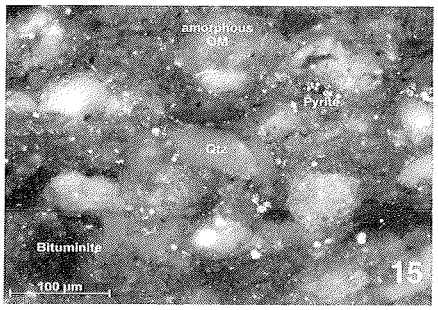
amorphous OM
Pyrite
Qtz
Bituminite
100 µm
15

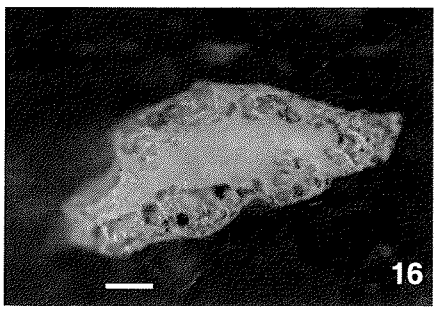
16

Plate IIICore 6814/04-U-02

All pictures were taken with a Zeiss AxioCam® digital video camera (maximum resolution 3600 x 3600 pixel) mounted on a Zeiss Axiophot light microscope using reflected white light (RWL) and ultraviolet light (UV). Depth is given in meters below sea-floor, i.e. core depth, and reflects also the sample number given in previous data tables.

Fig. 1 Depth: 10.94 m, Vitrinites, sub-angular, silt-grade quartz, RWL, 500 x magnification
Fig. 2 Depth: 10.94 m, Vitrinites, silt-grade quartz, FL, 500 x magnification, scale bar equals 20 µm
Fig. 3 Depth: 10.94 m, Vitrinite (80 µm), angular, RWL, 500 x magnification, scale bar equals 20 µm
Fig. 4 Depth: 136.62 m, Sporinite, alginite, typical "Hekkingen Formation", FL, 200 x magnification
Fig. 5 Depth: 10.94 m, Amorphous material, uncertain origin, FL, 200 x magnification, scale bar equals 100 µm
Fig. 6 Depth: 57.70 m, Alginite(?), oil-secreting, FL, 500 x magnification, scale bar equals 20 µm
Fig. 7 Depth: 57.70 m, Vitrinite, vascular bundle (150 x 20 µm), RWL, 500 x magnification, scale bar equals 20 µm
Fig. 8 Depth: 68.40 m, Telalginite, probably dinoflagellate cyst, FL, 500 x magnification, scale bar equals 20 µm
Fig. 9 Depth: 109.93 m, Sporinite, heavily degraded, FL, 500 x magnification, scale bar equals 20 µm
Fig. 10 Depth: 109.93 m, Sporinite and amorphous matter, FL, 500 x magnification, scale bar equals 20 µm
Fig. 11 Depth: 128.49 m, Telalginite, colonial, *Botryococcus*(?), FL, 500 x magnification, scale bar equals 20 µm
Fig. 12 Depth: 128.49 m, Resinite(?), bedding diagonal to image, FL, 500 x magnification, scale bar equals 20 µm
Fig. 13 Depth: 128.49 m, Telovitrinite (100 µm), immature, angular, shattered, RWL, scale bar equals 20 µm
Fig. 14 Depth: 109.93 m, Amorphous matter (algae/bacteria?), sporinite, silty sequence, RWL, 200 x magnification
Fig. 15 Depth: 106.62 m, A coarse-grained silt facies, RWL, 200 x magnification
Fig. 16 Depth: 136.62 m, Telalginite, crosscut, degraded, FL, 500 x magnification, scale bar equals 20 µm

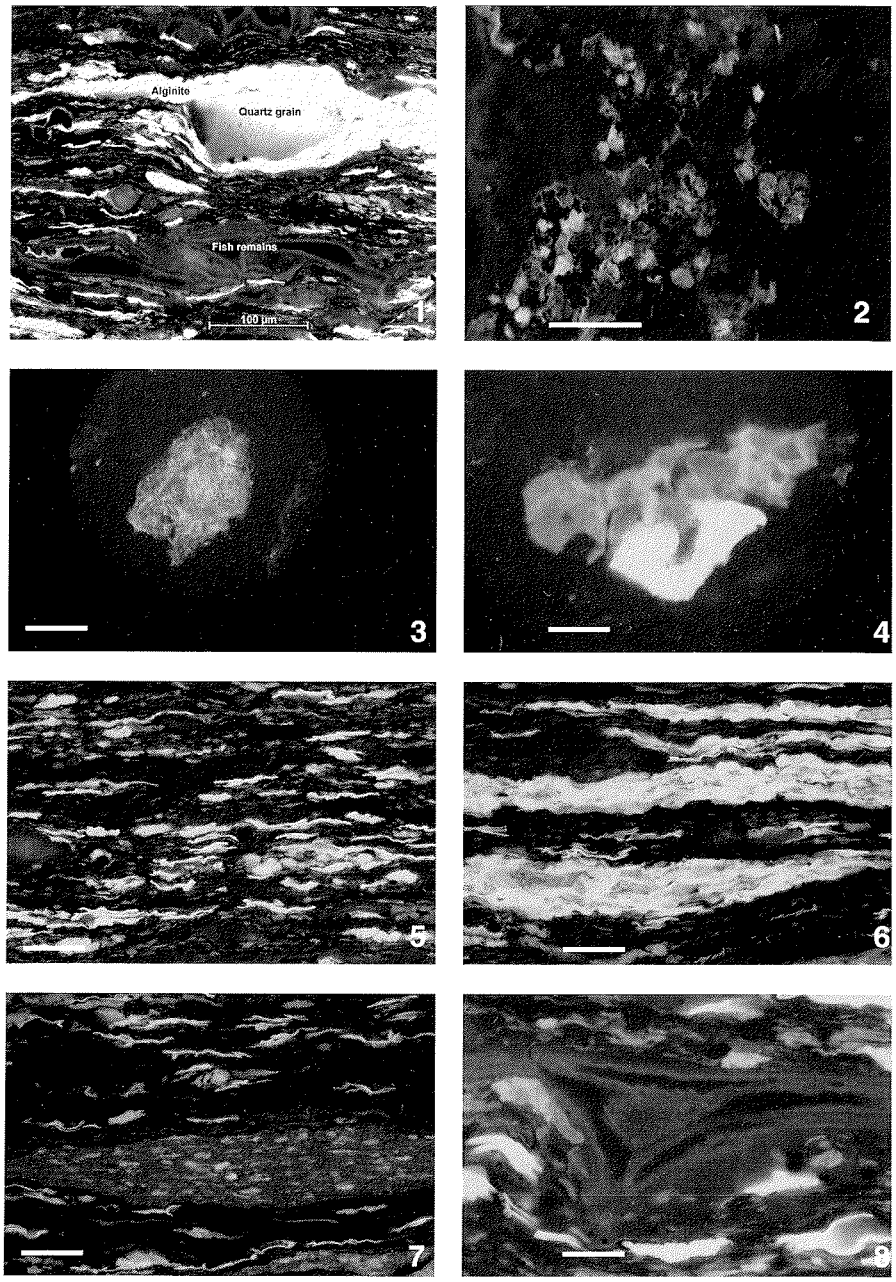
Alginite
Quartz grain
Fish remains
100 µm
1
2
3
4
5
6
7
8

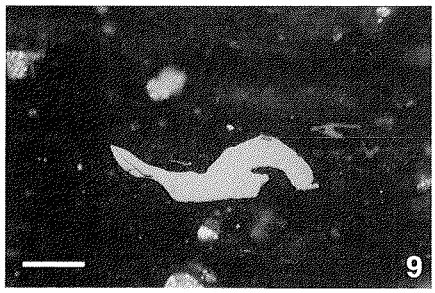
9

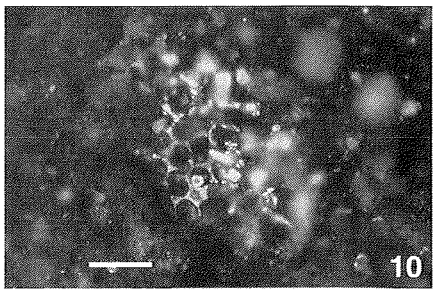
10

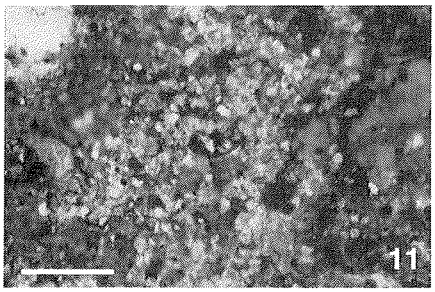
11

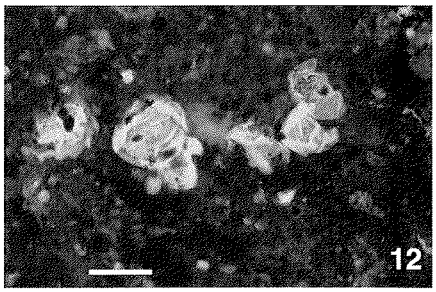
12

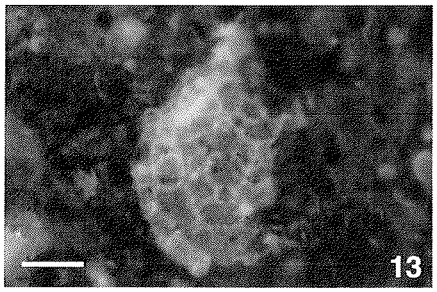
13

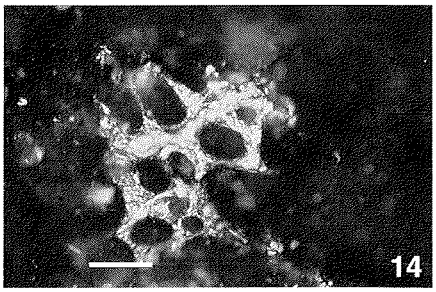
14

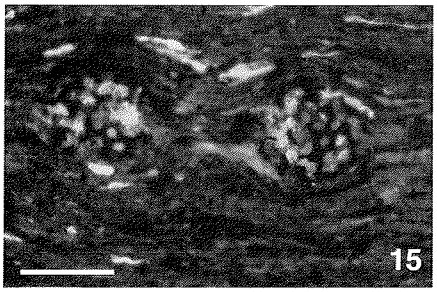
15

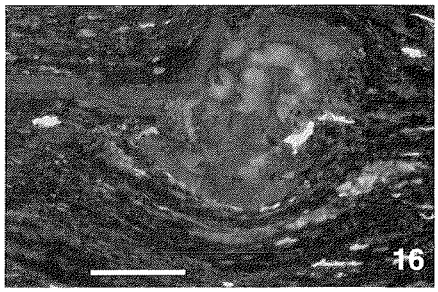
16

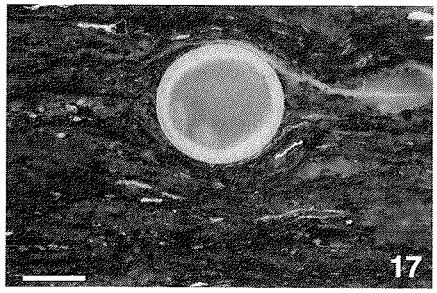
17

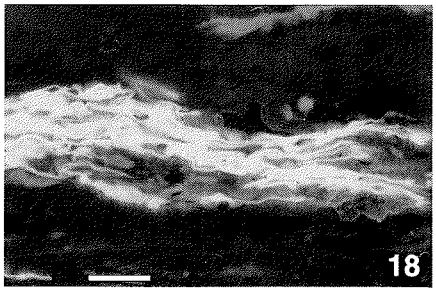
18

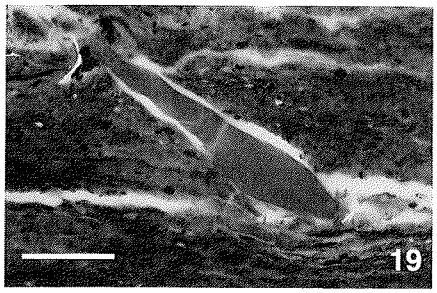
19

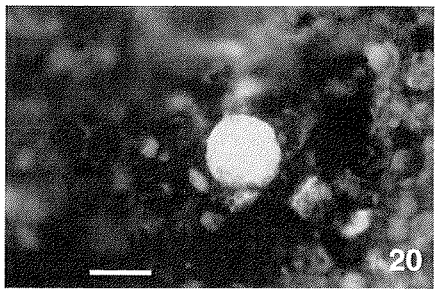
20

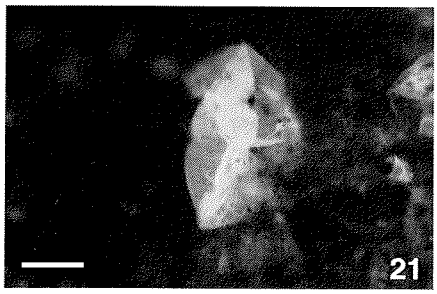
21

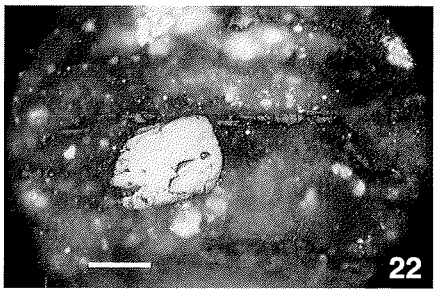
22

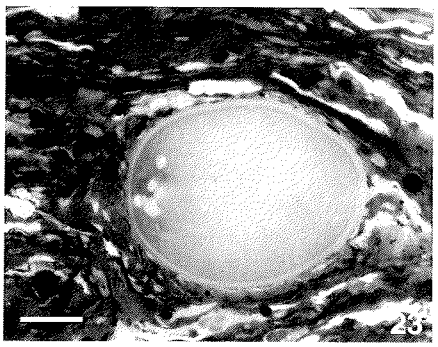
23

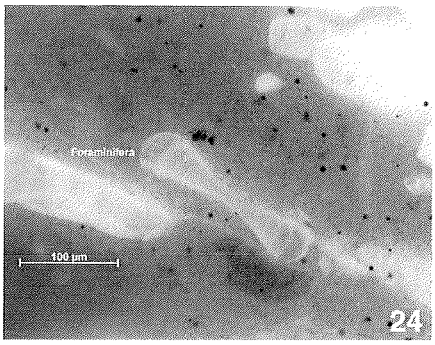
Cytheridella
100 µm
24

Plate IV Core 7430/10-U-01

All pictures were taken with a Zeiss AxioCam® digital video camera (maximum resolution 3600 x 3600 pixel) mounted on a Zeiss Axiophot light microscope using reflected white light (RWL) and ultraviolet light (UV). Depth is given in meters below sea-floor, i.e. core depth, and reflects also the sample number given in previous data tables.

Fig. 1 Depth: 49.95 m, Alginite, fish remains, well-preserved, fine-sand quartz (upper left center), FL, 200 x magnification
Fig. 2 Depth: 48.72 m, Alginite, bloom of *Leiosphaeridia*(?), FL, 200 x magnification, scale bar equals 100 µm
Fig. 3 Depth: 48.72 m, Alginite, physically degraded, FL, 500 x magnification, scale bar equals 20 µm
Fig. 4 Depth: 48.72 m, Liptodetrinite (resinite and cutinite?), FL, 500 x magnification, scale bar equals 20 µm
Fig. 5 Depth: 49.95 m, Alginite, layered deposition, FL, 200 x magnification, scale bar equals 100 µm
Fig. 6 Depth: 49.95 m, Alginite, warves of algae, prob. reflect. annual cycles, FL, scale bar equals 20 µm
Fig. 7 Depth: 49.95 m, Alginite, sporinite, two facies, FL, 500 x magnification, scale bar equals 20 µm
Fig. 8 Depth: 49.95 m, Fish remains, algae, well-preserved, FL, 500 x magnification, scale bar equals 20 µm
Fig. 9 Depth: 49.95 m, Semifusinite, bronze hue, RWL, 500 x magnification, scale bar equals 20 µm
Fig. 10 Depth: 50.31 m, Funginite, pyritized, RWL, 500 x magnification, scale bar equals 20 µm
Fig. 11 Depth: 50.31 m, Alginite, bloom of *Leiosphaeridia*(?), FL, 200 x magnification, scale bar equals 100 µm
Fig. 12 Depth: 50.31 m, Alginite, spherical form, thin-walled, extremely well-preserved, FL, scale bar equals 20 µm
Fig. 13 Depth: 50.31 m, Alginite, remain, colonial, *Botryococcus*(?), FL, scale bar equals 20 µm
Fig. 14 Depth: 50.31 m, Inertinite (funginite?), "Lochsiebstruktur", RWL, scale bar equals 20 µm
Fig. 15 Depth: 52.00 m, Uncertain origin (fungal remain?), both ends spherical, FL, scale bar equals 100 µm
Fig. 16 Depth: 52.00 m, Fish remains, end of 2.5 mm long particle, unbroken, FL, scale bar equals 100 µm
Fig. 17 Depth: 52.00 m, Telalginite, *Tasmanites* (100 µm), FL, 500 x magnification, scale bar equals 20 µm
Fig. 18 Depth: 52.00 m, Alginite, band of filamentous algae, inertinite (black), FL, 500 x magnification, scale bar equals 20 µm
Fig. 19 Depth: 52.50 m, Fish remain, penetrated sediment surface, FL, 200 x magnification, scale bar equals 100 µm
Fig. 20 Depth: 53.59 m, Alginite, *Pediastrum* (30 µm), very well-preserved, FL, 500 x magnification, scale bar equals 20 µm
Fig. 21 Depth: 53.59 m, Alginite, quenched *Leiosphaeridia*(?), FL, 1000 x magnification, scale bar equals 10 µm
Fig. 22 Depth: 59.74 m, Semifusinite (sub-rounded) and telovitrinite (angular), RWL, scale bar equals 20 µm
Fig. 23 Depth: 52.50 m, Sporinite (probably pollen grain), alginites, all excellently preserved, FL, scale bar equals 20 µm
Fig. 24 Depth: 39.74 m, Foraminifers (various benthic and plankton) and diatoms, FL, scale bar equals 100 µm